A STUDY OF
ABSOLUTE ATOMIC TRANSITION PROBABILITIES;
THE CORRELATION OF OSCILLATOR STRENGTHS
AND VAPOR PRESSURE

Thesis by

Norton Leonard Moise

In Partial Fulfillment of the Requirements

For the Degree of

Doctor of Philosophy

California Institute of Technology

Pasadena, California

1963

ACKNOWLEDGEMENTS

This research has been carried out under the supervision of Professor Robert B. King. The author wishes to express his gratitude for Dr. King's guidance and assistance, which were generously given throughout the project.

Mr. George Lawrence and Mr. John Link built the photometric system used, and their assistance in the use of this apparatus has been very helpful.

This research was supported, in part, by the Office of Naval Research under Contract Nonr 220(06).

ABSTRACT

A discussion of the absolute f-value of atomic transitions is given and the resulting relation between the equivalent width of an absorption line and the density is derived. This relation, referred to as the curve of growth, is examined in detail over a large range of the density factor; that is, for values beyond the linear region. Accurate computations are made for various values of the ratio of natural to Doppler broadening and tables presented in the appendices.

An optical quartz cell was designed with a variable optical path length. This cell was used in conjunction with an electric furnace to construct the curve of growth entirely from the experimental data. The curves of growth were then correlated to the latest vapor pressure data yielding f-values for nineteen resonance lines of ten elements.

The lines studied and the resulting f-values were Cu, λ3247 (0.322) and λ3274 (0.153); Ag, λ3281 (0.451) and λ3381 (0.175); Au, λ2676 (0.76); Zn, λ3076 (0.992×10^{-4}); Cd, λ3261 (2.05×10^{-3}); Ga, λ4033 (0.095); In, λ3039 (0.339) and λ4101 (0.172); Tl, λ2767 (0.219) and λ3775 (0.108); Sn, λ2863 (0.332), λ3009 (0.042), and λ3175 (0.065); and Pb, λ2833 (0.229), λ3639 (0.106), λ3683 (0.243), and λ4057 (0.419).

These results are correlated to those of other investigators and comments made on the connection between the f-value and the energy of the transition. For those elements which have a well-known f-value, the vapor pressure data are discussed. Corrections to the solar abundances are made on the basis of the results obtained.

TABLE OF CONTENTS

TABLE OF CONTENTS
(Continued)

LIST OF TABLES

LIST OF TABLES
(continued)

LIST OF FIGURES

LIST OF FIGURES
(continued)

I. INTRODUCTION

A. Background - There are two quantities which characterize an atomic transition. The first is the energy level separation of the initial and final states, and the second is the transition probability between the two states. The wavelength is inversely proportional to the energy gap and is almost always known to six or seven significant figures. The second is the matrix element (usually for a dipole operator) between initial and final states; it is inversely proportional to the lifetime of the upper state, and is rarely known to two significant figures.

One basic reason for the difficulties encountered in the transition probability measurement is that the wave functions of the atom are strongly affected by collisions, temperature effects, magnetic fields, etc., while the energies are not. For example, pressure effects cause the wavelength to shift only a small fraction of a percent while the lifetime may be shortened by a factor of two. Likewise, the nuclear magnetic moment causes a hyperfine splitting which may not be detectable on the spectrograph, yet it needs to be accounted for in determining the transition probabilities or lifetime. Therefore, the lack of available data on transition probabilities is understandable, but these difficulties encourage one to attempt to fill this gap in atomic information.

Many attempts have been made to calculate transition probabilities, such as the coulomb approximation of

Bates and Damgard.[1] The self-consistent field method was applied by Hargreaves,[2] Bates and Damgard,[3] Hartree,[4] and Misra,[5] to various transitions, primarily in light atoms. Recently, the f-value of Pb was calculated by Helliwell[6] using simple wave functions, and Atlick[7] has used the random phase method for calculating the f-values of six elements. All of this work involves approximating the wave function and then accounting for exchange and other purely quantum mechanical effects afterwards. The general agreement with experiment is not remarkable, although some particular calculations are in agreement with experiment.

On the experimental side, the method of total absorption has been used by A. S. and R. B. King,[8] R. B. King and D. C. Stockberger[9] and F. B. Estabrook.[10] They have been able to obtain vapor pressure determinations of absolute f-values for about ten elements. Kepferman and Wessel[11] developed an atomic beam method which has been improved upon by Bell, Davis, King, and Routly[12] who measured the f-value of the Mn line $\lambda = 4031$ Å, and by Bell and King[13] who measured the Pb line $\lambda = 2833$ Å. More recently G. Lawrence[14] and J. Link [15] have extended this method to include other elements.

Another method, referred to as the Hook Method, has been used by D. S. Rozhdestvenskii and N. P. Penkin[16] and extended by Ostrovskii and Penkin.[17]

Direct lifetime measurements have been made by K. Ziock,[18] Ottinger and Ziock,[19] and W. Demtroder[20] In these experiments the light is modulated and the phase shift or time delay of the remitted radiation is sought.

C. H. Corliss and W. R. Bozman[21] have attempted to correlate the f-values of seventy elements using an emission method.

The various experimental techniques are not in good agreement. This fact is brought out in Table I, in which several of the experimental values are compared.

TABLE I - COMPARISON OF f-VALUES

Element	____	Atom Beam	Abs. Tube	Emission[21]	Lifetime
Cu	3247	0.31	0.42 0.74	0.32	0.67
Cu	3274	0.16	0.22	0.16	
Ag	3281	0.48		0.27 0.29	
Ag	3383	0.22	0.14	0.115	

These few samples are indicative of some of the "better known f-values." It is, therefore, clear that much is left to be done in this field.

The resulting f-values or transition probabilities are of particular interest in astrophysics, since the verification of various theories of stellar and solar composition depends

on a knowledge of these constants. The work of Aller, et al,[22] on the abundances of the elements in the sun, is critically dependent on not only the f-values but also on a knowledge of the curve of growth. That is, the complete relationship between the spectral line itensity and the number of atoms is required. The f-value can be thought of as the ratio of the quantum mechanical oscillator, strength to the classical harmonic oscillator strength so that knowledge of the number of atoms involved in a spectral line is proportional to the f-value. Investigations of stellar composition by Goldberg, Miller, and Aller[23] and by Greenstein and Coworkers[24] similarly require knowledge of the transition probabilities.

B. Definitions - If a beam of light of intensity I_o passes through a gas absorption takes place at those frequencies which excite the atoms from their initial state to a final state. The intensity then has the form,

$$I(\nu) = I_o e^{-k(\nu)x} \tag{1}$$

where, $k(\nu)$ is the absorption coefficient; a function of the frequency ν, and x is the optical path length. We define f as the number of classical harmonic oscillators present in the atom, therefore, $k(\nu)$ for a resonance line has the form,

$$k(\nu) = N_\ell f \frac{e^2}{mc} \frac{\gamma/4\pi}{(\nu-\nu_o)^2+(\gamma/4\pi)^2} \tag{2}$$

In this equation N_e is the number of absorbing atoms per unit volume in the initial state and γ is the half-width of the transition. The total absorption coefficient is then,

$$k_o = \int_0^\infty k(\nu)\,d\nu = \pi N_e f\, e^2/mc \qquad (3)$$

This total absorption coefficient is independent of the half-width γ, and therefore, the method of damping does not affect the result. This is a vital fact in measurements because the instruments have imperfect resolution; so that, the line shape is lost. The total process is depicted in Figure 1, where it can be seen that the natural resonance shape with half-width is exponentially broadened by the Gaussian velocity distribution of the absorbers. The line is then folded by the spectrograph. That is, each infinitesimal part of the line is broadened by the spectrograph resolution. The last curve in figure 1 shows the line very much broadened by the scanning and filtering of the photoelectric sensor.

Because of the change in line shape one studies, instead of k_o, the equivalent width W, defined by,

$$W = \int_0^\infty \frac{I_o - I(\lambda)}{I_o}\,d\lambda$$

$$= \int_0^\infty \left\{1 - \exp\left[-\int_0^L k(\lambda,x)\,dx\right]\right\} d\lambda \qquad (4)$$

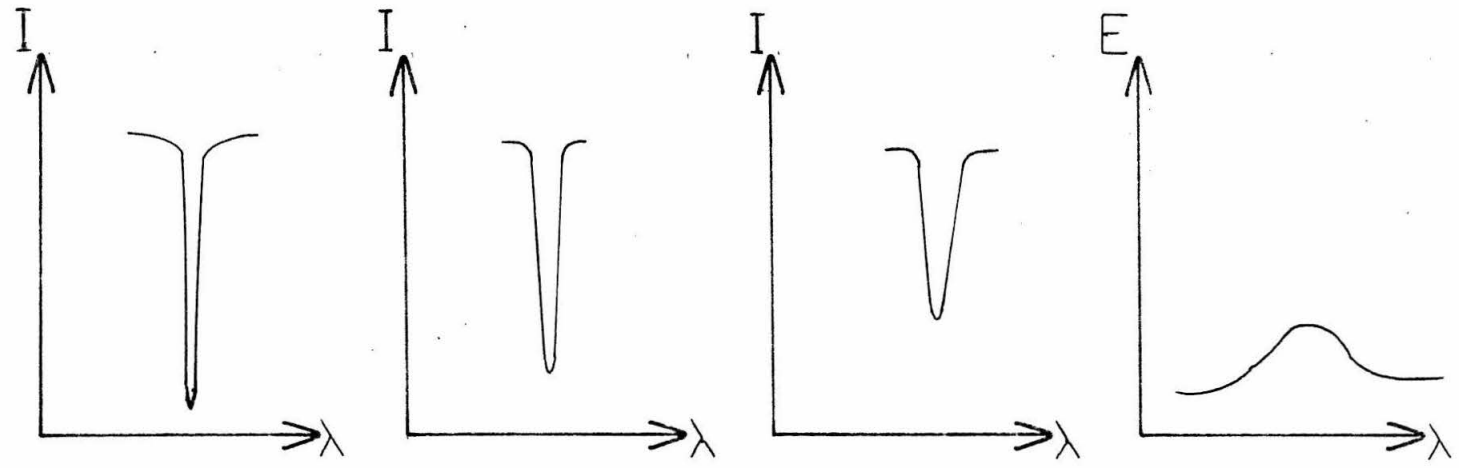

THE DEVELOPMENT OF THE BROADENED SPECTRAL LINE

FIGURE 1

This is the equation relating k(ν) or K(λ) to the equivalent width. It should be remarked that the atoms in the upper state can spontaneously emit and return to the lower state. Einstein showed that thermodynamic equilibrium requires that,

$$\frac{\text{Tran Prob}(u \to \ell)}{\text{Tran Prob}(\ell \to u\,;\, I_\nu)} \qquad \frac{2h\nu^3}{c^2}\,\frac{g_\ell}{g_u}$$

so that, equation 3 becomes

$$k_o = \frac{\pi e^2}{mc} N_\ell f \left(1 - \frac{g_\ell N_u}{g_u N_\ell}\right) \tag{5}$$

Here, the statistical weights g are given by

$$g = 2j + 1$$

where, j is the total angular momentum. Therefore, the curve of growth is given by,

$$W = \int_0^\infty \left\{1 - \exp\left[-\frac{e^2 f}{mc} \int_0^L N_\ell(x) \frac{\gamma(x)/4\pi \, dx}{\left(\frac{\gamma(x)}{4\pi}\right)^2 + (\lambda - \lambda_o)^2}\right]\right\} d\lambda \tag{6}$$

Experimentally it is possible to keep the temperature quite uniform over the small length of the vapor column, so that the x integration is trivial for pure resonance broadening. However, if we assume that the Doppler effect due to the temperature distribution of velocities is

gausian, then each small increment of the line between $\lambda+\Delta\lambda$ and $\lambda-\Delta\lambda$ is broadened by the Doppler effect. Then, the exponent in equation 6 becomes,

$$-\sqrt{\pi}\, r_0 \lambda_0^2 f \int_0^L \frac{a N_\ell}{\sqrt{\pi}\,\Delta\lambda_D} \int_{-\infty}^{\infty} \frac{e^{-t^2} dt}{a^2+\left(\frac{\lambda}{\Delta\lambda_D}-t\right)^2} dx$$

Thus, the curve of growth is (assuming that conditions are uniform along the path),

$$\frac{W}{\Delta\lambda_D} = \int_{-\infty}^{\infty} dw \left\{1-\exp\left[-\frac{Ca}{\sqrt{\pi}} \int_{-\infty}^{\infty} \frac{e^{-t^2} dt}{a^2+(w-t)^2}\right]\right\} \qquad (7)$$

where,

$$a = \frac{\Delta\lambda_R}{\Delta\lambda_D} \qquad (8)$$

and the density function C is,

$$C = \frac{\sqrt{\pi}\, r_0 \lambda_0^2 N L f}{\Delta\lambda_D} \left[1-\frac{g_\ell}{g_u} e^{-\frac{(E_u-E_\ell)}{kT}}\right] \qquad (9)$$

The factor N is the density of atoms in the lower state, L is the total optical path length in the gas, $\Delta\lambda_D$ is the half width of the Doppler broadening gaussian, the exponential in the temperature T is the Boltzmann Factor for the relative occupation of the upper state, and r_0 is the classical electron radius equal to e^2/mc. The Doppler half-width is

$$\Delta\lambda_D = \frac{\lambda_0}{c}\left(\frac{2RT}{M}\right)^{1/2}$$

and the resonance broadening is a combination of the natural width and collision or pressure broadening. Thus,

$$a = \frac{\Delta\lambda_R}{\Delta\lambda_D} = \frac{4\pi n_o f}{\Delta\lambda_D}\frac{g_\ell}{g_u} + \frac{\Delta\lambda_P}{\Delta\lambda_D}$$

It is apparent that the parameter a <u>is not constant</u>. It varies at $T^{-\frac{1}{2}}$ and since the pressure broadening (Unsold,[25] Lindholm[26]) is proportional to $N f \lambda^2 \sigma_p$, at higher temperatures it becomes more strongly dependent on the temperature. The term σ_p is the collision crossection.

At the lower end of the temperature and pressure ranges used in this experiment, the pressure broadening is much less than the natural width so that

$$a \propto T^{-1/2}$$

Typically, the temperature range was two hundred degrees out of one thousand degrees, so that, "a" varies by about ten percent. It will be shown that the curve of growth is a slowly varying function of "a" for values of C less than one hundred. Therefore, it is a good approximation to take "a" equals a constant;

$$a \cong \frac{4\pi n_o f}{\Delta\lambda_D(ave)} \cdot \frac{g_\ell}{g_u}$$

One crude method of approximating the f-value would be to determine the value of the parameter "a". At higher temperatures the dependence of the pressure broadening on the

density predominates, so that "a" is not a constant.

C. The Experiment - In this research, the curve of growth is determined entirely from experimental data, yielding the values of Nf as a function of the temperature. The value of f is chosen to yield the best fit to the vapor pressure data over several orders of magnitude. For the most part, the latest vapor pressure data of the University of California Metallurgy Group[27] was used. In a few cases this useage was qualified and compared to other data given by Stulle and Sinke[28] and by Kelley[29].

The curve of growth was then, afterwards, fitted with the best theoretical curve using the value of "a" calculated with the resulting f-value, and utilizing the known hyperfine and isotope splitting (as given in Landholt and Bornstein[30]). This fit verifies the theory of the curve of growth, the detailed calculations for the non-linear portions of the curve, and furnishes an approximate cross-check on the f-value.

The data for Cd, Tl, Ag, and Pb were taken over a large enough temperature range to detect the change in "a" at higher pressures, thus, the pressure coefficient σ_p can be found as a by-product of this experiment.

There has been considerable discussion of the effects of Zeemann splitting due to the magnetic fields present in the electric furnace. This effect was sought experimentally but was not measureable in this experiment.

II. THE EQUATION FOR THE CURVE OF GROWTH

A. Analytical Considerations - In this section equation 7 will be examined from an analytical standpoint. The equation relates $W/\Delta\lambda_D$ and the density factor C, with "a" as a parameter. That is,

$$W/\Delta\lambda_D = W/\Delta\lambda_D\,(C;a)$$

$$= W/\Delta\lambda_D\left(\frac{NLf}{\Delta\lambda_D};\ \frac{bf+cNf}{\Delta\lambda_D}\right) \qquad (13)$$

The density N appears in two different contexts. The first, and most obvious, is through the variable C and the second is in the parameter "a". Also, the f-value appears in each of the variables. The temperature dependence is very complicated since N is a strong function of T and $\Delta\lambda_D$ is a slowly varying function of T. We assume that for the lower part of the temperature range

$$b >> cN$$

so that,

$$a \sim b' f T_{(ave)}^{-1/2}$$

and we temporarily ignore the cfN term. We also take the average temperature. Then $W/\Delta\lambda_D$ becomes a function of the single variable C. In this approximation, the density N occurs only in the form $NLT^{-\frac{1}{2}}$. The results of this research verify the validity of these assumptions.

If two different temperatures are chosen and, simultaneously, two different optical path lengths are used, such that,

$$N_1 L_1 T_1^{-1/2} = N_2 L_2 T_2^{-1/2} \tag{14}$$

then, to this approximation,

$$W_1/\Delta\lambda_{D1} = W_2/\Delta\lambda_{D2} \tag{15}$$

Conversely, if equation (15) is valid,

$$\frac{N_2}{N_1} = \frac{L_1 T_2^{1/2}}{L_2 T_1^{1/2}}$$

This is strictly true only if,

$$a(T_1) = a(T_2)$$

but, it turns out to be a very good approximation for most of the experimental conditions utilized. This assumption leads to a family of curves of the form of equation 13 for various values of "a". The slow change in this parameter will then be accounted for by the gradual crossing of an actual curve of growth from one member of the family to another.

B. <u>Method of Calculation</u> - In most treatments the assumption "a" equals zero is used because the limiting solution (Unsold[25]) may be expressed in the form

$$W/\Delta\lambda_D = \int d\omega \left\{ 1 - \exp - C e^{-\omega^2} \right\}$$
$$= \sqrt{\pi}\, C \left(1 - \frac{C}{2!\sqrt{2}} + \frac{C^2}{3!\sqrt{3}} - \cdots \right) \tag{16}$$

This resulting solution has the wrong asymptotic form for large values of σ and is far from correct for any case in which σ is greater than unity. In fact, "a" is proportional to the f-value. In the case of Zn, for example,

$$a \geq 10^{-4}$$

Zn has the lowest value of "a" among the elements studied in this work. For Pb on the other hand, the value at the low temperature limit is,

$$a \sim 10^{-2}$$

and, of course, when T becomes very large, pressure broadening increases this value.

The next most sophisticated treatment (Mitchel[31]) is to form a power series expansion about $a = 0$. This requires the calculation of the derivatives with respect to "a". That is

$$\frac{W}{\Delta\lambda_D} = \frac{W}{\Delta\lambda_D}(a=0) + a\left(\frac{\partial}{\partial a}\frac{W}{\Delta\lambda_D}\right)_{a=0}$$

The first partial derivative has been calculated by Mitchel and is discussed in Appendix A. The result may be expressed in the form

$$\frac{\partial}{\partial a} k(\nu) = -\frac{2C}{\sqrt{\pi}}\left[1 - 2\omega e^{-\omega^2}\int_0^{\omega} e^{y^2} dy\right] \qquad (17)$$

This term goes to zero very strongly as $\omega \to \infty$. In fact at $\omega = 6$ the term

$$1 - 2\omega F(\omega) \sim 10^{-2}$$

where,

$$F(\omega) = e^{-\omega^2}\int_0^{\omega} e^{y^2} dy$$

Succeeding terms become more difficult to calculate and every odd term contains a derivative of $F(\omega)$. Therefore, a thorough computation was necessary and the computations done are discussed in Appendix B. In Appendix C tables of $W/\Delta\lambda_D$ vs. C have been presented for

$$a = 2^m \times 10^{-4} \qquad m = 1, 2, \cdots 10$$

The method consists of integrating

$$\int \frac{a\, e^{-t^2}}{a^2 + (\omega - t)^2}\, dt$$

for each value of ω and then computing the integral over ω. Since the integrands approach zero as ω get large, it is possible to cut off each of the infinite integrals without appreciable error.

These tables were necessary in order to fit any theory to the data. Furthermore, the hyperfine splitting needs to be accounted for. The value of N is actually given by,

$$N = \sum_{f=1}^{2F+1} N_f$$

where there are $2F + 1$ degenerate states due to the nuclear magnetic moment. Furthermore, there may be several isotopes, so that

$$N_f = \sum_k N_{fk}$$

where the summation is taken over the k isotopes. Now in some cases the hyperfine splitting is appreciable; i.e.,

$$\Delta\lambda_{H.F.} > \Delta\lambda_D$$

Then, the different components each has its own curve of growth and

$$\frac{W}{\Delta\lambda_D} = \sum_k \frac{W}{\Delta\lambda_D}\left(N_k ; a\right) \tag{18}$$

It is assumed that the small hyperfine splitting

$$\Delta\lambda_{H.F.} \sim 10^{-5}\lambda$$

does not affect the f-value. Thus, each of the components has the same values of "a" and f. Furthermore, the Boltzmann Factors are assumed to be unity and the relative strength of the different components is known, i.e.,

$$f N_b = B_b f N$$

It is also an assumption that the isotopic composition is known, so that

$$N_k = b_k N \quad .$$

with the b_k's as the known concentration of the k^{th} isotope. Then,

$$\frac{W}{\Delta\lambda_D} = \sum_{k,f} \frac{W}{\Delta\lambda_D}\left(b_k B_f C ; a\right) \tag{19}$$

In many cases where $\Delta\lambda_{HF}$ is larger than $\Delta\lambda_D$, the spectrograph fails to resolve the lines. In some cases, such as Tl, the scanning system smears the nearby lines together, even though the spectrograph resolves them. In these cases the composite curve of growth (equation 19) must be used. In those cases where

$$\Delta\lambda_{H.F.} < \Delta\lambda_D$$

F is no longer a good quantum number and the transition must be treated as a single component. The intermediate cases

$$\Delta\lambda_{H.F.} \sim \Delta\lambda_D$$

cause the curve of growth to lie between two theoretical curves. Thus, if one imagines that the nuclear magnetic moment is turned on gradually, the curve of growth moves from the single component equation 13 to the composite form of equation 19.

It should be remarked that certain authors have attempted to split the equivalent width W into isotopic parts, and then compute the inverse function

$$C = C(W/\Delta\lambda_D) = \sum C\left(b_k \frac{W}{\Delta\lambda_D}; a\right)$$

But it is clear that the density function is the one for which the division into components is known. On the linear portion of the curve of growth the difference is negligible, but, on the non-linear portions of the curve of growth this technique causes a large error. This fact is illustrated in paragraph D of this section and in figure 4.

III. CONSTRUCTION OF THE CURVE OF GROWTH

A. The Variable Path Length - The quartz cells used to hold the vapor have three or four different optical path lengths. At a given temperature the equivalent width is measured for each path length. (L_i, I=1,2,3,4). The range of L was as large as possible, so that,

$$\frac{L_4}{L_1} \sim 60$$

Thus, the variable C is changed over the same range at each temperature. The data consists of four equivalent widths per temperature point, i.e., one has

$$W = W_{ij}(T_j, L_i, N(T_j))$$

for various temperatures Tj. The ratios of the Ci are known precisely, that is,

$$\frac{C_{i+1}}{C_i} = \frac{L_{i+1}}{L_i}$$

The points are then plotted on a log-log scale as shown in Figure 2 for several temperatures. The main point is that the ranges of $W/\Delta\lambda_D$ for the adjacent temperatures overlap strongly. Thus, for some value of L(Tj)

$$L_1 < L(T_j) < L_4$$

$$\frac{N(T_j)L(T_j)}{\Delta\lambda_j} = \frac{N(T_{j+1})L(T_{j+1})}{\Delta\lambda_{j+1}} \qquad (20)$$

which clearly means that,

$$C_j(L(T_j)) = C_{j+1}(L(T_{j+1})) \qquad (21)$$

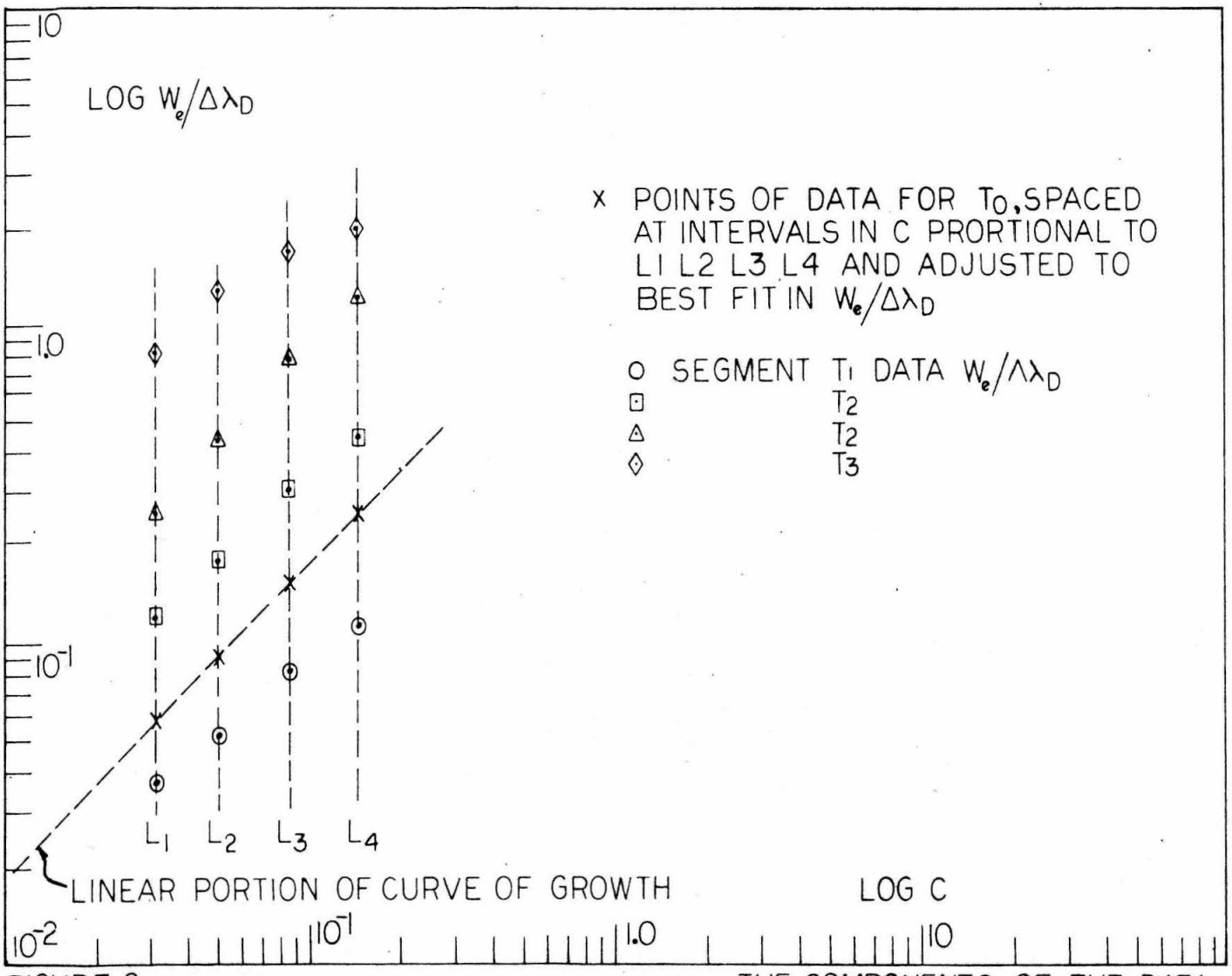

FIGURE 2 THE COMPONENTS OF THE DATA

B. Construction of the Curve - The curve of growth is now constructed from the data shown in Figure 2 by using the result of equation 21. The four data points, at an appropriate temperature, (with small values of $W/\Delta\lambda_D$) are put on the known "linear" portion of the curve of growth picked from the tables in Appendix C. The value of "a" is taken from the closest guess of the f-value. The other segments of the data are moved laterally to give the best least squares overlap. This technique is illustrated in Figure 3. The method is not very sensitive to the guess of the value of "a" since the variation between the family of the curves of growth in the linear portion is very slight.

C. Calculation of the Parameter "a" - In the manner depicted in Figure 3, the first approximation to the curve of growth is made. The final step is to account for the change in the parameter "a" on the extreme upper part of the curve. A small adjustment is made for the change in "a" due to the small change in $\Delta\lambda_D$. Equation 17 for the partial derivative of k(v) is approximated, and thus the change in $W/\Delta\lambda_D$ for a change in "a" is made. This amounts to fitting the upper portions of the curve on the high side of the best overlap.

After constructing the curve and drawing the "best fit" smooth curve through the data the values of C for each are read off and compared to the vapor pressure data. In other words Pf is calculated for each temperature, and then the value of P is used to yield a datum point for the

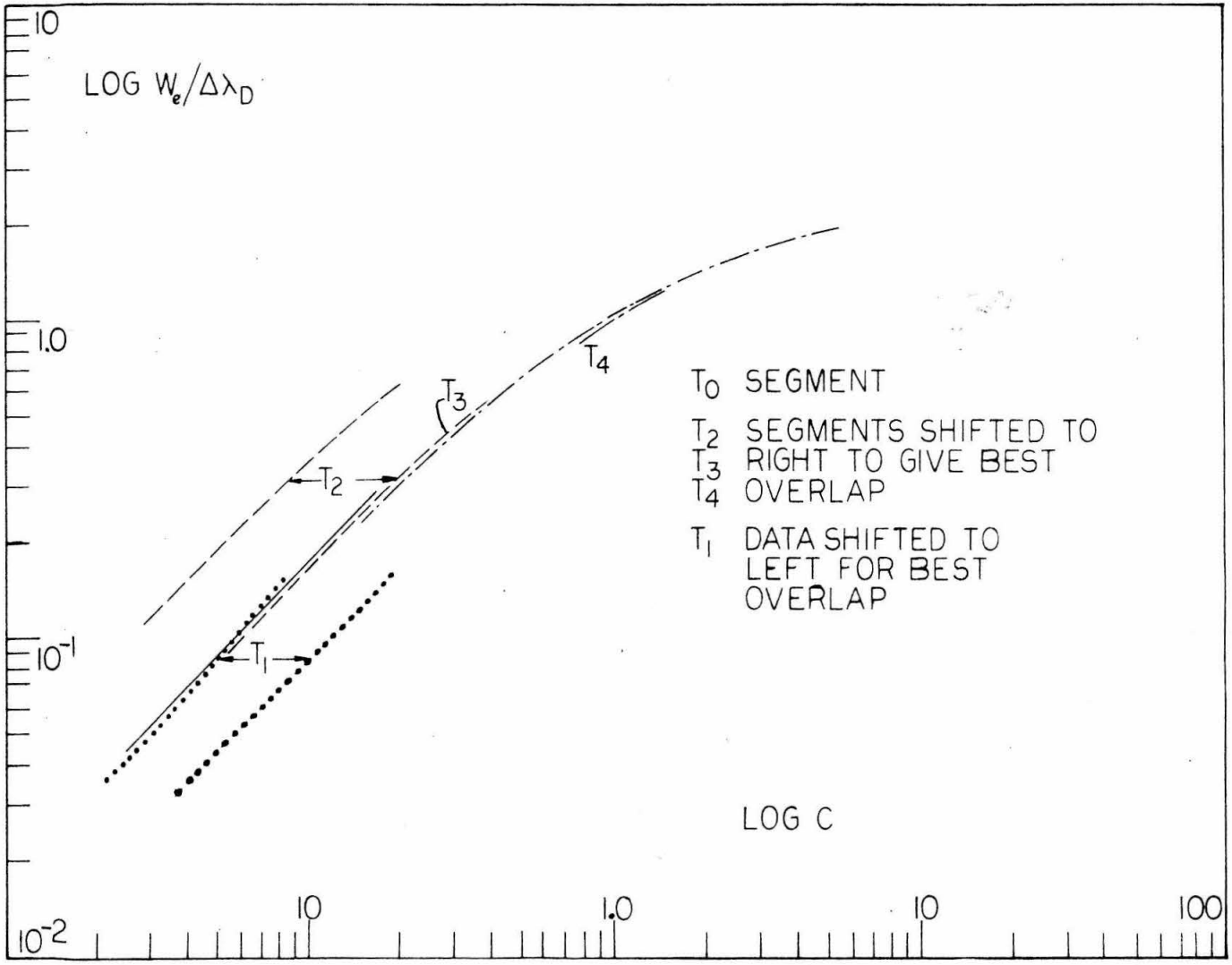

FIGURE 3 CONSTRUCTION OF CURVE OF GROWTH

f-value determination.

D. Fitting the Theory - A typical example of a curve of growth is shown in Figure 4. In this Figure the outline of the final curve for Pb, $\lambda = 2833$ Å is shown as a solid line. The f-value is such that "a" is close to 0.0128. The theoretical curves for a single component transition with $a = 0.0001$ and $a = 0.0128$ are shown also, and obviously neither fits the data. In order to illustrate the difference between splitting $W/\Delta\lambda_D$ and splitting C into components (discussed at the end of Section II) the composite curves for the four known isotopic components split in each manner are shown. The curve with the C split (as it properly should be) fits the data well for

$$10^{-1} < C < 10^{3}$$

The composite curve for $a = 0.0256$ is also shown, and it is clear that as C varies from 5×10^2 to 5×10^5 the curve of growth moves over to the value for $a = 0.0256$. Therefore, if T_1 was the temperature for which $C = 5 \times 10^2$ then

$$\Delta\lambda_N + \sigma_p \lambda^2 N(T_1) f = \frac{1}{2}\left[\Delta\lambda_N + 10^3 \sigma_p \lambda^2 N(T_1) f\right]$$

or,

$$\sigma_p = \frac{\Delta\lambda_N}{10^3 \lambda^2 f N(T_1)}$$

For Pb, $T_1 = 9400°$C and Nf was 7×10^{12}. The value of is 3.3×10^{-12} cm. yielding

$$\sigma_p = 0.6 \times 10^{-18}\ \text{cm}^2$$

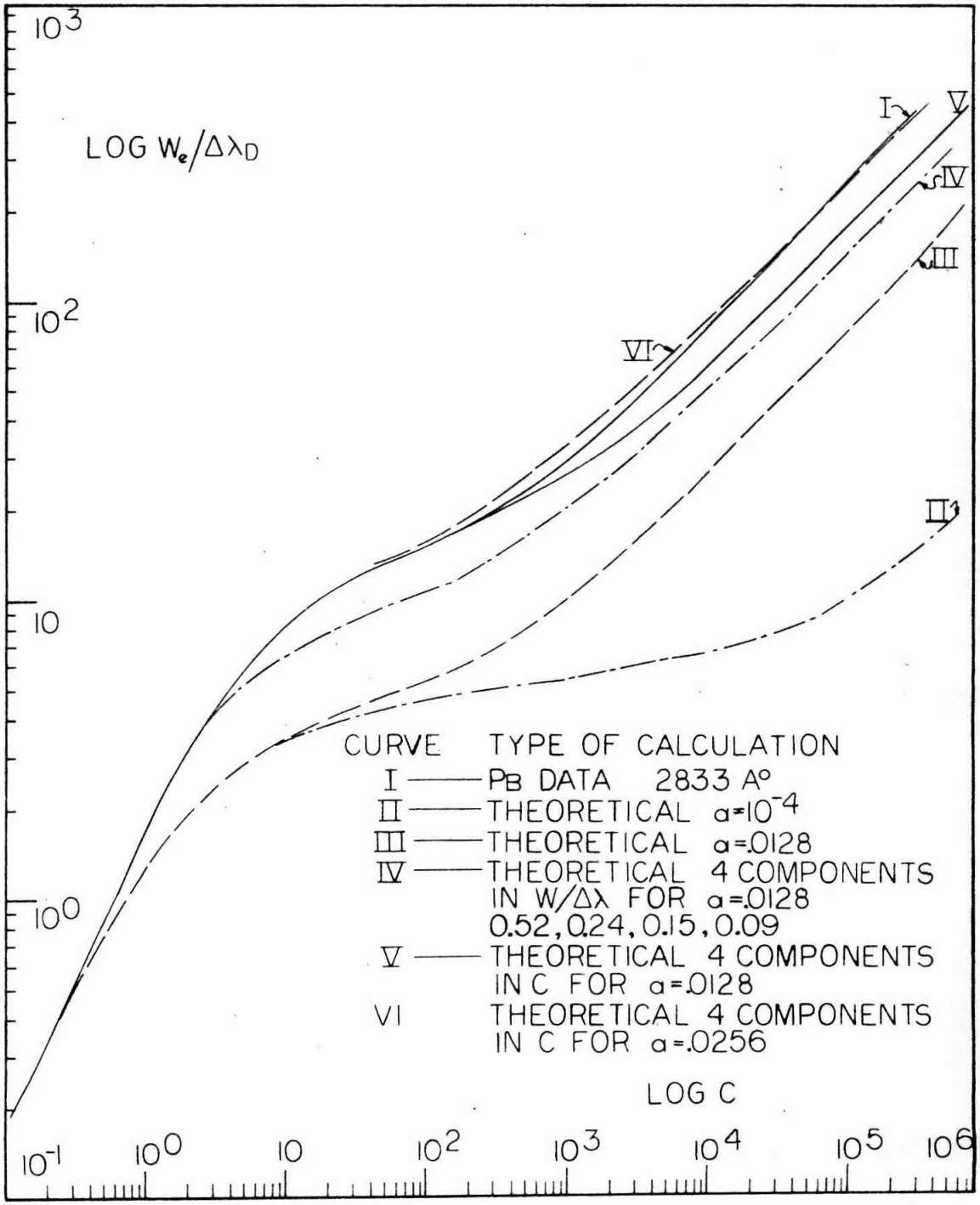

FIGURE 4 COMPARISON OF PB DATA TO THEORETICAL CURVES

This is the collision cross section for pressure broadening. there is no other experimental source of this number (known to the author) for comparison purposes.

IV. DESCRIPTION OF THE APPARATUS

A. The Optical System - A schematic diagram of the experiment is shown in Figure 5. A mercury capillary tube lamp was focused through a filter so that its image was in the step cell. The lenses used were acromats of 30 cm and 60 cm focal lengths. The long focal length guaranteed that all of the light passed through the same optical length since the lens aperture provided an angular opening of about three degrees. The second lens focused the image on the spectrograph slit which was set at thirty microns.

Two methods of detection were used. The first was by photographic emulsions which were exposed for ten minutes or so, depending on the wave length used. A calibrated neutral step filter furnished by the Hilger Company was used to make calibration plates. This method was used on one Pb run and checked against the second method. This second method used a photo cell technique developed for the most part by Mr. George Lawrence. Having compared the two methods, the photo tube seemed far superior and was used for most of the remaining data.

The step-cell was placed in the electric furnace and the entire furnace mounted on a mill-head traverse. The entire furnace assembly was moved laterally without disturbing the focused beam, in order to change the optical path length.

The temperatures were measured with Pt, Pt-10% Rh thermocouples calibrated at the National Bureau of Standards. The coils of the electric furnace were individually controlled

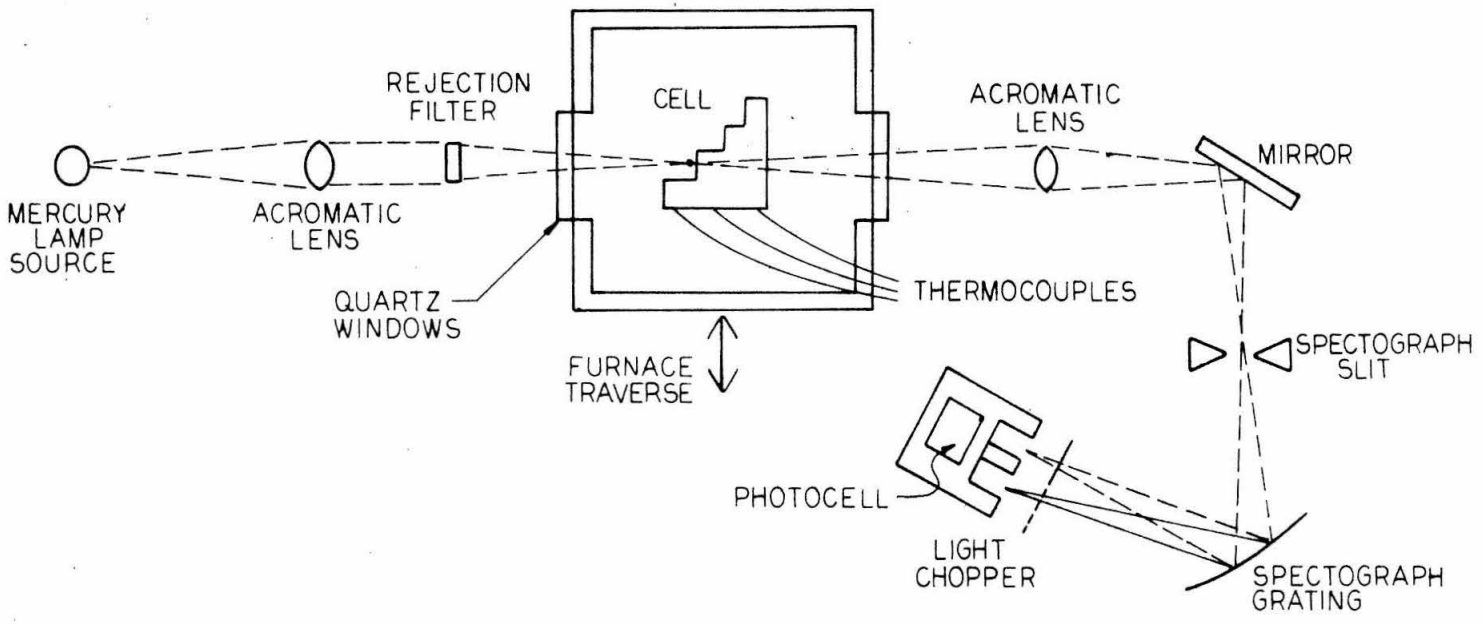

FIGURE 5 SCHEMATIC DIAGRAM OF OPTICAL APPARATUS

to obtain the best temperature uniformity over the cell length.

The entire system was easily aligned many times throughout the runs and was found to be more than adequate for this experiment.

B. Light Sources, Filters, and Lenses - For the most of the lines studied, a high pressure, capillary tube, mercury arc source was used. The lamp was supplied with about 1 ampere at 1000 volts DC from a regulated motor generator set. The lamp had a quartz water jacket supplied with tap water for cooling. Periodically, the water jacket was flushed out with dilute HCl. This dissolved the salt deposits which accumulated allowing maximum output intensity. The lamps were furnished by the P.E.K. Laboratories, of Palo Alto, California. The pressure broadened mercury lines furnished an excellent source, except for the λ4032 line of Galluim and the λ 2676 line of Gold. The slope of the continium caused an error in determining Io of less than 2% of the equivalent width.

In a few instances a Xenon arc source was used. This furnished a much smoother continuum but much less intensity. The lamp operated on 220 Volts AC except for starting. The arc itself is a point source so that the spectrograph slit could not be filled. The lamp was manufactured by Osram Kommanditgellshaft in Germany.

The filters used were Corning Glass Co. #7-59, #7-54, and #5-57. These filters transmitted in the regions 2600 - 3800 Å, 3300-4100 Å, and 3600-4600Å, respectively. The trans-

mission in these bands was greater than 70 per cent and the rejection outside of the bands was very efficient.

One very important point was the placement of the filters ahead of the absorbing gas. Whenever the upper state has transition probabilities to other still higher states, the effective width of the upper state is modified according to the strength of these higher transitions. By putting the filters ahead of the gas no photons were available to induce these upper transitions. In all cases except Cd and Zn, the f-values of all available transitions were much smaller than those being measured. Therefore, no errors could be introduced due to secondary transitions. The lower f-values of Zn and Cd mean that the upper state is very well defined (by the uncertainty principle). With a broad band filter, the lines Cd λ2881 and Cd λ4799 were found. In the cases of Zn and Cd almost all available transitions were blocked out by the placement of the filter, so that light, of the correct frequency for stimulating these upper lines, was absent from the filtered source.

Both of the lenses used were Lithium-Floride acromats, ground by the optics laboratory of the Mount Wilson Observatory.

C. The Optical Cell - The step cells were handmade of optical quality fused quartz furnished by the Amerisil Company. The body of the cell was made out of 37mm diameter tubing and 1.5mm flat plate. After completing the body and attaching the graded seal for filling purposes, the optical windows

were fused on at 1750°C. The entire cell was washed with 5% HFl for 5 minutes to remove the silicon oxides formed. The washing did not adversely affect the optical transmission of the cells.

The cells were then cleaned three times with aqua regia and three times with triply distilled water to remove any residues. The cells were attached to the all-glass vacuum system, filled and flushed under a nitrogen pressure, and evacuated to less than 10^{-7}mm of Hg. After evacuation the cells were heated to 500°C to drive off the absorbed gases and sealed off.

Figure 6 is a photograph of a typical cell. The optical path lengths were 0.14, 0.49, 1.58, and 6.21cm. An attempt was made to have the lengths equally spaced on a logarithmic scale.

D. The Electric Furnace - The furnace consisted of an 18-inch long brass pipe of less than 12 inches inside diameter. The walls contained water jackets in which ordinary tap water flowed. The end plates were brass and also contained water jackets. They were sealed on the furnace with 12-inch "O-rings", and the quartz windows used 3-inch "O-rings". The furnace was evacuated through a mechanical pump to about 10^{-3}mm of Hg. The pressure was checked with a Phillips Gauge. Figure 7 is a photograph of the furnace and mount.

The heater coils were wound of #25 gauge molybdenum wire on an aluminum core, and then were covered with Saverelsea #1 alumdum cement. The main heater coil was capable of carrying

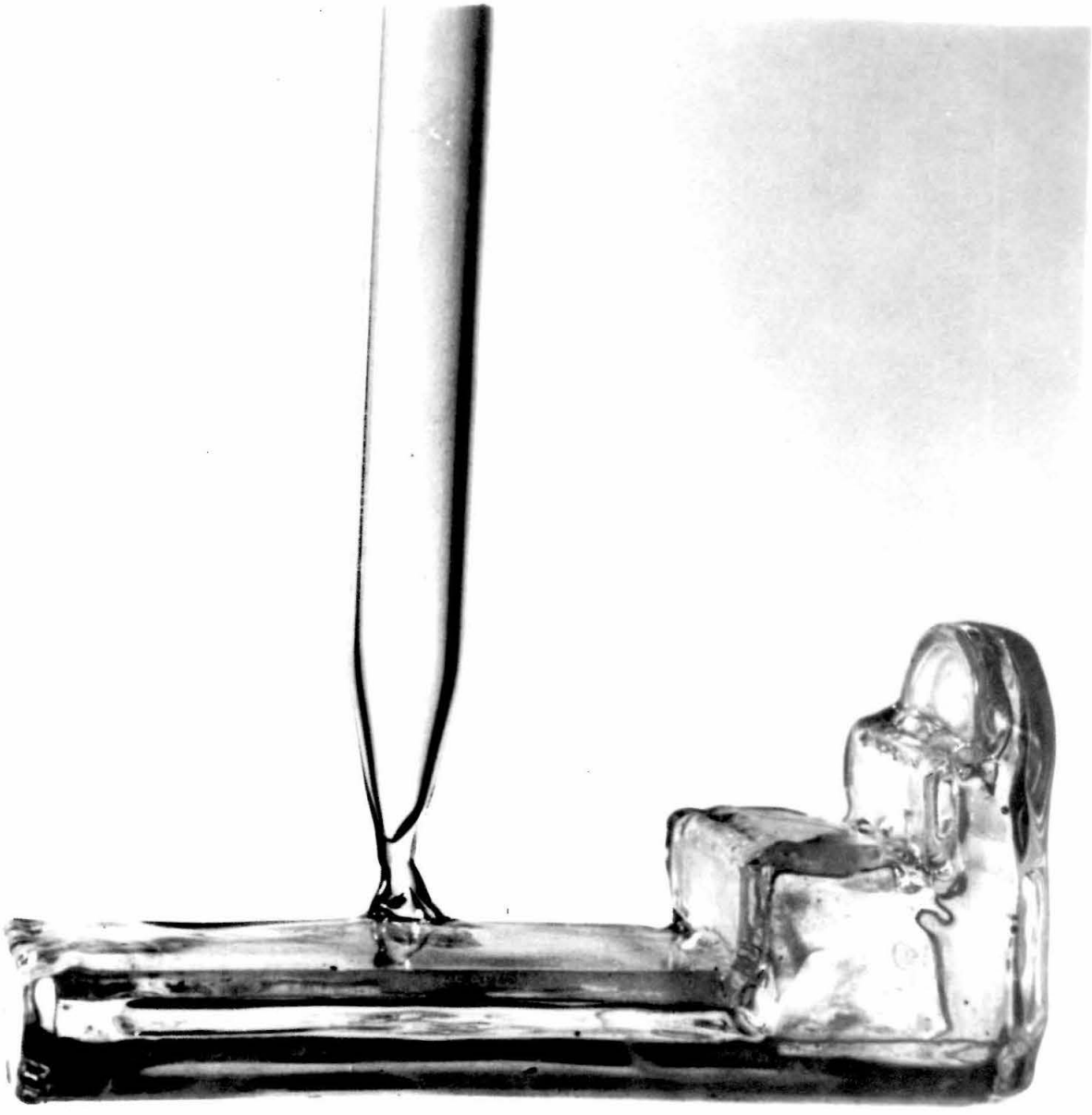

FIGURE 6. PHOTOGRAPH OF STEP-CELL

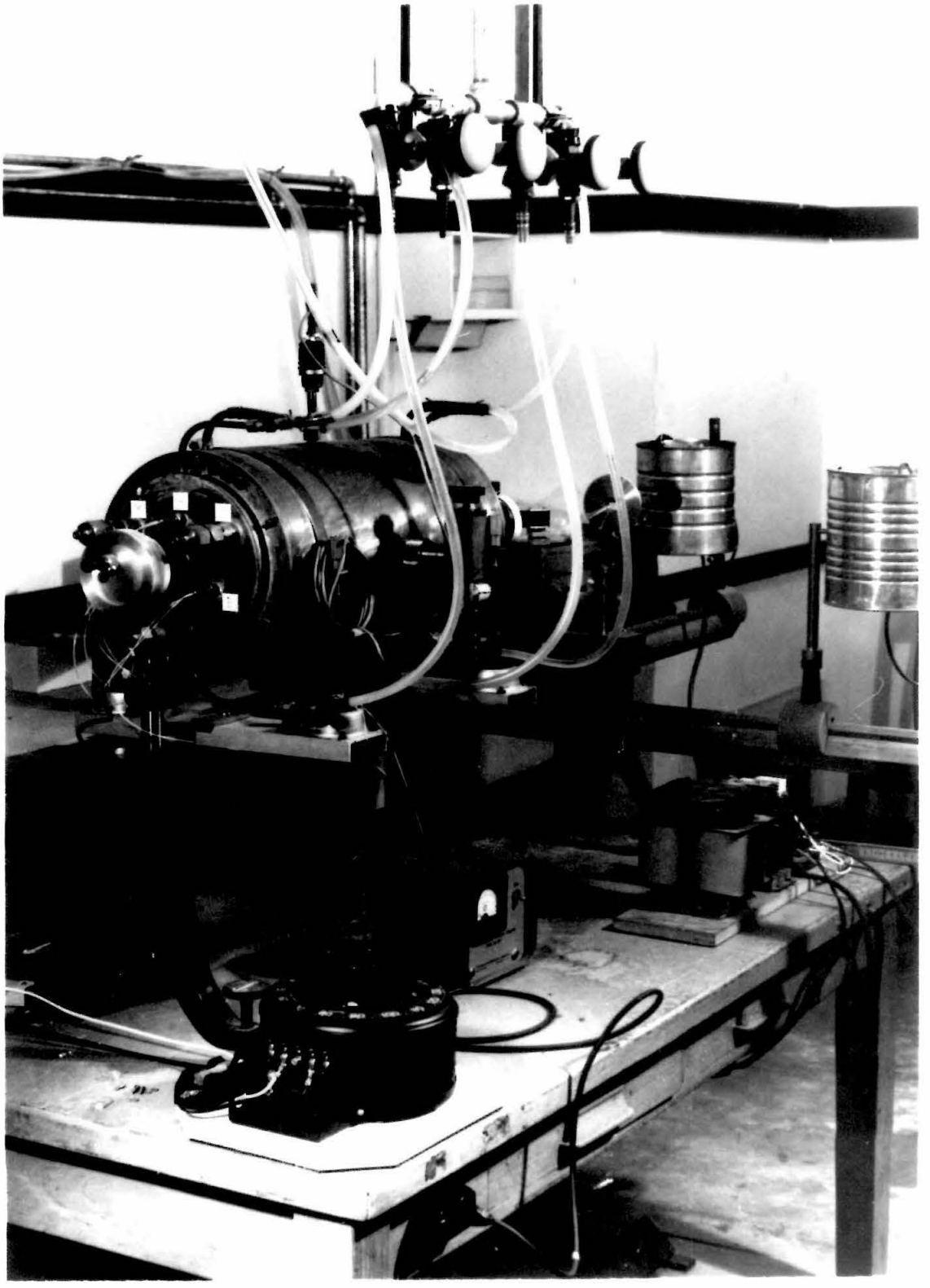

FIGURE 7. PHOTOGRAPH OF ELECTRIC FURNACE

6 amperes at 1300 watts and each of the trim coils could carry 5 amperes at 300 watts. The two trim coils were oppositely wound.

The cell was placed in a molybdenum baffle inside the aluminum core as shown in figure 8, and inserted into the furnace.

The temperature was measured with three thermocouples of Pt; Pt-10% Rh, furnished by Leeds and Northrup Company and calibrated by the National Bureau of Standards. The reference junction was in ice water at $0^{o}C$. The reference temperature was checked periodically. The accuracy of the thermocouples was much better than the ability to obtain uniform temperatures. The three thermocouple readings were kept within $\pm 0.5^{o}C$ for almost all readings. This was more than adequate for all of the elements except Cd. In the case of Cd, the density changes by several per cent per ^{o}C depending on the temperature. Special care had to be exercised in order to achieve reliable data. The E.M.F. was compared to a Weston Model 17199 Standard Cell using the Rubicon #52904 potentiometer and #3415 galvanometer.

Because of some suggestions concerning the Zeemann effect, a side experiment was done. In this experiment Ag was used and the temperature was about $1200^{o}K$. This was the maximum temperature obtainable with full capacity of the outer coils and with the center coil current down to 0.5 amperes. With this arrangement the temperature was sufficient to achieve very large values of $W/\Delta\lambda_{D}$. However, there was a

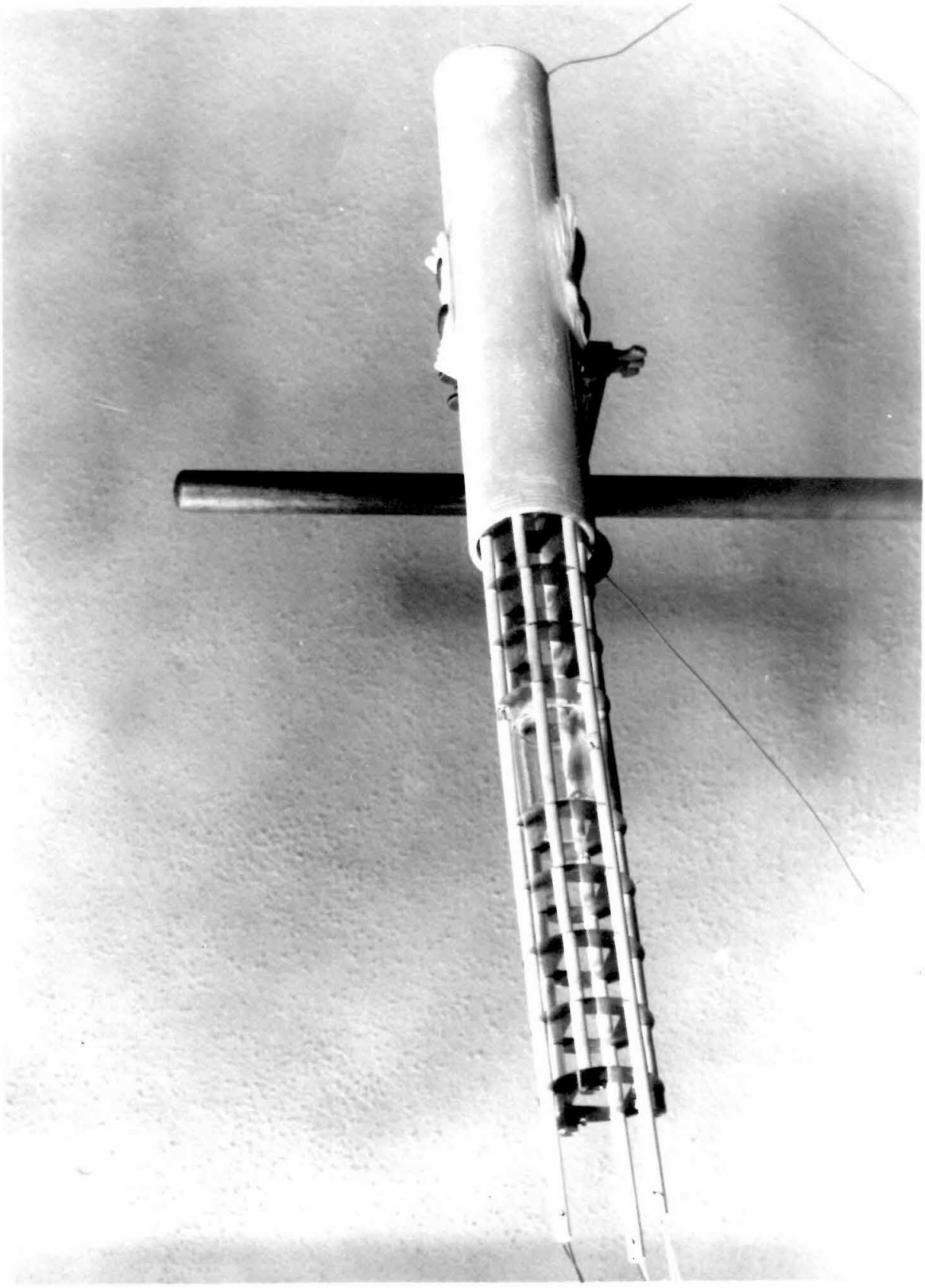

FIGURE 8. PHOTOGRAPH OF ALIGNMENT OF CELL

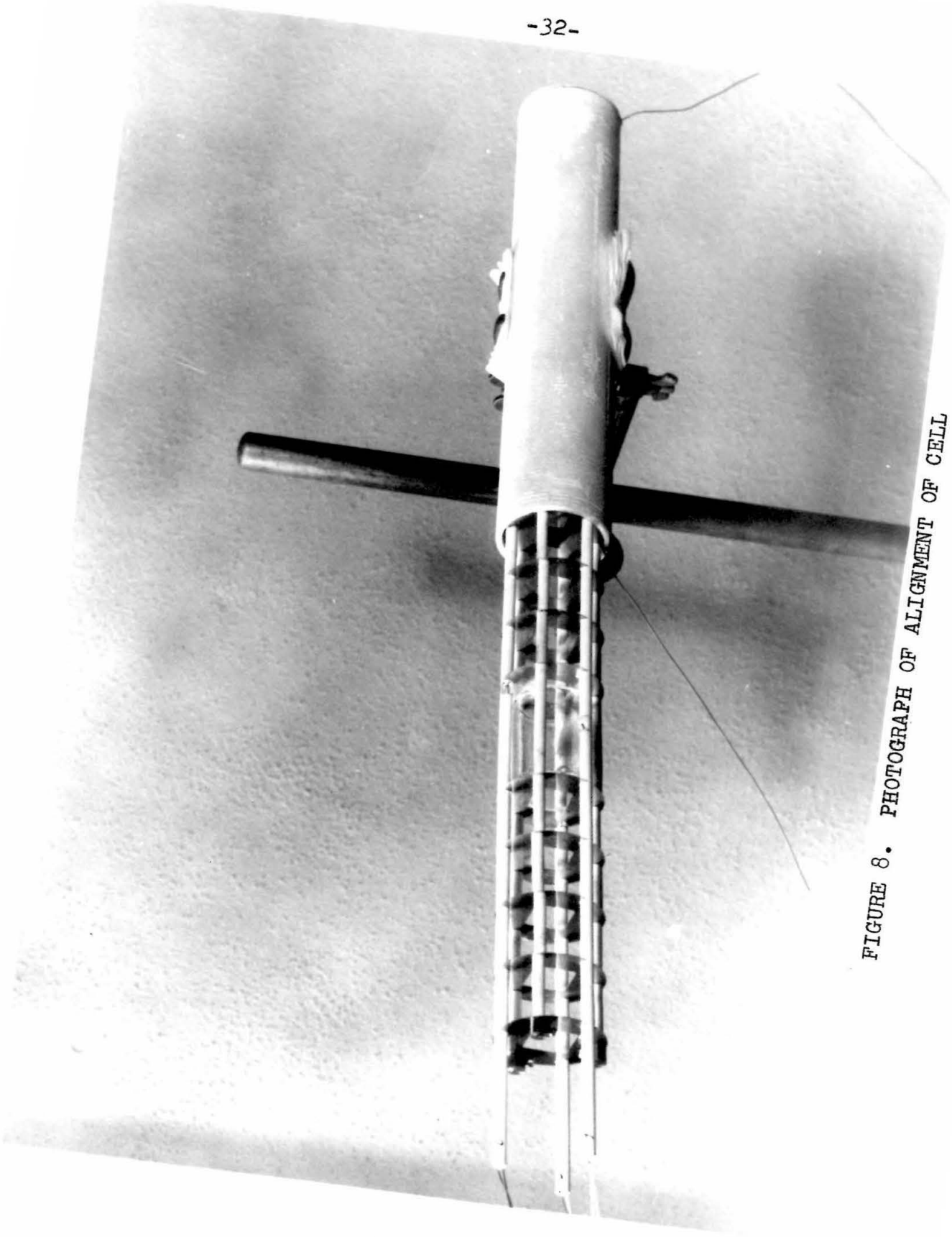

FIGURE 8. PHOTOGRAPH OF ALIGNMENT OF CELL

deterioration in temperature uniformity of $\pm 2^{\circ}$C. Four pieces of data for the four-step cell were taken. Then the outer coils were turned off and the same temperature achieved with about 3.5 amperes in the inner coil, and the data rerun. Despite the 7-fold increase in the magnetic field strength, the difference between the two sets of data was of the same order as the random scatter due to the scanning system. These data were not as consistent as usual because of the temperature non-uniformity. The experiment was repeated several times with negative results. It was therefore concluded that the Zeemann effect does not significantly affect the curve of growth.

E. The Photoelectric Scanner - There are two main advantages of this device over the photographic method. The first is its ability to measure much smaller lines and the second is that the data can be observed as they are taken. The difficulties have to do with the intensity variation of the lamp during the scanning period. This effect was greatly diminished by the use of a light chopper.

Figure 9 is a schematic diagram of the detector. Two slits are used, separated by about 2Å. The first is the measuring slit and the second a reference slit. The shutter alternately opens one of these and simultaneously throws the electrical switch at a repetition rate of 4cps. The two signals are fed into matched DC amplifiers and the 4cps chopper frequency is filtered out. The signals and the reference are subtracted and the difference recorded on a Brown Instrument

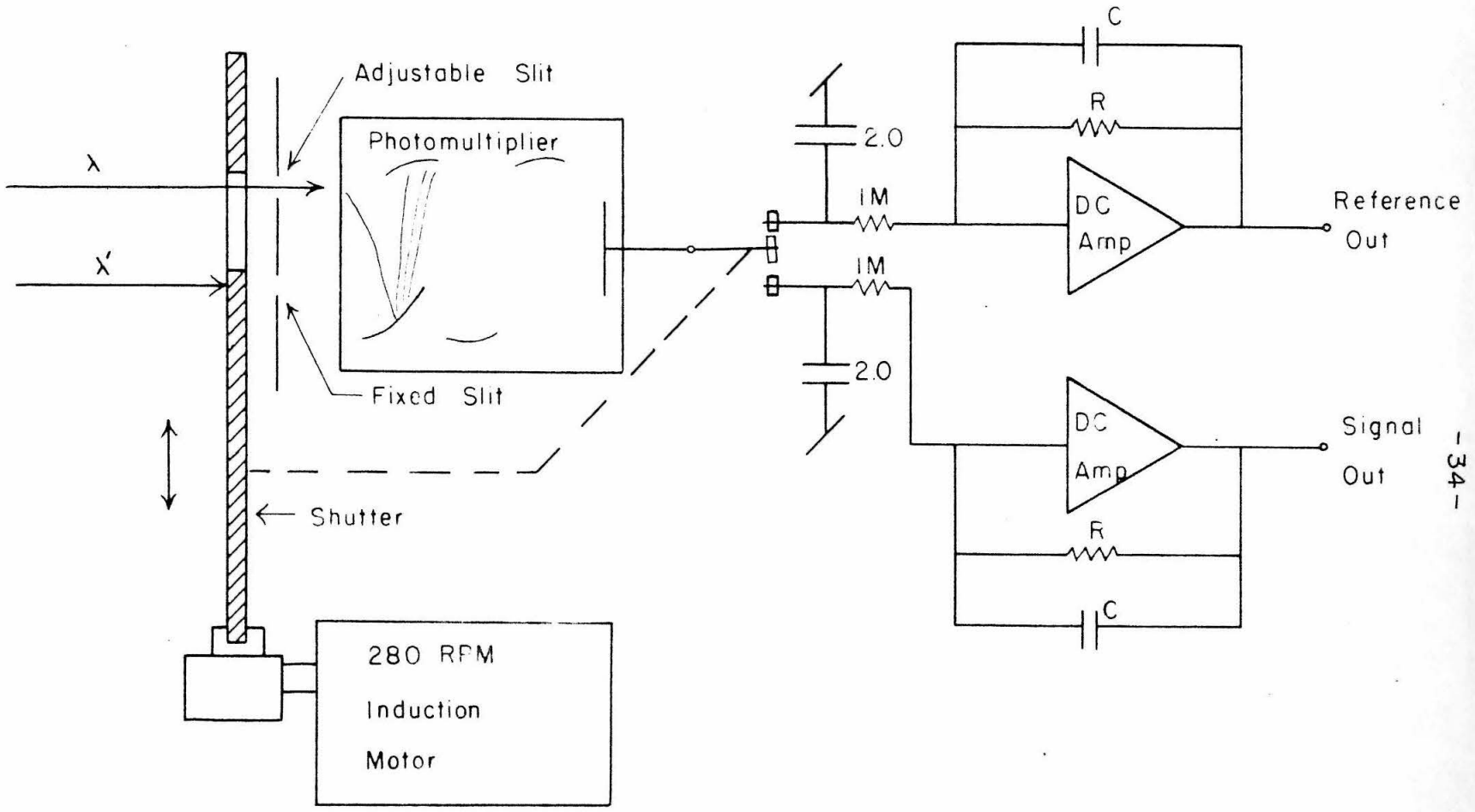

FIGURE 9 LIGHT CHOPPER, SYNCHRONIZER, AND DETECTOR

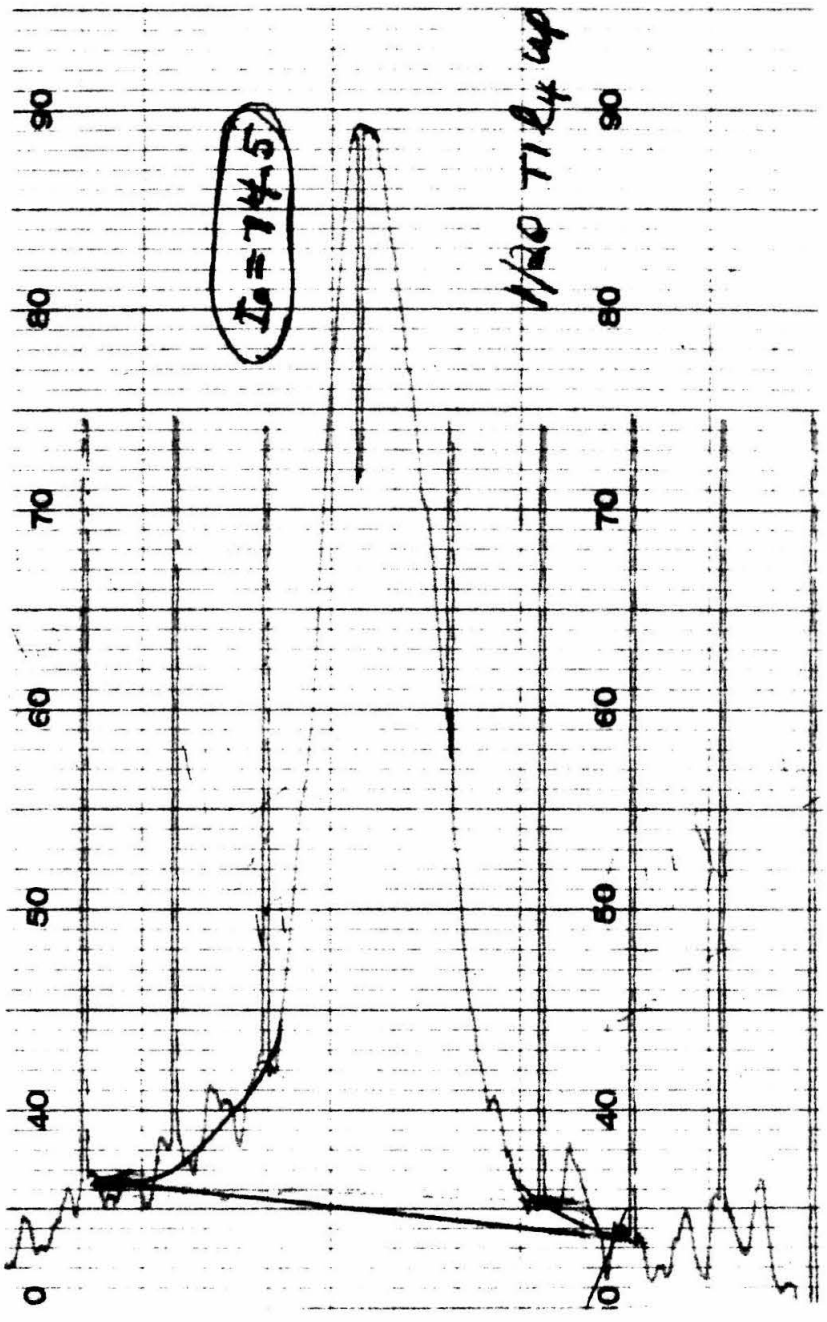

FIGURE 10 TYPICAL RECORDING OF DATA

Company pen recorder. At equally spaced intervals the trace was interrupted and the amplified signal interjected so that the data included both I_0-$I(\lambda)$ and $I(\lambda)$. Figure 10 is a sample recording which illustrates the noise in the base line and the general shape of the scanned line. This line had an equivalent width of 0.75mÅ, which would be difficult to accurately measure photographically. The photocell was a 9526B, Serial No. 5916, designed for spectrographic work by the E.M.I. Corporation of England. It has a fused quartz window.

The entire apparatus is driven laterally at a constant speed of 79.5mÅ/minute. Figure 11 is a photograph of the scanner and figure 12 shows the scanner mounted on the spectrograph.

The linearity of the device was checked against the Hilger neutral filter and agreed within ½%. The two main sources of random error are the base line noise which causes an error in determining the bottom of the line, and the random fluctuations of the light chopper repetition rate. These errors were estimated at 10% by repeating several lines twenty times and observing the scatter of the data. The main sources of systematic error are the variation in scanning speed and the accuracy of measuring the area under the line. These were estimated at 3% and 2%, respectively.

F. The Spectrograph - The spectrograph was the Institute's 21-foot Rowland Spectrograph. This instrument has been described by several investigators. The main problem which had to be studied was that of scattered light. G. D. Bell[32] in

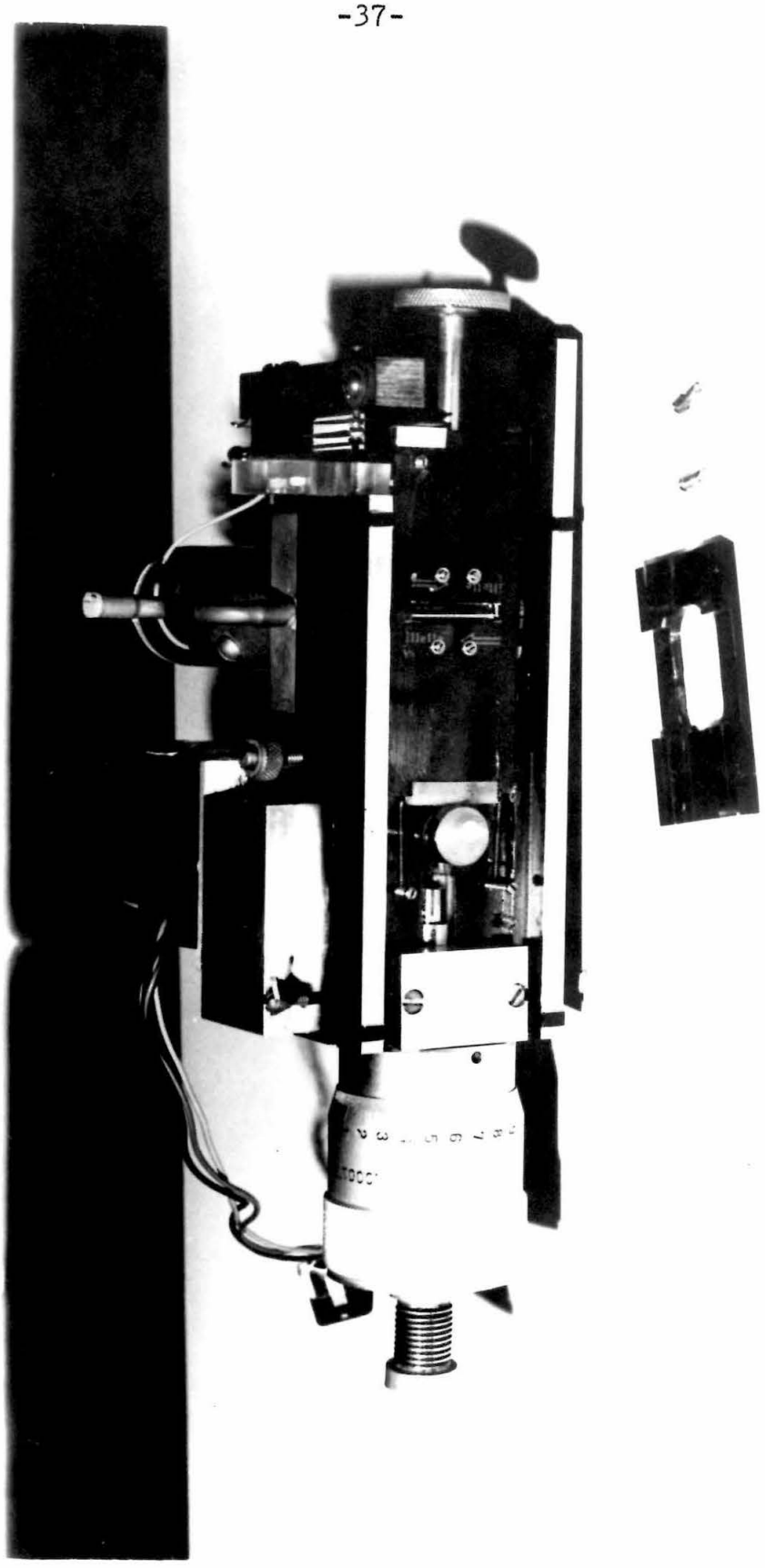

FIGURE 11. PHOTOGRAPH OF PHOTOELECTRIC SCANNER

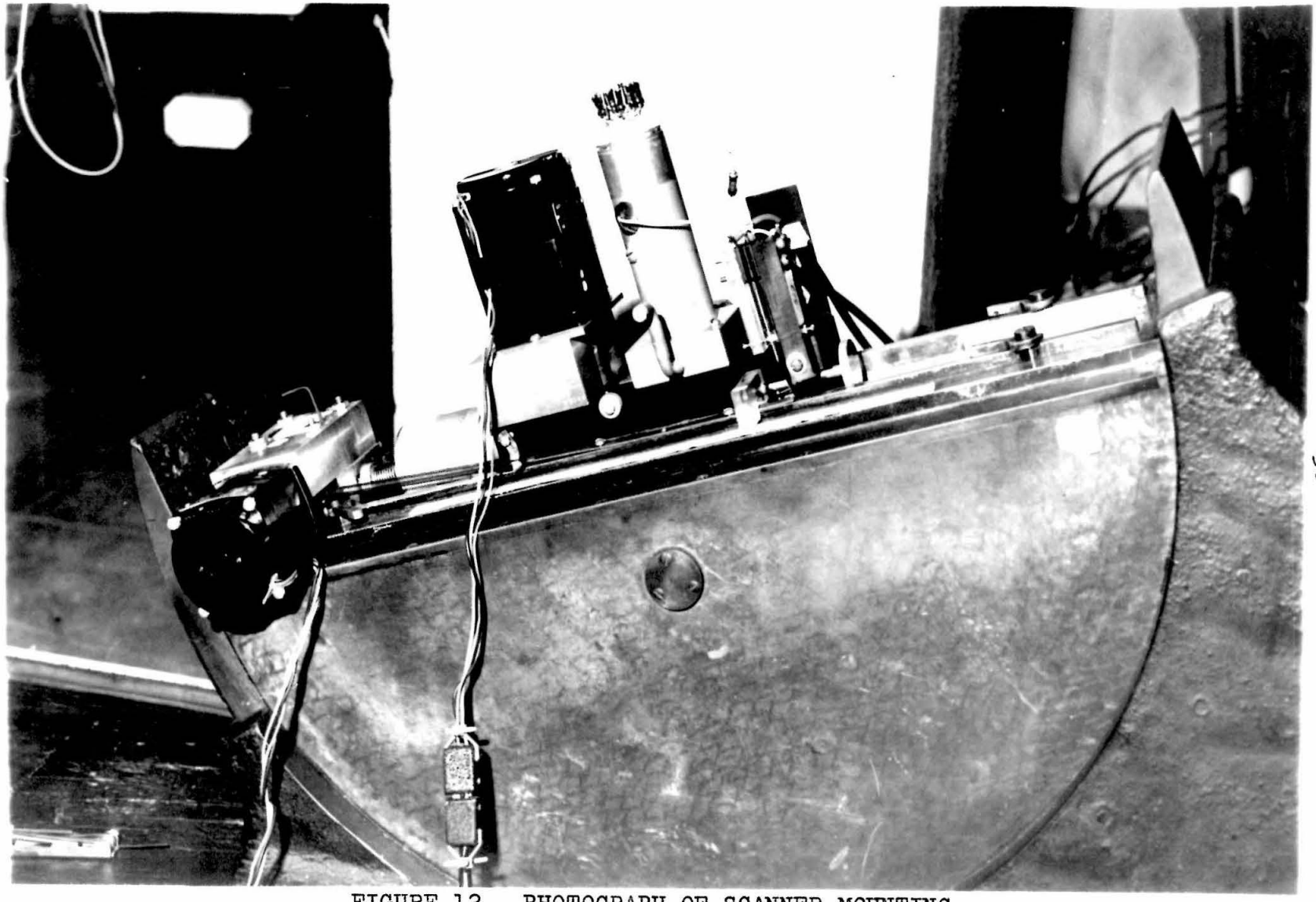

FIGURE 12. PHOTOGRAPH OF SCANNER MOUNTING

his PhD Thesis found the scattered light to be about 30% for the grating then in use, however, he was able to use a fore-prism to reject the optical light. In order to measure the scattered light, an exposure was made over a 500Å range and the intensities recorded at various values of λ. Assuming that the relative intensities of the source lamp do not change, a filter which cut off half of the range was inserted. The ratios between points in and out of the transmission band were re-measured. The transmission side of the exposure was reduced by 30% and the rejection side by 98%. Thus, the scattered light is less than 2%. With the photoelectric scanner, only the difference between the intensity of the signal, I( ), and that of the reference, I_0, is used for determining the line shape, so that only the denominator I_0 in the equivalent width should be affected. One line at λ=3775Å was scanned using a #7-54 filter which passes 2600-3800Å. The equivalent width was measured. Then a #5-57 filter was also inserted. This filter transmits between 3600Å and 4600Å, yielding a combined range of only 3600-3800Å. The observed equivalent width changed by less than the random error in the scanner; therefore, it was concluded that scattered light was not a problem with the filtered beam.

G. Summary of Experimental Errors - The errors which have been individually discussed are summarized in table 2.

TABLE 2

Source of Error	Random Error	Systematic Error
Continuum Slope	---	2%
Scattered Light	---	2%
Scanning	10%	3%
Area Measurement	2%	1%
Temperature	2%	---

The total R.M.S. random error was therefore less than about 10.5%. Enough readings were taken so that the effect of the random errors on the resulting f-value is much smaller than this value. The total systematic errors were less than 8%, except for Od.

V. RESULTS FOR COPPER, SILVER, AND GOLD

A. The Cu λ3247 and λ3274 lines are a doublet from the $4\,^2S_{\frac{1}{2}}$ ground state to the $4\,^2P$ state at an energy of 3.80 and 3.77 eV for the j=3/2 and j=1/2, respectively. There are two isotopes, namely Cu^{63} and Cu^{65}, with the normal isotopic concentration being 69% and 31%, respectively.

The two odd copper isotopes have a nuclear spin of 3/2. Thus, the $^2S_{\frac{1}{2}}$ ground state is split into two components and the $^2P_{3/2}$ state, which is the upper state of the 3247 transition, is split into four components. The upper state of the 3274 transition is $^2P_{\frac{1}{2}}$ which is split into two components. The selection rule $\Delta F=0, \pm 1$ allows for four components for each isotope in the λ3247 transition. Using the rules for computing statistical weights of the hyperfine states (Kuhn[33]), and referring to the tables of Landholt and Bornstein[29] for the hyperfine splitting, one arrives at the splitting shown below. The components appear to be

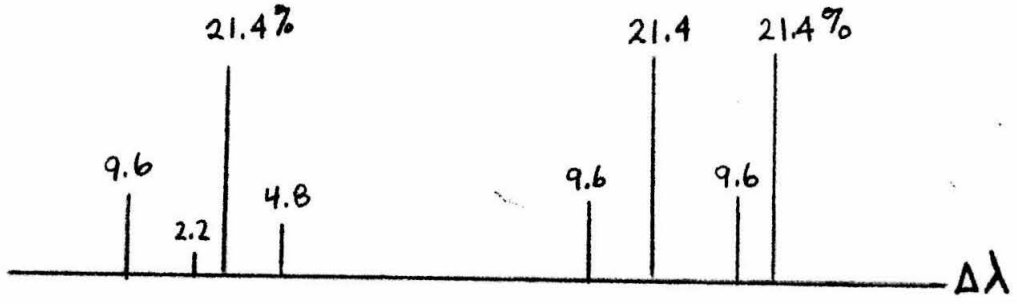

separated into two major groups, which have spreads of 2.5mÅ (63%) and 3.9mÅ (37%). The typical value of the doppler width in the experiment was 6.2mÅ, so that one

expects to be able to treat the λ3247 line as a two component line with the ratio of strengths being 0.38:0.62 and splitting of about 40mÅ between the two components.

The λ3274 line has the splitting shown below. This line

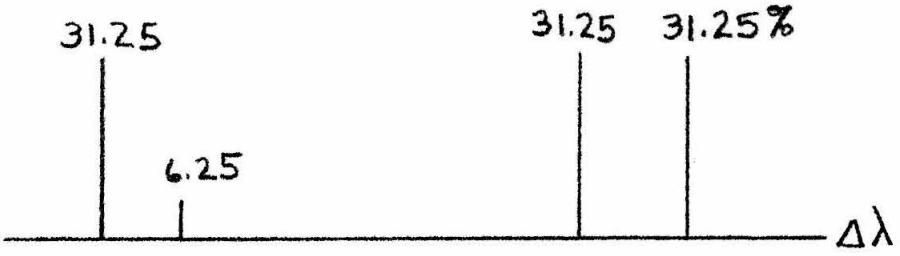

is essentially two components about 38mÅ apart with an intensity ratio of 38:62.

The experimental curves of growth for the two lines are shown in figures 13 and 14, and the experimental data are shown in table 3. On each of the curves of growth, two theoretical curves are shown. One is a single component curve and the other a two component curve. It is clear that the data imply that the lines do not behave as if they were completely split. The calculations for λ3247 are shown in table 4 and yield

$$f(3247) = 0.322 \pm 0.014$$

while the calculations of table 5 yield

$$f(3274) = 0.153 \pm 0.009$$

The vapor pressure data used are a combination of results compiled by The University of California metallurgy group[27]. Previous results of Bell, Davis, King, and Routly[12] obtained by the atomic beam method (similar to the apparatus used by Link and Lawrence) gave 0.31 for the

λ3247 line. In this paper the authors explained the higher results of King and Stockbarger[9] (0.62) on the basis of the fact that newer vapor pressure data tend to reduce the results of King and Stockbarger to 0.42. This experiment, using the most recently compiled data, gave about 50% lower results than those obtained in 1940. The fact that the agreement with the atomic beam apparatus is excellent tends to support the data obtained here. The fit to the vapor pressure data is shown in figure 15, and is quite good over several hundred degrees.

B. The two Silver lines are the same doublet as those of copper. The isotopic splitting consists of Ag^{107} (52%) and Ag^{109} (48%) with each nucleus having $I=\frac{1}{2}$. The isotopic splitting and hyperfine splitting are each smaller than those for copper. The curves of growth shown in figures 16 and 17, indicate that the data lie between the theoretical curves for the split and unsplit lines. In the case of Silver, one might more nearly expect the single component theory to hold since the $\Delta\lambda_{HF} \sim \Delta\lambda_{D}$. The data for these two curves of growth are presented in tables 6 and 7.

The vapor pressure data used were measured in 1960 by The University of California[27]. Using this latest available data, the calculations of tables 8 and 9 yield

$$f(3261) = 0.451 \pm 0.034$$

$$f(3383) = 0.175 \pm 0.015$$

Current experiments of G. Lawrence[14] on the atomic beam

yield values of 0.45 and 0.22, while Minov and Kohn[34] in an experiment on flame emission gave 0.39 for the f(3280). Filipov obtained results of 0.46 and 0.22 by the hook method.

One important feature of the present experiment is that the relative f-values are very likely reliable. The temperature measurements are quite repeatable and the experimental situation is in equilibrium, while other techniques involve atoms in a beam. Therefore, one suspects that the relative f-values measured here are accurate.

The results of Corliss and Bozman[21] (f(3280) = 0.53; f(3381) = 0.23) are probably in error since they involve a temperature normalization procedure which depends on other data for its success.

C. The experiment was attempted for the Gold transition of the 2676Å line; however, the quartz cells seemed to deteriorate rapidly in regard to transmitting in the short wavelength region (2400 - 2700Å). The filters used were also not as efficient as for longer wavelengths. Four data points were achieved, however. They are shown in table 10 on the following page.

The small dispersion of the data is believed to be just a fortuitous accident, since the predicted experimental errors exceed the dispersion. Corliss and Bozman give f = 0.08 from an emission method.

TABLE 10

Data on Au $\lambda = 2675\text{Å}$

T (°K)	$W_1/\Delta\lambda_D$	f
1368.2	0.021	0.077
	0.062	0.071
	0.194	0.076
	0.646	0.080

$\bar{f} = 0.076 \pm 0.005$

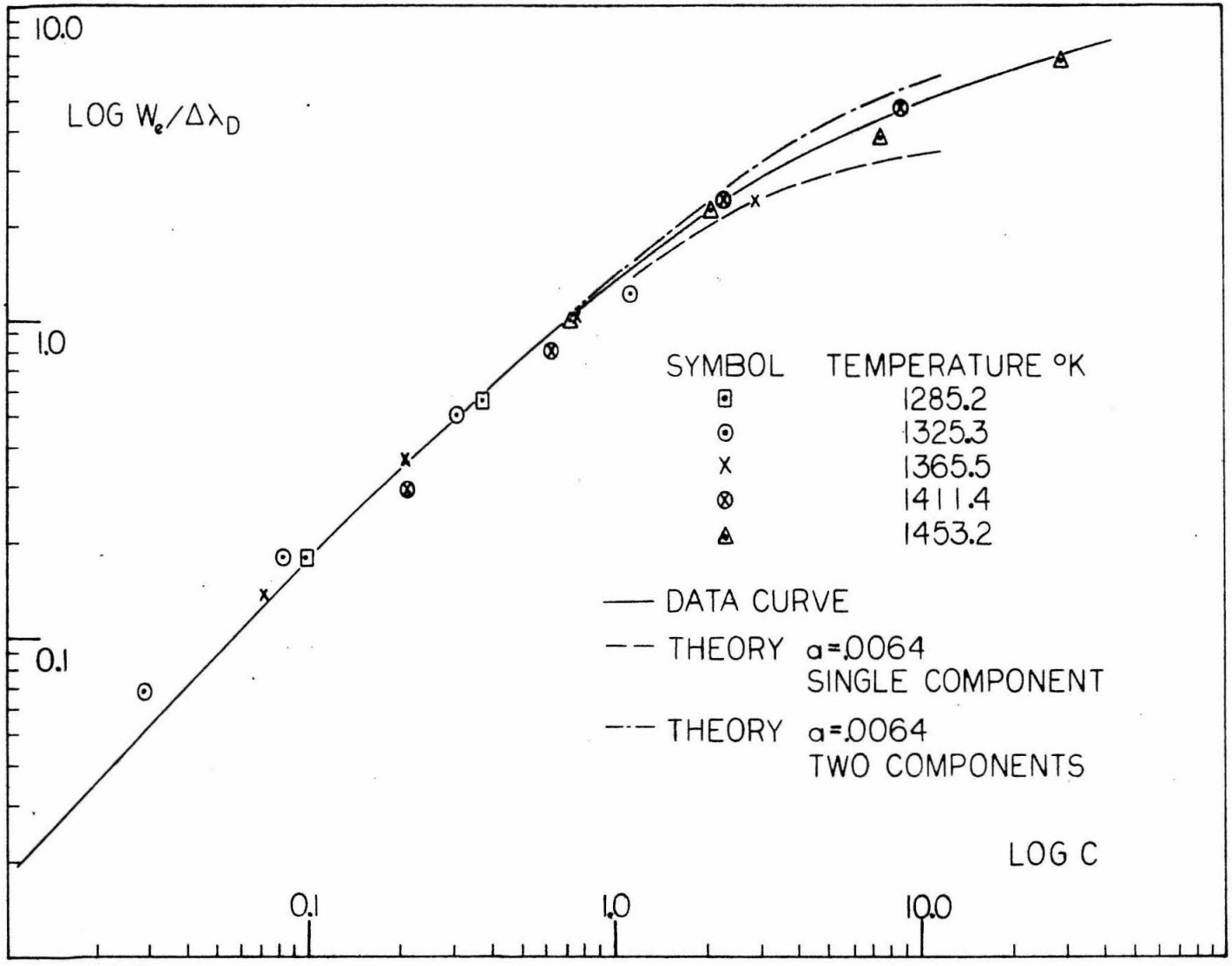

FIGURE 13 CURVE OF GROWTH OF Cu λ=3247.54 A°

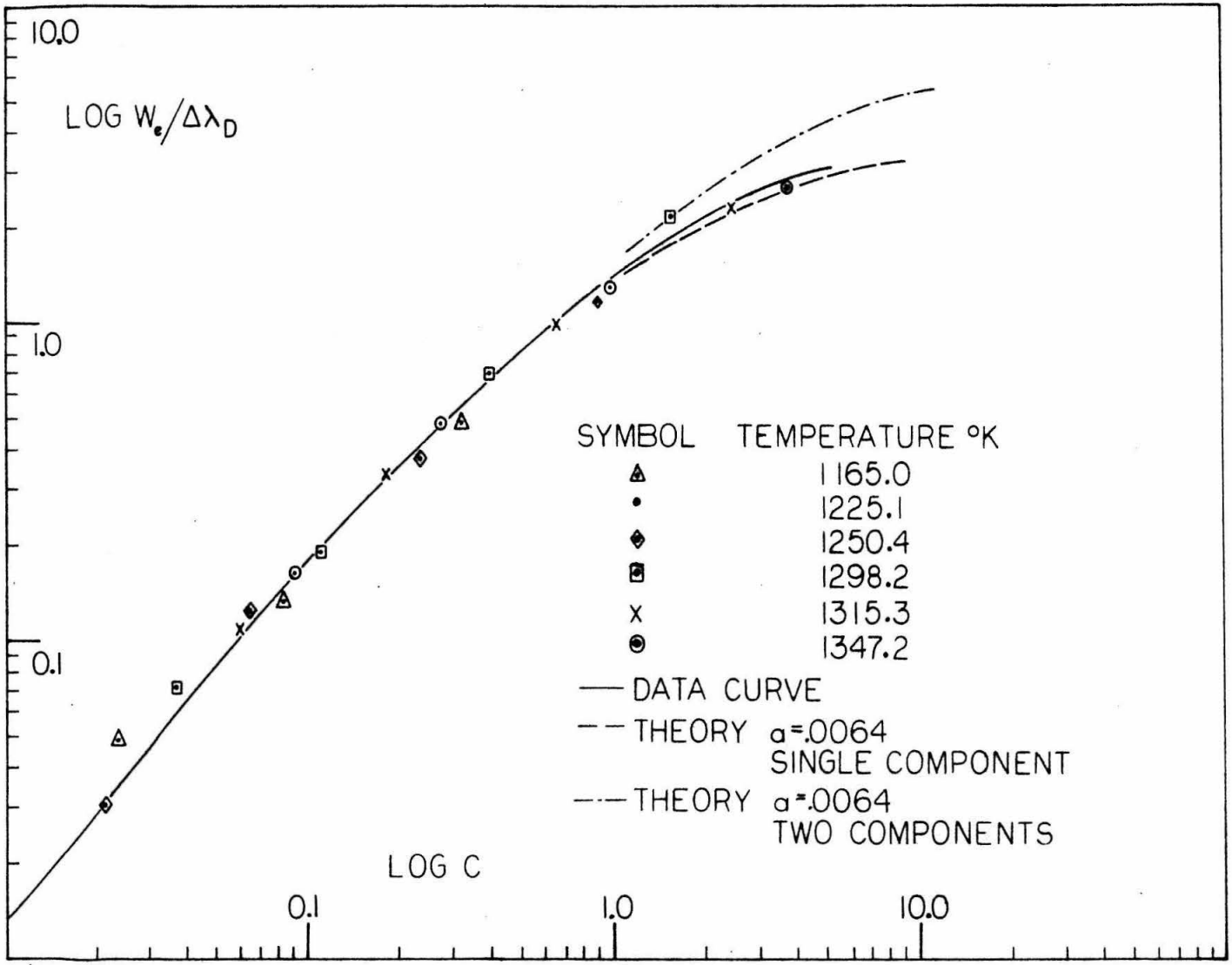

FIGURE 14 CURVE OF GROWTH OF Cu λ=3273.96 A°

TABLE 3

Experimental Data For Cu.

$\lambda = 3247.54$ Å

T (°K)	$\Delta\lambda_D$ (mÅ)	W_{L1} (mÅ) L1=.152	W_{L2} (mÅ) L2=.445	W_{L3} (mÅ) L3=1.59	W_{L4} (mÅ) L4=6.26	$W_{L1}/\Delta\lambda_D$	$W_{L2}/\Delta\lambda_D$	$W_{L3}/\Delta\lambda_D$	$W_{L4}/\Delta\lambda_D$
1162.2	5.977	0.13	0.30	1.04	3.20	0.021	0.050	0.175	0.535
1209.3	6.099	0.42	1.10	2.96	7.21	0.068	0.179	0.485	1.181
1238.5	6.175	0.83	2.20	6.24	14.81	0.135	0.357	1.010	2.398
1279.4	6.254	1.78	4.99	15.37	29.52	0.285	0.798	2.458	4.720
1331.2	6.406	6.25	14.50	24.62	40.46	0.976	2.263	3.843	6.317

$\lambda = 3273.96$ Å

1176.0	6.057		0.29	0.78	2.84		0.048	0.130	0.470
1196.1	6.115		0.42	1.58	4.57		0.070	0.258	0.748
1217.4	6.170	0.19	0.73	2.28	7.05	0.030	0.118	0.369	1.142
1248.2	6.251	0.44		4.31	13.42	0.070		0.689	2.147
1263.3	6.288	0.68	2.09	6.14	14.15	0.107	0.332	0.976	2.250
1277.4	6.320	1.01	2.98	8.05	16.44	0.160	0.472	1.274	2.601

TABLE 4

Calculations For The f-Value Of Cu. λ=3247.54 Å

E.P.=0.0000 eV

T (^{o}K)	C(T), (L)	Nfx10^{-10}	NfTx10^{-13}	Pfx10^{8}	Px10^{8}	f*(abs)
1160.2	0.027(2)	0.692	0.804	0.109	0.331	0.329
	0.097(3)	0.692	0.804	0.109		0.329
	0.365(4)	0.663	0.770	0.105		0.317
1209.3	0.037(1)	2.82	0.340	0.414	1.24	0.334
	0.101(2)	2.63	0.318	0.433		0.349
	0.313(3)	2.28	0.275	0.375		0.302
1238.5	0.073(1)	5.63	6.97	0.951	2.91	0.327
	0.217(2)	5.72	7.08	0.965		0.332
	0.753(3)	5.56	6.89	0.939		0.323
	2.65 (4)	4.97	6.16	0.839		0.288
1279.4	0.196(1)	15.32	19.58	2.67	8.48	0.315
	0.573(2)	15.30	19.57	2.67		0.315
	2.27 (3)	16.99	21.71	2.96		0.349
	8.95 (4)	16.98	21.61	2.95		0.348
1331.2	0.716(1)	57.32	76.40	10.4	30.8	0.338
	2.03 (2)	55.52	74.04	10.1		0.328
	6.60 (3)	50.58	67.45	9.19		0.298
	27.8 (4)	54.05	72.07	9.82		0.319

$\bar{f}$=0.322±0.014

TABLE 5

Calculations For The f-Value Of Cu. λ=3273.96 Å

E.P.=0.0000 eV

T (^{o}K)	C(T), (L)	$Nf \times 10^{-10}$	$NfT \times 10^{-13}$	$Pf \times 10^{8}$	$P \times 10^{8}$	f^{*}(abs)
1176.0	0.075 (3)	0.536	0.630	0.0858	0.510	0.168
	0.266 (4)	0.481	0.566	0.0772		0.151
1196.1	0.043 (2)	1.109	1.32	0.180	1.06	0.170
	0.146 (3)	1.047	1.25	0.171		0.161
	0.520 (4)	0.950	1.14	0.155		0.146
1217.4	0.021 (1)	1.598	1.95	0.266	1.77	0.150
	0.068 (2)	1.766	2.15	0.293		0.166
	0.213 (3)	1.569	1.88	0.256		0.145
	0.808 (4)	1.490	1.82	0.248		0.140
1248.2	0.043 (1)	3.306	4.13	0.563	3.68	0.153
	0.420 (3)	3.090	3.86	0.526		0.143
	1.95 (4)	3.639	4.55	0.620		0.168
1263.3	0.061 (1)	4.714	5.96	0.812	5.19	0.156
	0.182 (2)	4.812	6.08	0.829		0.160
	0.606 (3)	4.489	5.67	0.773		0.149
	2.32 (4)	4.361	5.53	0.753		0.145
1277.4	0.090 (1)	6.992	8.93	1.22	8.14	0.150
	0.268 (2)	7.118	9.09	1.24		0.152
	0.925 (3)	6.884	8.79	1.20		0.147
	3.65 (4)	6.882	8.79	1.20		0.147

$\bar{f}$=0.153 ± 0.009

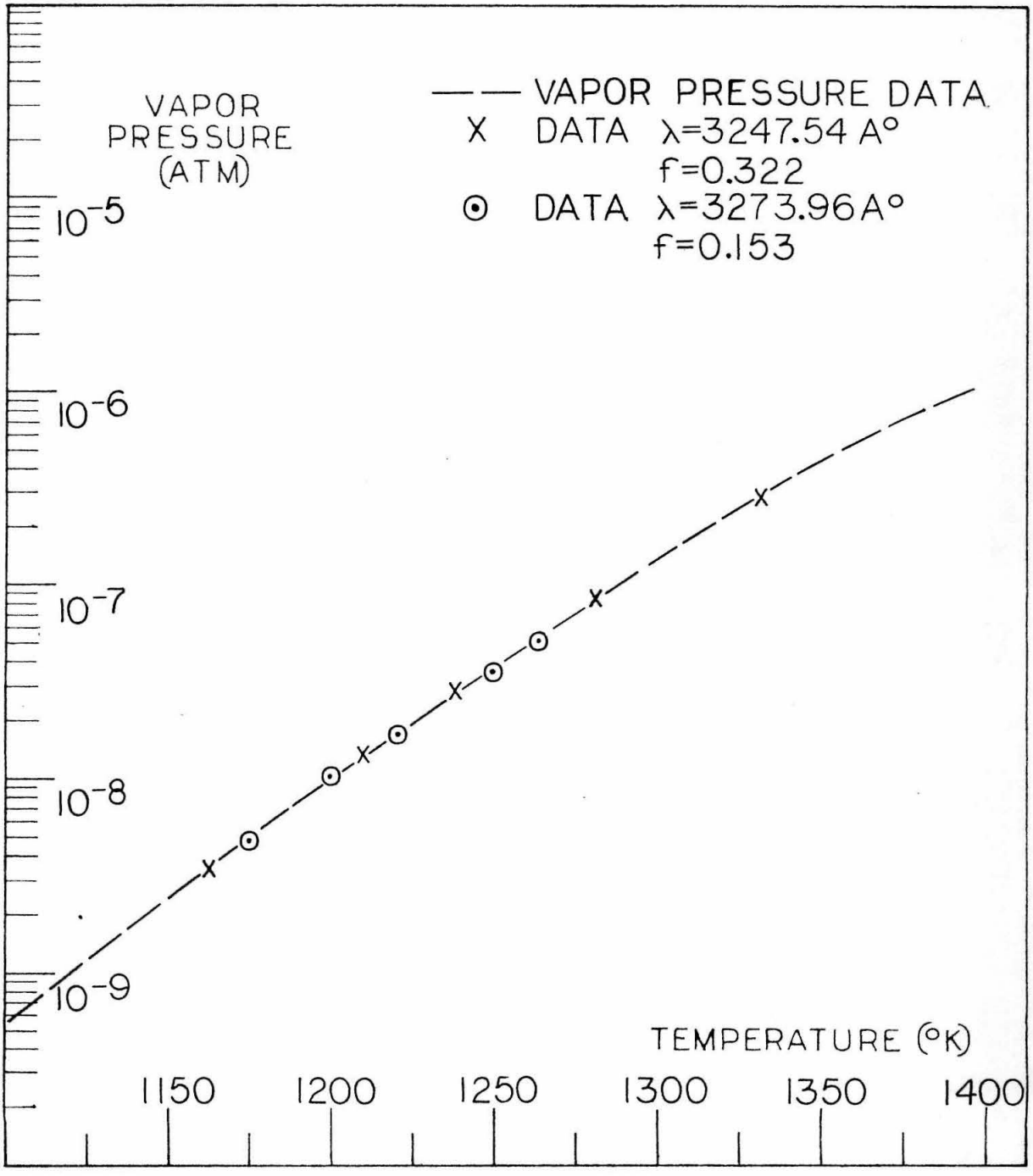

FIGURE 15 VAPOR PRESSURE OF Cu VS TEMPERATURE

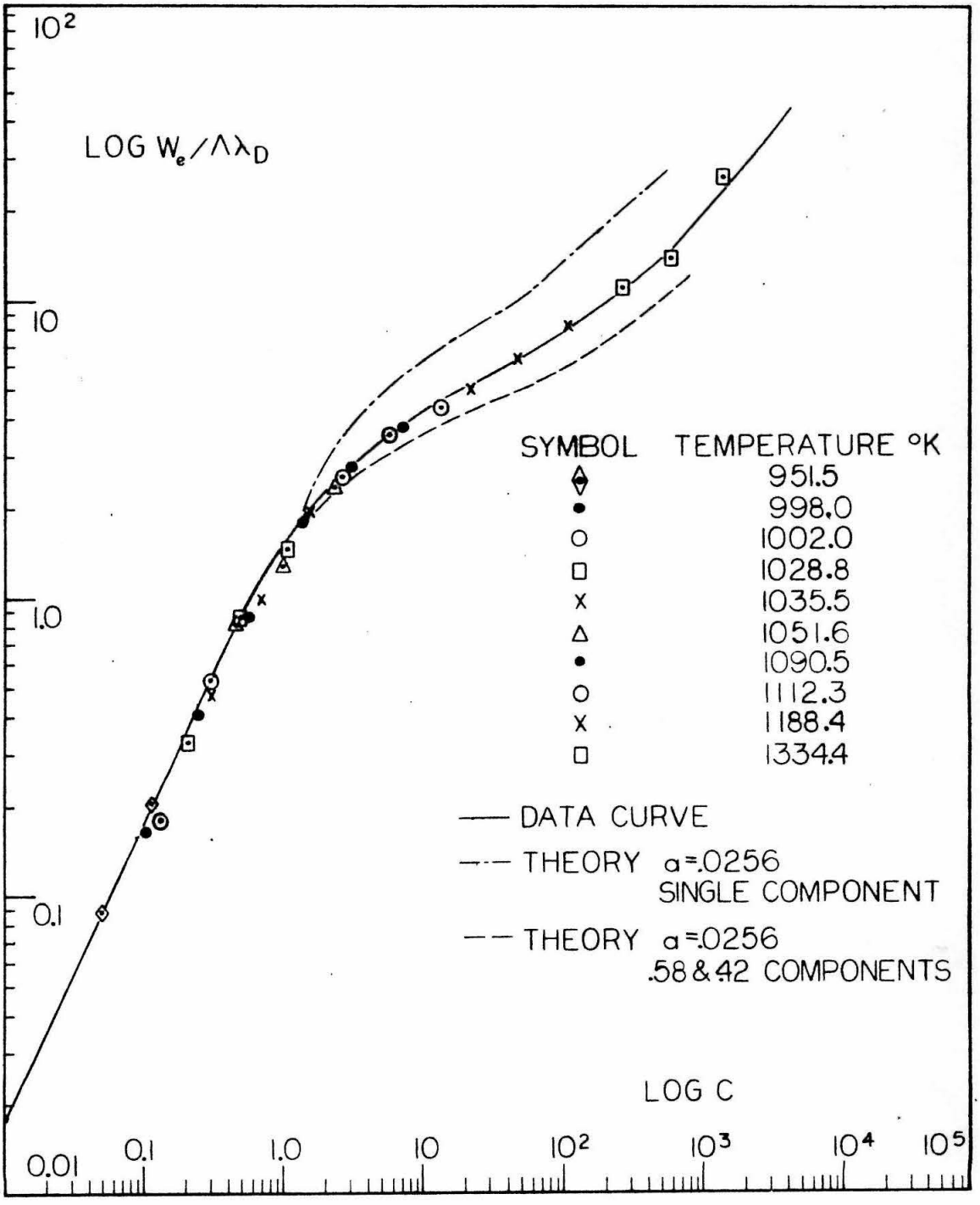

FIGURE 16 CURVE OF GROWTH OF Ag λ=3280.68 A°

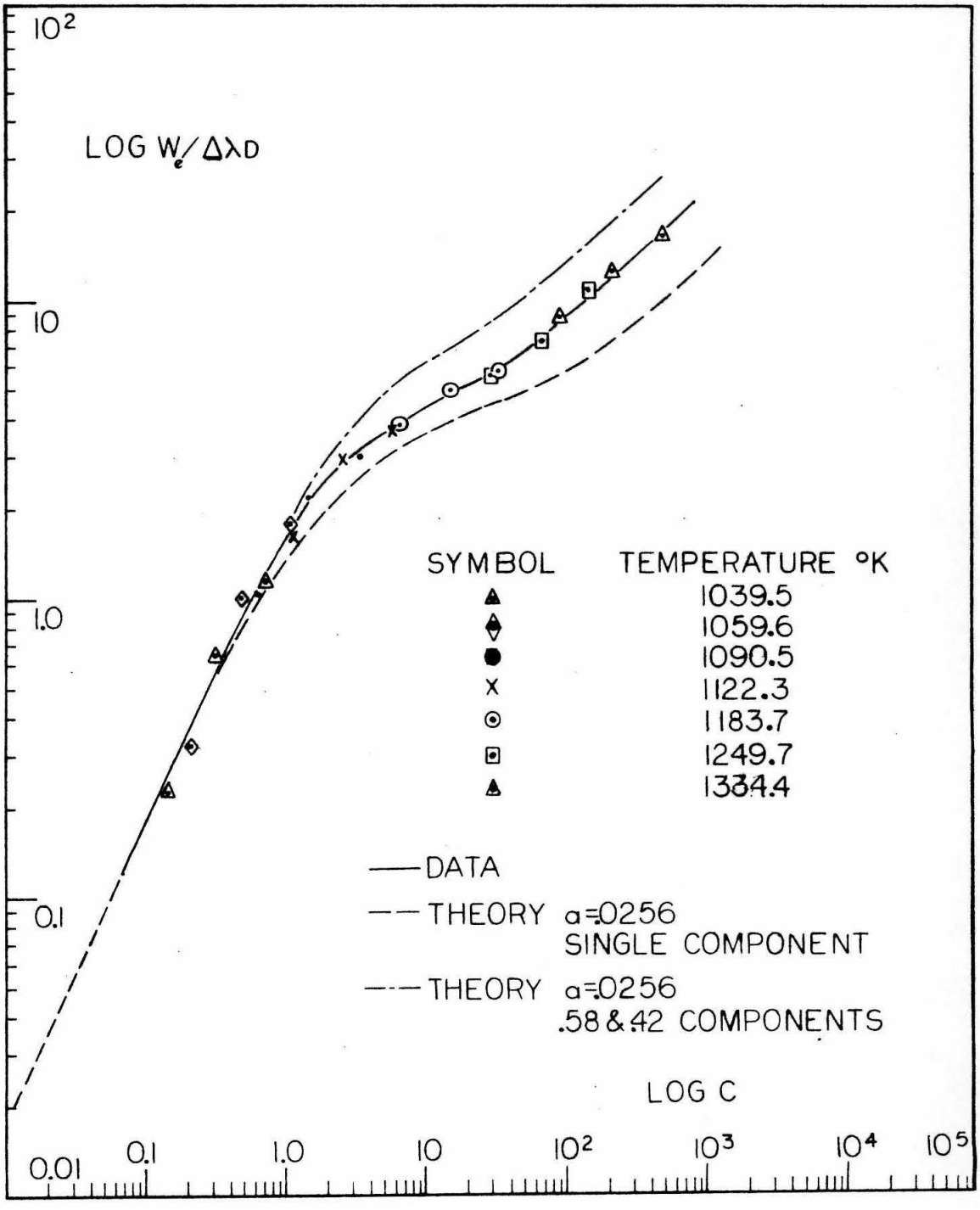

FIGURE 17 CURVE OF GROWTH OF Ag λ=3382.89 A°

TABLE 6

Experimental Data For Ag. $\lambda = 3280.68$Å

T (°K)	$\Delta\lambda_D$(mÅ)	W_{L1}(mÅ) L1=0.42	W_{L2}(mÅ) L2=0.95	W_{L3}(mÅ) L3=2.10	$W_{L1}/\Delta\lambda_D$	$W_{L2}/\Delta\lambda_D$	$W_{L3}/\Delta\lambda_D$
951.5	4.188		0.365	0.857		0.087	0.203
998.0	4.290	0.740	1.73	3.71	0.172	0.403	0.865
1002.8	4.299	0.691	2.29	4.08	0.160	0.532	0.946
1028.8	4.355	1.39	3.79	6.40	0.319	0.870	1.469
1035.5	4.371	2.02	4.26	8.35	0.461	0.975	1.911
1051.6	4.403	3.57	5.54	10.49	0.810	1.258	2.382
1090.5	4.485	8.04	12.30	16.74	1.792	2.742	3.732
1112.3	4.531	11.44	15.98	19.50	2.524	3.526	4.306
1199.4	4.703	23.66	30.54	39.25	5.029	6.491	8.343
1334.4	4.961	56.03	72.08	131.1	11.29	14.53	26.42

TABLE 7

Experimental Data For Ag. $\lambda = 3382.89\text{Å}$

T (°K)	$\Delta\lambda_D$ (mÅ)	W_{L1} (mÅ) $L1=0.42$	W_{L2} (mÅ) $L2=0.95$	W_{L3} (mÅ) $L3=2.10$	$W_{L1}/\Delta\lambda_D$	$W_{L2}/\Delta\lambda_D$	$W_{L3}/\Delta\lambda_D$
1039.5	4.515	1.04	2.94	5.23	0.226	0.651	1.160
1059.6	4.557	1.47	4.58	8.09	0.321	1.005	1.772
1090.5	4.664	4.83	10.17	13.83	1.045	2.201	2.998
1121.3	4.692	7.62	13.73	17.35	1.624	2.926	3.697
1183.7	4.815	18.50	24.15	28.00	3.841	5.014	5.813
1250.7	4.950	28.60	36.80	49.90	5.777	7.434	10.080
1334.4	5.015	45.41	62.16	84.84	8.858	12.15	16.566

TABLE 8

Calculations For The f-Value Of Ag. λ=3280.68 Å

I.P.=0.0000 eV

T (°K)	C(E), (L)	$fx10^{-11}$	$Ffx10^{-14}$	$Pfx10^{8}$	$Px10^{8}$	f^{*}(ata)
951.5	0.044 (2)	0.0361	0.034	0.046	0.101	0.460
	0.114 (3)	0.0421	0.040	0.054		0.540
998.0	0.091 (1)	0.173	0.173	0.236	0.530	0.445
	0.231 (2)	0.194	0.194	0.264		0.498
	0.495 (3)	0.188	0.188	0.256		0.483
1002.8	0.108 (1)	0.204	0.205	0.279	0.611	0.456
	0.289 (2)	0.238	0.238	0.325		0.532
	0.575 (3)	0.219	0.219	0.299		0.489
1028.8	0.192 (1)	0.371	0.382	0.521	1.25	0.417
	0.495 (2)	0.422	0.434	0.592		0.474
	0.982 (3)	0.379	0.390	0.532		0.426
1035.5	0.275 (1)	0.533	0.552	0.752	1.80	0.418
	0.625 (2)	0.535	0.554	0.755		0.419
	1.52 (3)	0.589	0.609	0.830		0.461
1051.6	0.475 (1)	0.927	0.975	1.32	3.05	0.433
	0.885 (2)	0.752	0.791	1.08		0.354
	2.20 (3)	0.859	0.903	1.22		0.400

(cont'd)

TABLE 8a

Calculations for the f-Value of Ag. λ=3280.68 Å

I.P.=0.0000 eV

r (^{o}A)	U(T), (L)	$fx10^{-11}$	$Sf\ x10^{-14}$	$Pfx10^{8}$	$Px10^{8}$	f(calc)
1090.5	1.33(1)	2.644	2.883	3.93	10.1	0.397
	2.95(2)	2.593	2.828	3.85		0.389
	6.90(3)	2.744	2.993	4.08		0.412
1112.3	2.48(1)	4.980	5.539	7.55	17.2	0.514
	5.45(2)	4.836	5.379	7.33		0.499
	12.2 (3)	4.895	5.444	7.42		0.505
1199.4	20.5 (1)	42.75	51.29	69.9	155.	0.451
	47.0 (2)	43.32	51.97	70.8		0.457
	109. (3)	45.45	54.52	74.3		0.480
1334.4	275. (1)	605.0	807.5	1100.	2550.	0.431
	545. (2)	534.1	713.1	972.		0.381
	1400. (3)	614.8	827.5	1120.		0.439

f=0.451 ± 0.034

TABLE 9

Calculations for the f-Value of Ag. $\lambda = 3382.89$ Å

I.P. = 0.0000 eV

T (°K)	S(T), (L)	$f \times 10^{-11}$	$Lf \times 10^{-14}$	$P \times 10^{8}$	$P \times 10^{7}$	f(abs)
1039.5	0.128(1)	0.241	0.251	0.342	0.220	0.155
	0.360(2)	0.302	0.314	0.428		0.195
	0.695(3)	0.261	0.271	0.369		0.168
1059.6	0.198(1)	0.386	0.409	0.557	0.321	0.174
	0.580(2)	0.487	0.516	0.703		0.219
	1.24 (3)	0.471	0.499	0.680		0.212
1090.5	0.625(1)	1.205	1.31	1.79	0.990	0.181
	1.51 (2)	1.285	1.39	1.90		0.192
	3.12 (3)	1.206	1.31	1.79		0.181
1121.3	1.09 (1)	2.13	2.39	3.26	2.09	0.156
	2.45 (2)	2.12	2.38	3.24		0.155
	5.60 (3)	2.19	2.46	3.35		0.160
1183.7	6.45 (1)	12.9	15.3	20.9	11.3	0.185
	11.2 (2)	10.0	11.8	16.1		0.142
	28.0 (3)	11.2	13.3	18.1		0.160
1250.7	28.2 (1)	58.2	72.7	99.1	52.5	0.189
	62.6 (2)	57.0	71.2	97.0		0.185
	140. (3)	57.7	72.1	98.3		0.187
1334.4	91.5 (1)	195.4	261.	355.	235.0	0.151
	231.0 (2)	217.3	290.	395.		0.168
	480.0 (3)	204.3	273.	372.		0.158

$\bar{f} = 0.175 \pm 0.015$

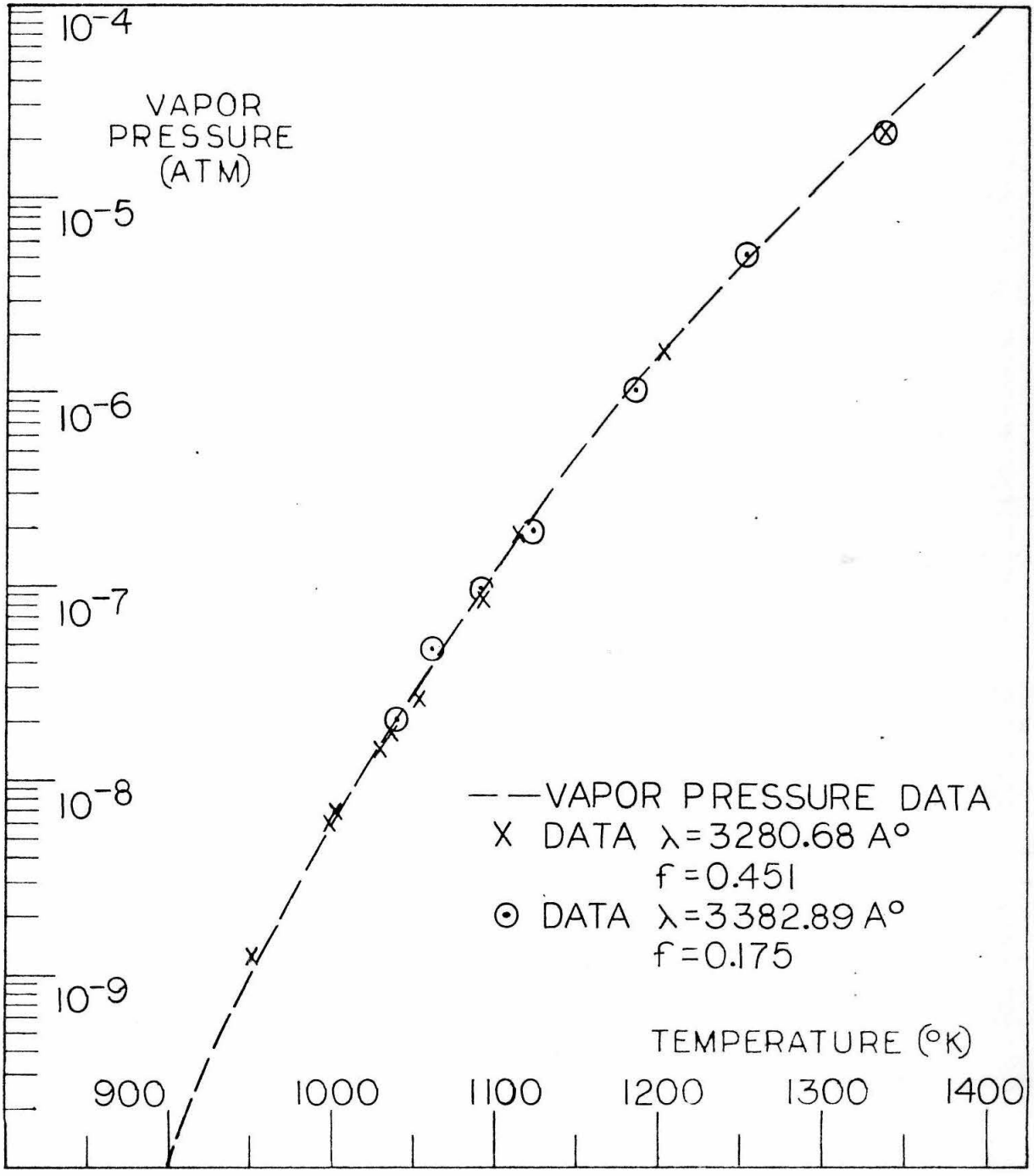

FIGURE 18 VAPOR PRESSURE OF Ag VS TEMPERATURE

VI. THE RESULTS FOR ZINC AND CADMIUM

A. The main resonance lines for Zn and Cd are below the wavelength region obtainable in this experiment. Therefore, the weak transitions $4^1S - 4^3P$, $\lambda 3075$ and $\lambda 3261 \mathring{A}$, were studied for the Zn and Cd atoms. These are j=0 to j=1 transitions.

The isotopic composition of Zn is 48.9% (Zn^{64}), 27.8% (Zn^{66}), 4% (Zn^{67}), 18.6% (Zn^{68}) and 0.7% of (Zn^{70}). The even isotopes compose most of the total Zn atoms so that the hyperfine splitting of the 4% (Zn^{67}) was ignored. The isotopic splitting is given below (due to nuclear volume effects, presumably).

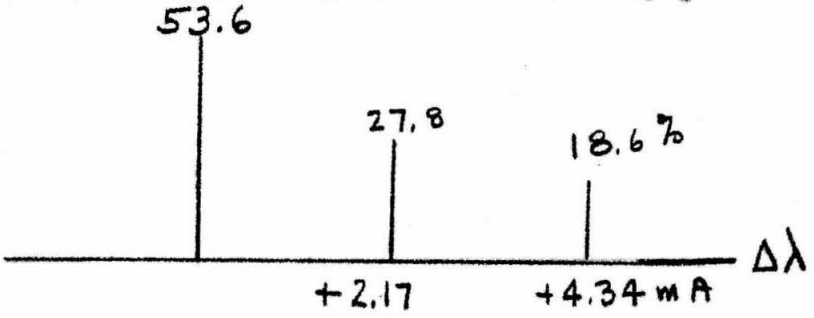

The doppler width was approximately $4.3 m\mathring{A}$, so that, one expects the Zn line to have the characteristics of a single component. This expectation was fulfilled as shown on the curve of growth of figure 19. The data from which the curve was derived is presented in table 11 and the calculation of the f-value is given in table 12. The resulting f-value was

$$10^4 f(\lambda=3075) = 0.992 \pm 0.051$$

There are twenty-four references given in the National Bureau of Standards "Bibliography on Atomic Transition Probabilities"[35], almost all of which deal with relative

f-values. The only absolute f-values are given by Soleillet[36] who found 2×10^{-4}, and Auslander[37] who reported 1.5×10^{-4}. Helliwell's calculated f(3076) is equal to 2.5×10^{-4}.

Figure 20 shows the fit of the spectroscopic data to the vapor pressure data which is quite good from 604°K to 820°K. The vapor pressure was from the standard reference[27] which agrees very closely in this temperature region with that of G. Gatlow and A. Schneider[38] and is the most recent data revised as of 1960. The fit over a 200°K temperature range lends credence to both the vapor pressure data and the f-value resulting from the fit. However, this f-value is lower than all of the previous results. The calculated values of Helliwell are higher than those of Bates and Damgard for the $^3P - {}^3S$ resonance lines and are higher than the experimental results for Cd, so that, the disagreement is not severe.

B. The Cadmium line, λ3261, has one of the best known f-values and has been measured by King and Stockbarger[9] (2.2×10^{-3}), Kuhn[39] (who found a value of 1.9×10^{-3}), and Koenig and Ellett[40] (1.9×10^{-3} from lifetime measurements). Helliwell's calculation[6] gave a value of 3×10^{-3}. This experiment yielded a measurement of 2.05×10^{-3}. The data are presented in table 13 and the calculations in table 14. The curve of growth is presented as figure 21 and the fit to the curve of vapor pressure data is depicted in

figure 22. The comparison of the results was more than adequate in King and Stockbarger's work, as well as in Helliwell's, and will not be repeated here.

One interesting result of the curve of growth is the fit to a theoretical curve. The Cadmium isotopic composition is 13%, 16%, and 29.5% in the even 110, 112, and 114 nuclei, respectively. The isotopic shift of the Cd^{112} and Cd^{114} nuclei is 1.6mÅ and 2.9mÅ from the Cd^{110} nucleus. The two odd nuclei have two components separated by 21.4mÅ. The net result is a group of three components in the intensity ratio 0.40:0.35:0.25 separated by considerably more than the Doppler width. The curve of growth of Cd does indeed fit the theory of several components, while the Zn curve fit the single component theory. These results clearly indicate the dependence of the curve of growth on the structure of the line.

The effects of pressure broadening are also clear. On the upper tail of the curve, the value of "a" has increased by 100 times for an increase in N of about the same amount. C. The ability to fit each of the Zn and Cd curves of growth with an explainable theory, the correlation of the spectroscopic data with the vapor pressure data over a fairly large temperature range, and the agreement of the Cadmium f-value with the results of other authors, lend credence to the Zinc f-value obtained here.

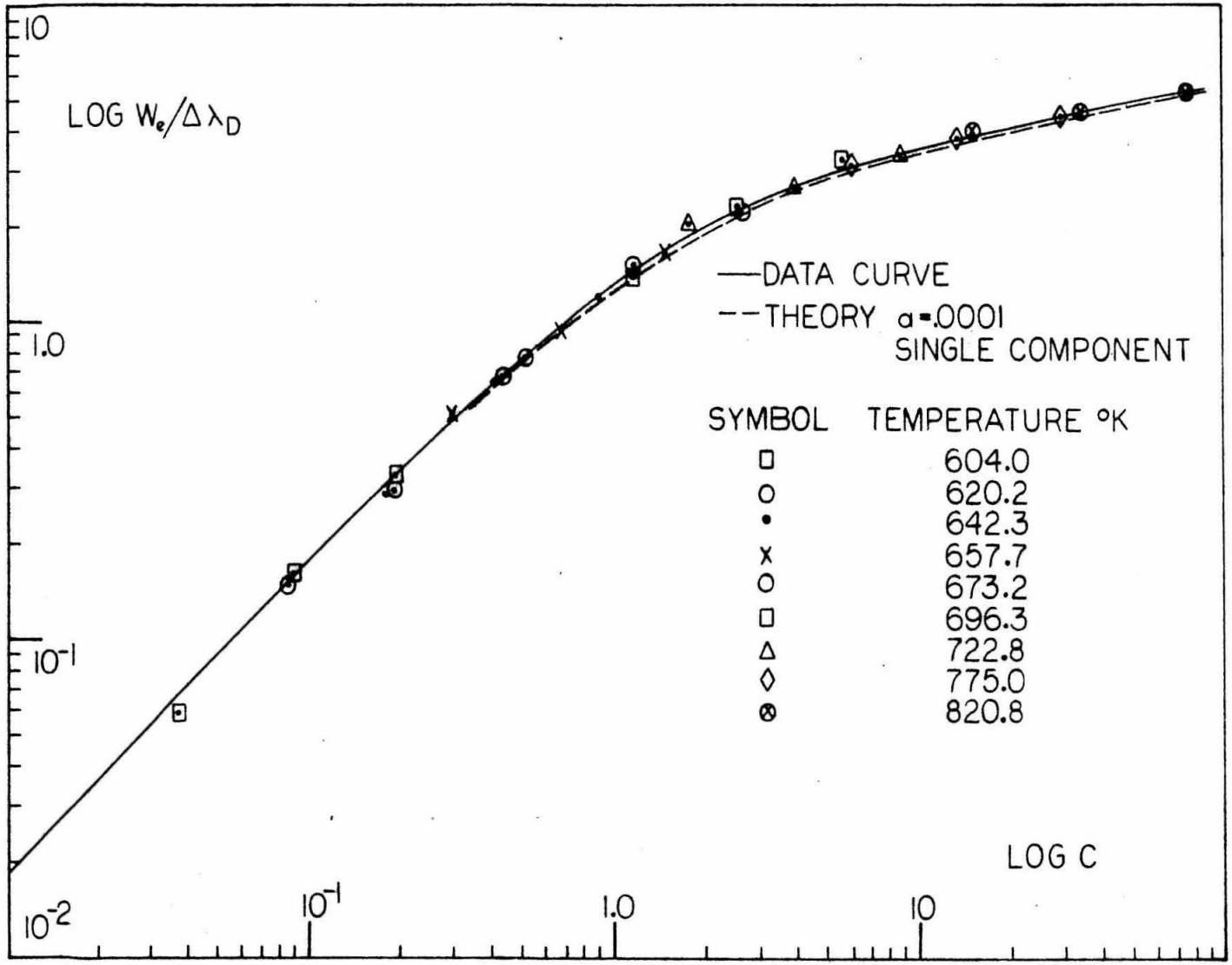

FIGURE 19 CURVE OF GROWTH OF ZN λ=3075.90 A°

TABLE 11

Experimental Data For Zn. $\lambda = 3075.90\text{Å}$

T (°K)	$\Delta\lambda_D$ (mÅ)	W_{L1} (mÅ) L1=0.42	W_{L2} (mÅ) L2=0.95	W_{L3} (mÅ) L3=2.10	$W_{L1}/\Delta\lambda_D$	$W_{L2}/\Delta\lambda_D$	$W_{L3}/\Delta\lambda_D$
604.0	4.018	0.230	0.671	1.29	0.057	0.167	0.321
620.2	4.072	0.600	1.16	2.69	0.147	0.285	0.661
642.3	4.144	1.04	2.58	4.75	0.251	0.623	1.146
657.7	4.193	2.10	3.82	6.80	0.501	0.911	1.621
673.2	4.242	3.26	6.31	9.10	0.768	1.487	2.145
696.3	4.314	5.72	9.56	13.40	1.326	2.216	3.106
722.8	4.396	8.19	11.32	14.25	2.000	2.575	3.242
774.0	4.550	13.68	17.12	20.27	3.005	3.760	4.451
320.8	4.952	19.57	21.89	25.17	3.951	4.420	5.083

TABLE 12

Calculations For The f-Value Of Zn. $\lambda = 3075.90\text{Å}$

E.P.= 0.0000eV

T (^{o}K)	C(T), (L)	$Nfx10^{-10}$	$NfTx10^{-13}$	$Pfx10^{9}$	$Px10^{5}$	f^{*}(abs)
604.0	0.034 (1)	0.682	0.412	0.562	0.674	0.833
	0.088 (2)	0.788	0.476	0.649		0.962
	0.187 (3)	0.758	0.458	0.624		0.925
620.2	0.082 (1)	1.684	1.044	1.42	1.46	0.973
	0.171 (2)	1.552	0.963	1.31		0.897
	0.422 (3)	1.733	1.075	1.47		1.007
642.3	0.172 (1)	3.594	2.308	3.15	3.42	0.921
	0.401 (2)	3.706	2.380	3.24		0.947
	0.862 (3)	3.603	2.314	3.15		1.026
657.7	0.301 (1)	6.413	4.218	5.75	6.04	0.952
	0.630 (2)	5.890	3.874	5.28		0.874
	1.42 (3)	6.005	3.949	5.38		0.891
673.2	0.507 (1)	10.84	7.297	9.95	10.2	0.976
	1.21 (2)	11.44	7.701	10.5		1.030
	2.52 (3)	10.78	7.250	9.88		0.969
696.3	1.12 (1)	24.36	16.96	23.1	23.6	0.979
	2.61 (2)	25.09	17.47	23.8		1.009
	5.82 (3)	25.32	17.63	24.0		1.018

(cont'd)

TABLE 12a

Calculations For The f-Value Of Zn. $\lambda = 3075.90$ Å

E.P.= 0.0000 eV

T (^{o}K)	C(T), (L)	$Nfx10^{-10}$	$NfTx10^{-13}$	$Pfx10^{9}$	$Px10^{5}$	f^{*}(abs)
722.8	1.85 (1)	41.36	29.90	40.8	45.1	0.905
	3.75 (2)	36.75	26.56	36.2		0.803
	8.35 (3)	37.02	26.76	36.5		0.810
774.0	5.85 (1)	134.3	104.1	142.	164.0	0.866
	13.5 (2)	137.0	106.2	145.		0.885
	29.0 (3)	133.2	103.2	141.		0.860
820.8	15.5 (1)	387.1	317.7	432.	482.0	0.897
	32.7 (2)	360.9	296.2	404.		0.839
	73.5 (3)	367.1	301.3	411.		0.854

$10^{4}\bar{f} = 0.923 \pm 0.051$

* This column is actually $10^{4}f$

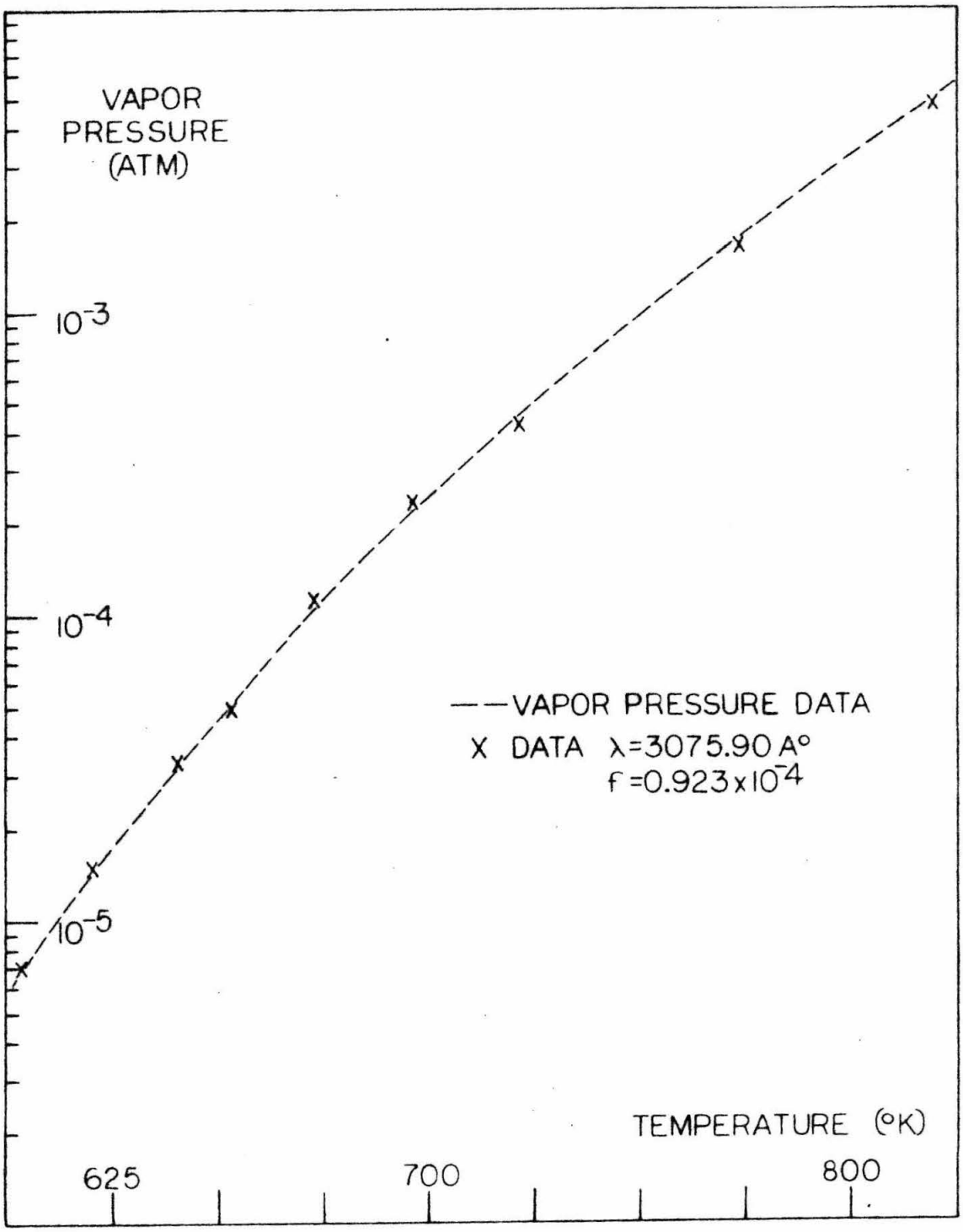

FIGURE 20 VAPOR PRESSURE OF Zn

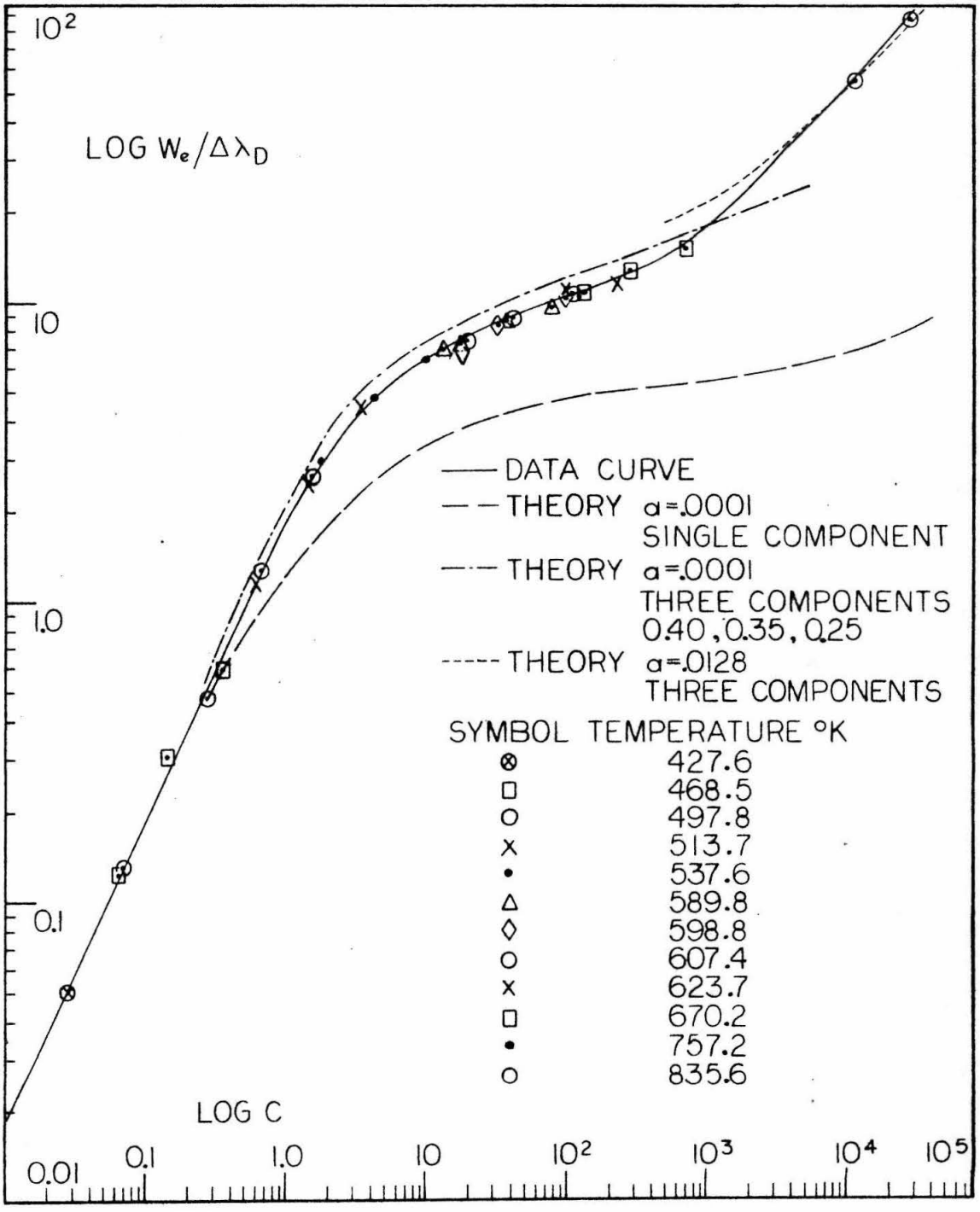

FIGURE 21 CURVE OF GROWTH OF Cd λ=3261.06 A°

TABLE 13

Experimental Data For Cd. $\lambda = 3261.06$ Å

T (°K)	$\Delta\lambda_D$ (mÅ)	W_{L1} (mÅ) L1=.431	W_{L2} (mÅ) L2=.960	W_{L3} (mÅ) L3=2.38	$W_{L1}/\Delta\lambda_D$	$W_{L2}/\Delta\lambda_D$	$W_{L3}/\Delta\lambda_D$
427.6	2.788		0.143	0.354		0.051	0.127
468.5	2.918	0.35	0.892	1.72	0.120	0.306	0.589
497.8	3.007	1.41	3.80	7.80	0.469	1.264	2.594
513.7	3.055	3.40	7.42	13.15	1.113	2.429	4.304
537.6	3.125	9.37	15.05	19.95	2.988	4.799	6.362
589.8	3.274	22.25	26.78	31.15	6.795	8.179	9.513
598.8	3.299	24.05	28.05	33.15	7.290	8.502	10.05
607.4	3.322	27.58	31.10	35.70	8.302	9.361	10.75
623.7	3.366	28.15	34.37	37.60	8.363	10.21	11.17
670.2	3.490	36.97	44.00	52.85	10.59	12.61	15.14
757.2	3.709		101.2	162.3		27.28	43.76
835.6	3.897	202.4	329.0	465.5	51.94	84.42	119.4

TABLE 14

Calculations For The f-Value Of Cd. λ=3261.06 Å

E.P.=0.0000 eV

T (°K)	C(T), (L)	Nfx10^{10}	NfTx10^{-12}	Pfx10^{10}	Px10^{7}	f*(abs)
427.6	0.027(2)	0.220	0.941	1.28	0.630	2.04
	0.071(3)	0.235	1.004	1.37		2.17
468.5	0.067(1)	1.281	6.01	8.19	3.90	2.09
	0.162(2)	1.387	6.49	8.86		2.27
	0.348(3)	1.203	5.64	7.69		1.98
497.8	0.265(1)	5.22	26.0	35.5	18.6	1.90
	0.695(2)	6.14	30.5	41.6		2.23
	1.60 (3)	5.70	28.4	38.6		2.08
513.7	0.620(1)	12.42	63.7	86.9	43.2	2.02
	1.42 (2)	12.75	65.5	89.3		2.06
	3.60 (3)	13.03	66.9	90.1		2.11
537.6	1.91 (1)	39.14	210.4	287.	146.0	1.96
	4.25 (2)	39.02	209.8	286.		1.96
	10.2 (3)	37.77	203.1	277.		1.90

(cont'd)

TABLE 14a

Calculations For The f-Value Of Cd. λ=3261.06 Å

E.P.=0.0000 cV

T (°K)	*** C(T), (L)	Nf x 10^{-12}	NfT x 10^{-15}	Pf x 10^{6}	P x 10^{3}	f (abs)
589.8	0.130(1)	2.791	1.646	0.224	0.113	1.99
	0.295(2)	2.839	1.674	0.229		2.02
	0.690(3)	2.677	1.579	0.215		1.90
598.8	0.181(1)	3.916	2.345	0.320	0.173	1.86
	0.531(2)	5.189	2.960	0.420		2.18
	0.997(3)	3.896	2.330	0.317		1.84
623.7	0.405(1)	8.994	5.854	0.809	0.397	2.04
	1.08 (2)	10.54	6.572	0.896		2.26
	2.25 (3)	8.98	5.598	0.763		1.93
670.2	1.37 (1)	31.35	21.01	2.86	1.40	2.05
	3.02 (2)	30.97	20.75	2.83		2.02
	4.20 (3)	29.78	19.96	2.72		1.94
757.2	26.50 (2)	289.	218.6	29.8	12.8	**2.32
	69.00 (3)	303.	229.5	31.3		**2.44

$10^{3}\bar{f}$ = 2.05 ± 0.11

* This column is actually 10^{3}f.
** Discarded in taking averages. This group of data was not overlapping the previous one in constructing the curve of growth.
*** This column is actually 10^{-2}C.

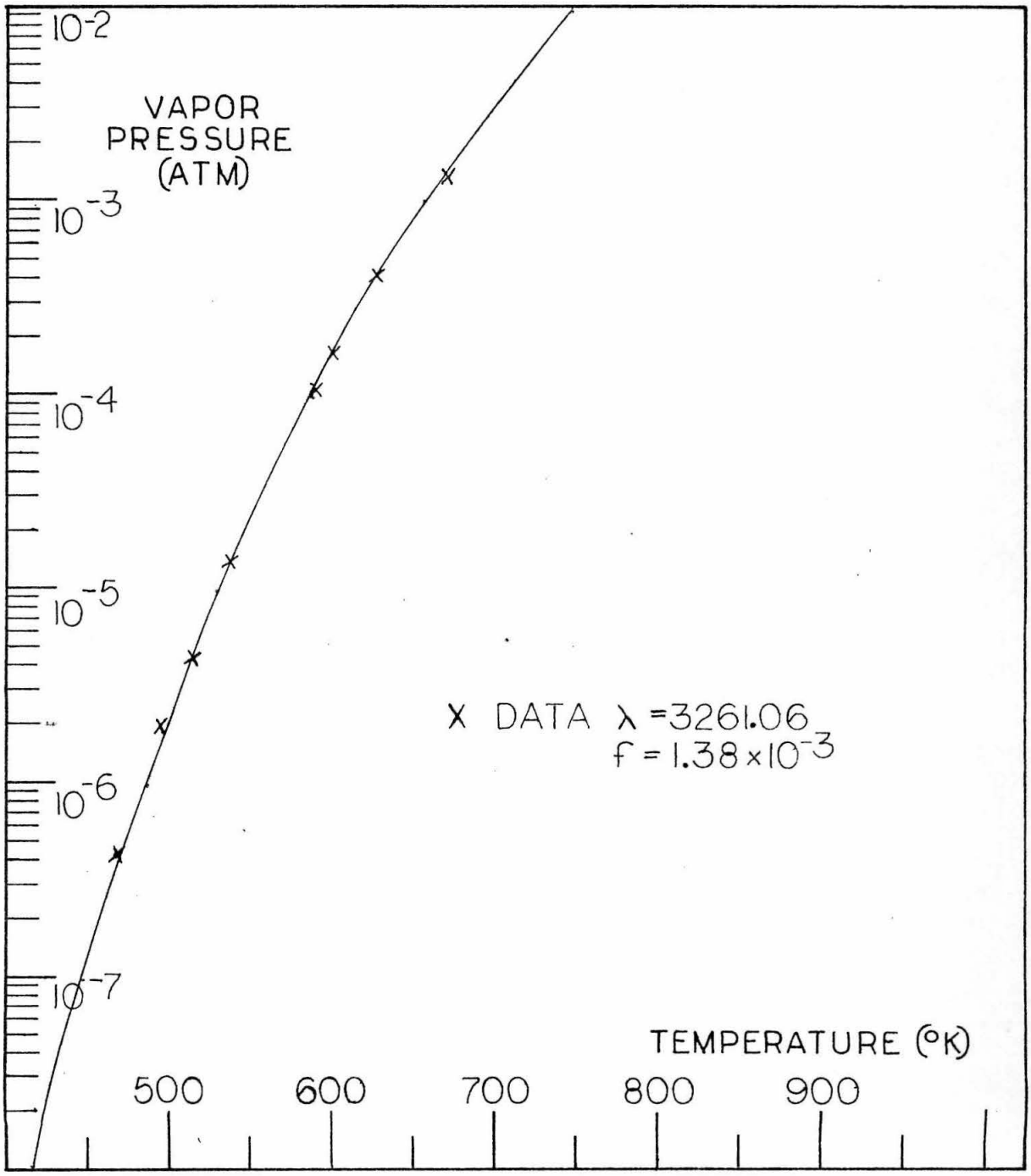

FIGURE 22 VAPOR PRESSURE OF Cd VS TEMPERATURE

VII. THE RESULTS OF GALLIUM, INDIUM, AND THALLIUM

A. The three elements under discussion have two different multiplets which were studied. The $np^1\ ^2P_{\frac{1}{2}} - nd^1\ ^2D_{3/2}$ transition lines, λ3039Å of Indium and λ2767Å of Thallium were studied. Also, the $np^1\ ^2P_{\frac{1}{2}} - np^1\ ^2S$ transitions, λ4033Å of Gallium; λ4102Å of Indium, and λ3775Å of Thallium were measured.

In all of these transitions the calculations are somewhat more complicated due to the existence of a nearby excited state. The excited states which are the substates of $^2P_{\frac{1}{2}}$ ground state are listed below.

Element	Ground State	Excited State	E.P.(eV)
Ga	$j = 1/2$	$j = 3/2$	0.10
In	$j = 1/2$	$j = 3/2$	0.27
Tl	$j = 1/2$	$j = 3/2$	0.96

Even though transitions from these states were not measured, they affect the ratio of N_ℓ and the total N. That is,

$$N_\ell = N_T g_\ell e^{-\frac{\Delta E_\ell}{kT}} \left[g_0 + \sum_{\ell'} g_{\ell'} e^{-\frac{\Delta E_{\ell'}}{kT}} \right]^{-1}$$

is used whenever more than one state needs to be considered. In some articles in the literature it is not clear that this was done. In the case of Tl the temperatures are low, thus,

$$kT \ll E.P.$$

and the approximation $N_\ell = N_T$ is a good one.

B. In the case of Gallium, the experiment was short-lived. The Gallium attacked the quartz surfaces in a few hours.

Because of this fact, the $\lambda 2874\text{Å}$ line was unobtainable but three data points were achieved for the $\lambda 4033\text{Å}$ line. The data are shown below in table 15.

TABLE 15

Data for Ga.		$\lambda = 4033\text{Å}$
T (°K)	$W_1/\Delta\lambda_D$	f
1002°K	0.050	0.0986
	0.146	0.0955
	0.492	0.0915

$$\bar{f} = 0.0955 \pm 0.006$$

These data are too sparse for a really reliable determination of the f-value but are presented as the best that could be obtained with this cell. In section XI there is some discussion of how these data could be enlarged upon.

A recent determination has been made by Ostrovskii and Penkin[17] using the hook method (with Speiser and Johnston's data which agree with that used in this experiment to within several per cent). Their results were f(4033) = 0.129 ± 20% which is in agreement to within 20% with this result if the vapor pressure data is adjusted.

The atomic beam experiment by J. Link[15] yielded a result of f = 0.072. In this case, two comments are necessary. The first is that the atomic beam and lifetime experiments are independent of vapor pressure. The second is that the temperature is usually not critical in this experiment,

so that the temperature measured by an optical pyrometer is adequate. With the low-lying excited level, however, the temperature becomes more critical in the statistical calculations discussed in paragraph A. In view of these comments, the agreement between the hook method and this one indicates that vapor pressure leads to an f-value which is larger than that given by those methods which are independent of vapor pressure, which implies that the vapor pressure data is too low by about 14% to 20%.

C. The Indium 3039Å line goes from the $5p^1\ ^2P_{1/2}$ ground state to the $5d^1\ ^2D_{3/2}$ excited state; it is a $j = 1/2$ to $j = 3/2$ transition. The isotopic abundances of Indium are 95.8% of In^{115} and 4.7% of In^{113}. For the purposes of this experiment only the In^{115} is considered. This isotope has a nuclear spin of 9/2, which allows for two components; namely,

$$F = 5 \qquad I = 0.55$$
$$F = 4 \qquad I = 0.45$$

The two components are separated by about 33mÅ (which is greater than the Doppler width). Table 16 is the experimental data and table 17 the calculations for Indium. Figure 23 is the curve of growth of Indium. The results are

$$\bar{f}(\lambda 3039) = 0.339 \pm 0.013$$

and the theory fits the split line curve quite well.

The splitting of the λ4101Å line consists of four major components as shown.

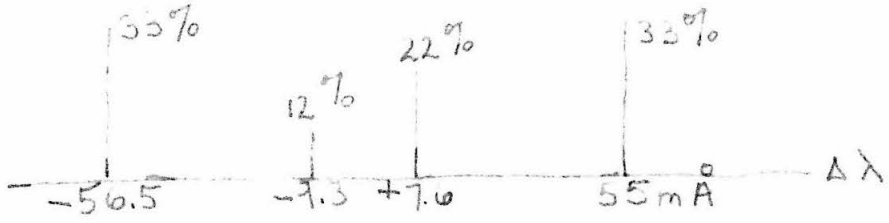

Table 18 shows a result,

$$\bar{f} = 0.172 \pm 0.022$$

and the curve of growth, as depicted in figure 24, indicates that the line comes closer to a single component curve. The reasons for this are now known.

Figure 25 is a vapor pressure graph for In with the spectrographic data shown. The fit is within 10% of the data of reference 27, which utilizes the data of J. S. Anderson[41] and A. P. and Y. N. Lyubimov[42]. Previous results of Penkin, et al[17], gave a result 0.201 ± 10%, which is in excellent agreement with this experiment. Their value for λ3039 was 0.50 however, which is higher than the results of this experiment. They used an equation to fit the data of Anderson which accounts for some of the difference.

J. Link[15] obtained the result f(λ3039) = 0.28 on the atomic beam, which is within 18% or so of these results. The temperature measurements and statistical corrections mentioned in the discussion of Ga might account for the difference between these data and the atomic beam data.

The emission results of the National Bureau of Standards[21] gives 0.495 and 0.235 as their respective values for λ3039 and λ4101. However, the agreement with the atomic beam experiment on the high side, and with the hook method on the low side (Penkin's vapor pressures tended to be low), indicates that the results of this experiment are reliable.

D. The Tl λ 3775 f-value has been measured by the emission method (0.11) and the lifetime method (0.12) and some unpublished data were taken by King (0.112). The magneto rotation measurements of Kuhn gave considerably higher results. For the λ2767 line, the N.B.S. report gives 0.24.

The λ2767 line has four components which group into two sub-lines with relative intensities of 75% and 25%, split by about 50mÅ. The data did not include high values of $W/\Delta\lambda_D$, so that the curve of growth was not fit with a theoretical one. The data are included (along with those for λ3775) in table 19 and the curve of growth is shown in figure 26. The results of the calculations in table 20 give,

$$f(\lambda 2767) = 0.219 \pm 0.020$$

The λ3775 line consists of six components as shown below.

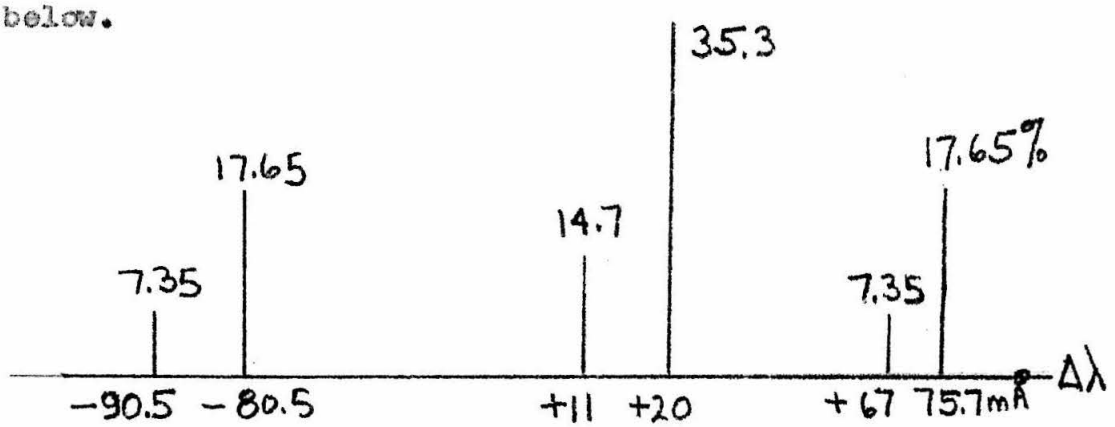

They arise from the two odd isotopes Tl^{203} (29.5%) and Tl^{205} (70.5%), each of which has a nuclear spin of $\frac{1}{2}$. The $^2P_{\frac{1}{2}}$ and $^2S_{\frac{1}{2}}$ states each has F = 0, 1 sub-levels, but the F = 0 to F = 0 transition is not allowed.

The curve of growth, shown in figure 27, illustrates once again the necessity of accounting for the hyperfine splitting. The results of table 21 are

$$f = 0.108 \pm 0.010$$

which is in good agreement with most of the previous results except those of Kuhn. The data fit the vapor pressure curve of figure 26 over a 300°K range, which would be difficult to do if the vapor pressure data were in error. Therefore, the agreement between this result, those of the lifetime measurements, and the total absorption data of King, implies that Kuhn's result was too high.

E. In the first two cases discussed in this section, there was some problem in containment of the element. Apparently, both Gallium and Indium penetrate quartz to some extent. After approximately ten or twelve hours, the supply of the element would be seriously depleted. Therefore, only the earliest part of the experiment gave reliable data.

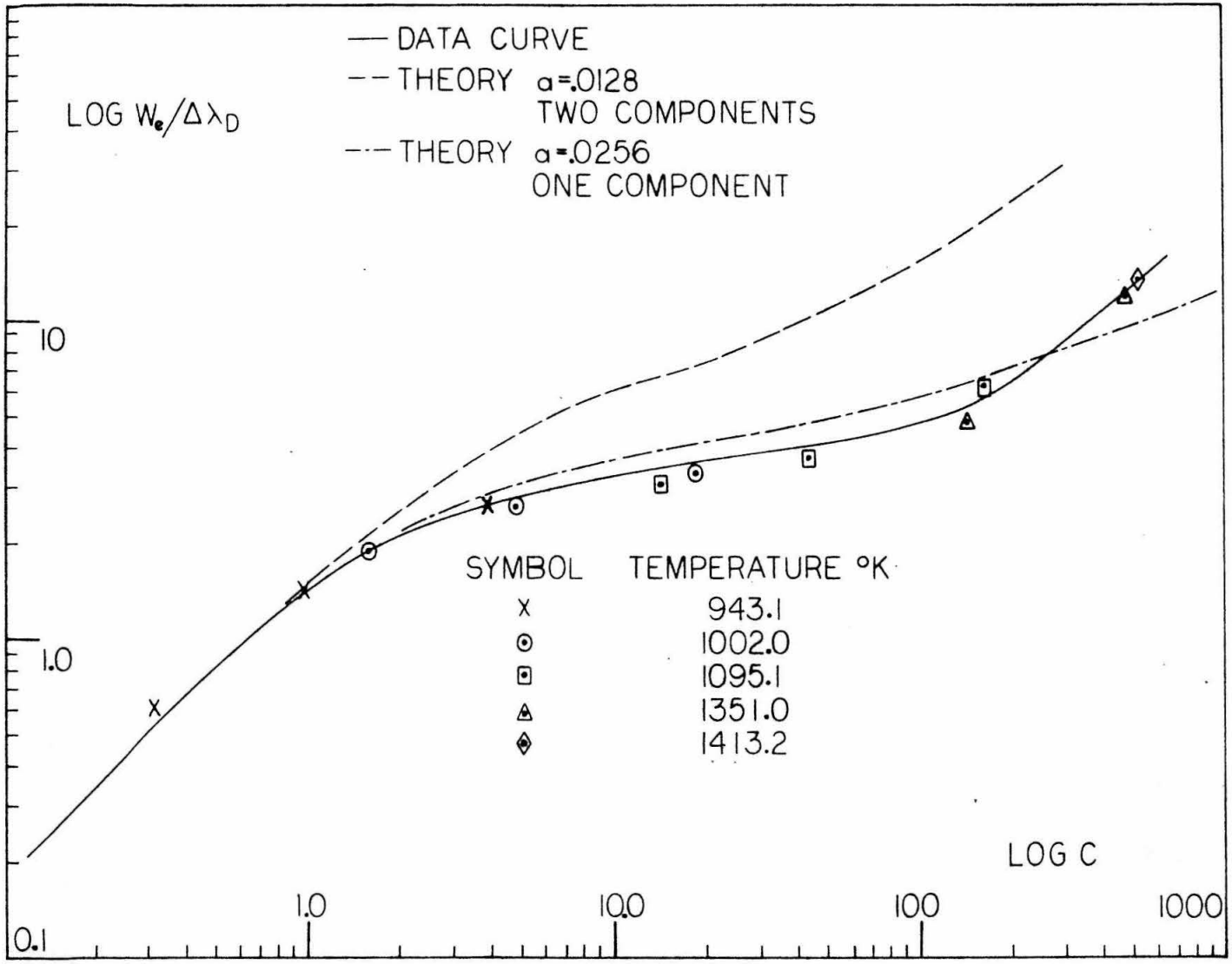

FIGURE 23 CURVE OF GROWTH OF IN λ=3039.36 A°

TABLE 16

Experimental Data For In. $\lambda = 3039.36$ Å

T (°K)	$\Delta\lambda_D$ (mÅ)	W_{L1} (mÅ) L1=.530	W_{L2} (mÅ) L2=1.60	W_{L3} (mÅ) L3=6.16	$W_{L1}/\Delta\lambda_D$	$W_{L2}/\Delta\lambda_D$	$W_{L3}/\Delta\lambda_D$
943.1*	3.757	2.22	5.28	9.40	0.591	1.405	2.502
1002.0	3.861	7.20	9.85	12.37	1.865	2.551	3.205
1095.1	4.035	12.37	14.96	25.11	3.065	3.708	6.223
1351.0	4.480	21.11	55.20		4.711	12.40	
1413.2	4.585	63.3			13.82		

$\lambda = 4101.76$ Å

911.0	4.976	0.80	2.46	6.95	0.160	0.495	1.402
943.1*	5.063	2.07	5.23	13.87	0.408	1.032	2.740
1002.1	5.204	5.41	13.64	17.44	1.039	2.621	3.351
1095.1	5.690	18.24	21.23	25.90	3.205	3.731	4.552

* Data taken on separate experimental runs. Some data lost due to adsorption of Indium on quartz cell.

TABLE 17

Calculations For The f-Value Of In. λ=3039.36 Å

I.P.=0.0000 eV

T (°K)	S(E), (L)	$gf\times10^{-11}$	$gfT\times10^{-14}$	$Pf\times10^{8}$	$P\times10^{6}$	f(abs)
943.1	0.341(1)	0.523	0.508	0.692	0.020	0.345
	0.918(2)	0.468	0.455	0.620		0.310
	3.69 (3)	0.490	0.476	0.650		0.325
1002.0	1.56 (1)	2.47	2.59	3.54	0.102	0.347
	4.77 (2)	2.50	2.63	3.59		0.352
	17.3 (3)	2.35	2.47	3.37		0.345
1095.1	13.3 (1)	22.01	26.51	36.3	1.05	0.343
	39.9 (2)	21.83	26.30	35.9		0.341
	158. (3)	22.46	27.04	37.9		0.350
1351.0	158. (1)	289.0	390.5	532.x10	150.0	0.355
	468. (2)	281.2	380.4	535.x10		0.357
1413.2	492. (1)	923.4	1305.0	$178.\times10^{2}$	524.0	0.340

f(abs)=0.339 ± 0.013

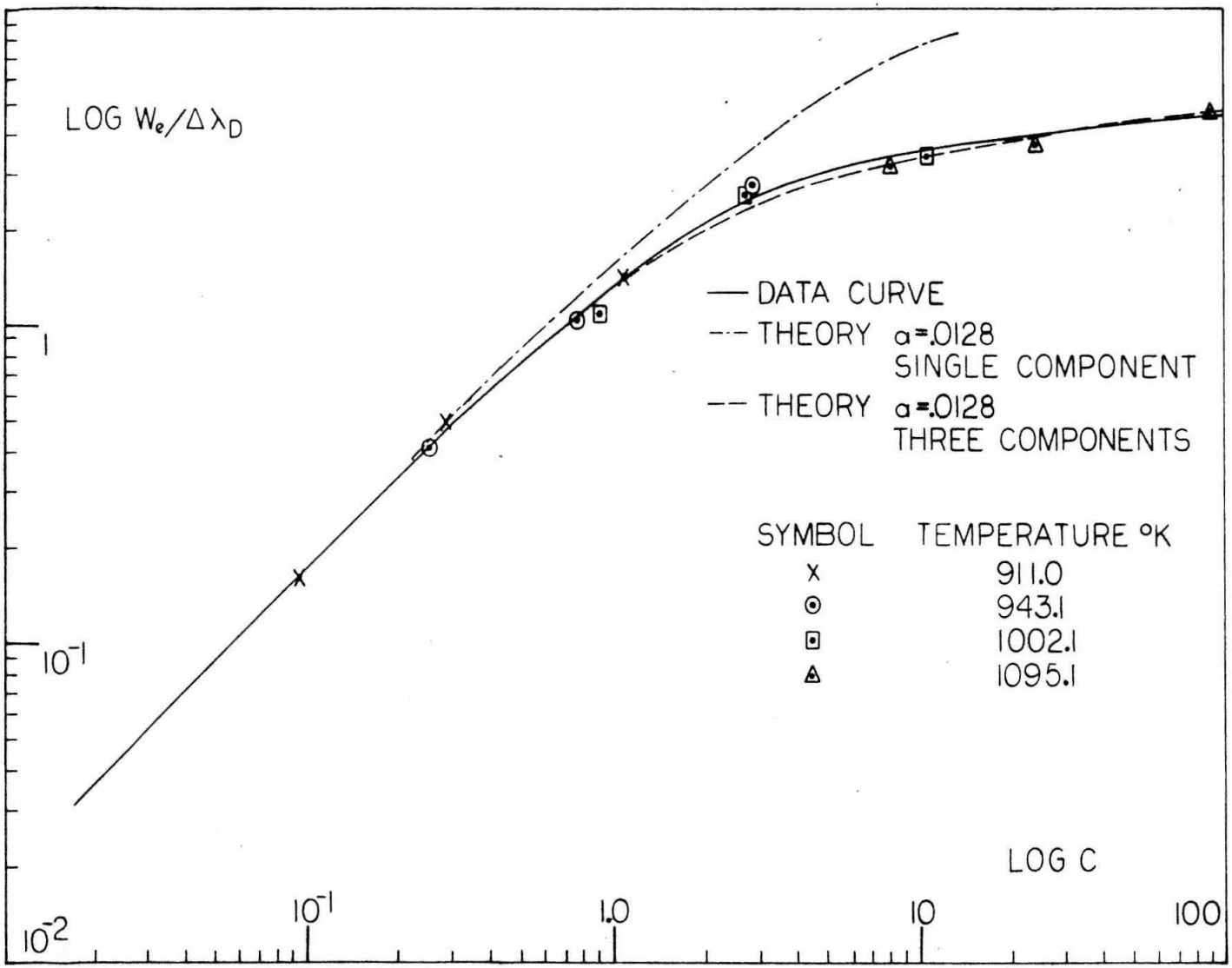

FIGURE 24 CURVE OF GROWTH OF In λ=4101.76 A°

TABLE 18

Calculations For The f-Value Of In. λ=4101.76 Å

L.P.=0.0000 eV

T (°K)	C(T), (L)	$Nf \times 10^{-10}$	$NfI \times 10^{-13}$	$Pf \times 10^{8}$	$P \times 10^{7}$	$\overset{*}{f}$(abs)
911.0	0.090(1)	1.072	0.997	0.135	0.069	0.197
	0.279(2)	1.043	0.970	0.131		0.191
	1.076(3)	1.035	0.963	0.129		0.188
943.1	0.235(1)	2.851	2.76	0.376	0.199	0.188
	0.702(2)	2.669	2.59	0.352		0.177
	3.26 (3)	3.190	3.08	0.419		0.210
1002.1	0.881(1)	10.30	10.8	1.47	1.02	0.144
	2.74 (2)	10.61	11.1	1.51		0.148
	10.6 (3)	10.69	11.2	1.53		0.150
1095.1	7.89 (1)	100.9	121.5	16.6	10.5	0.158
	23.5 (2)	99.6	120.0	16.4		0.156
	95.0 (3)	104.5	125.8	17.1		0.164

$\overset{*}{f}$(abs)=0.172 ± 0.022

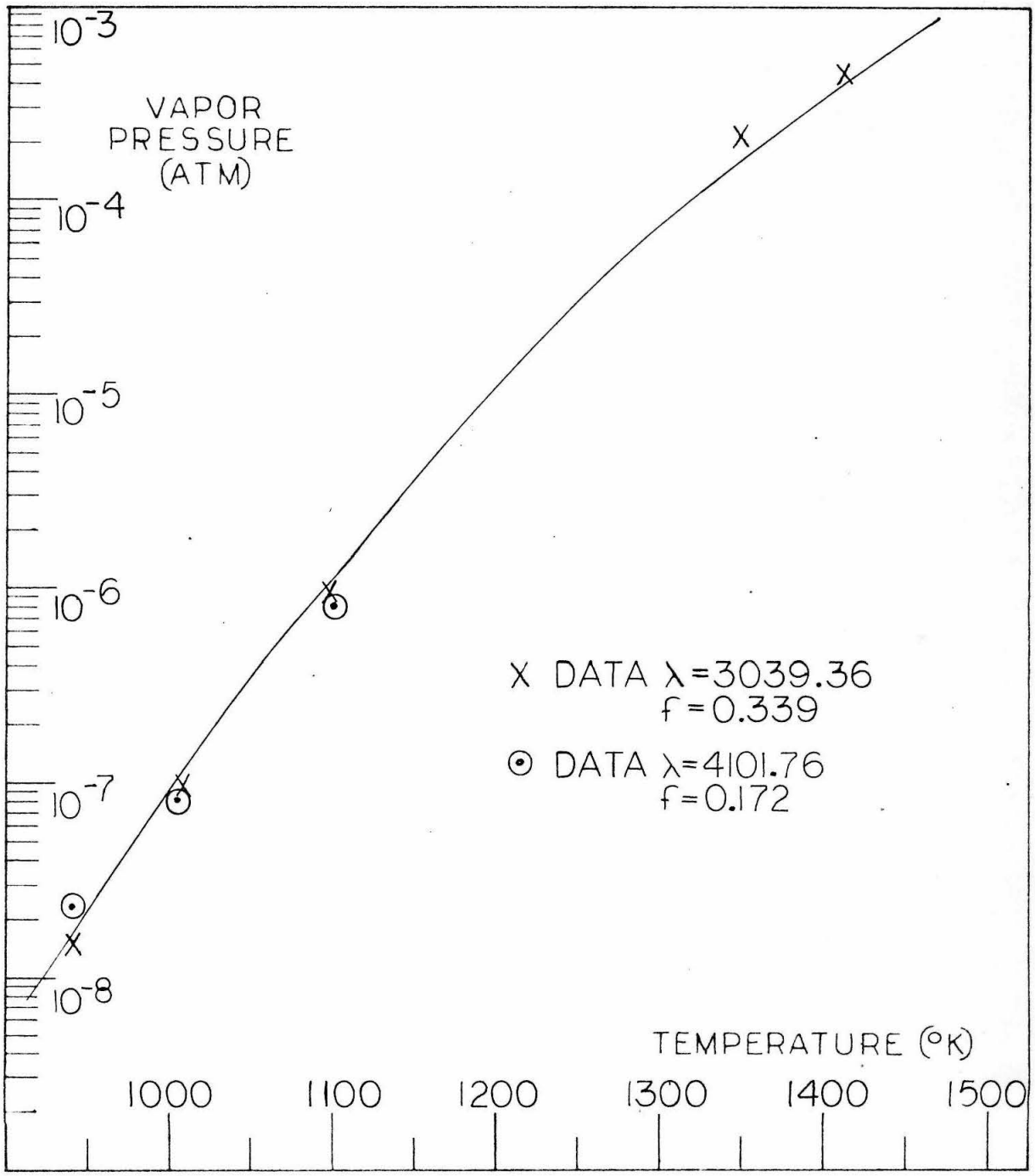

FIGURE 25 VAPOR PRESSURE OF In VS TEMPERATURE

TABLE 19

Experimental Data For Tl. $\lambda = 3775.72\text{Å}$

T (°K)	$\Delta\lambda_D$(mÅ)	W_{L1}(mÅ) L1=0.19	W_{L2}(mÅ) L2=.481	W_{L3}(mÅ) L3=1.55	W_{L4}(mÅ) L4=6.12	$W_{L1}/\Delta\lambda_D$	$W_{L2}/\Delta\lambda_D$	$W_{L3}/\Delta\lambda_D$	$W_{L4}/\Delta\lambda_D$
638.5	2.867			0.295	1.16			0.103	0.406
659.5	2.912		0.213	0.684	3.16		0.073	0.235	1.087
694.0	2.992	0.246	1.06	2.79	9.54	0.082	0.354	0.934	3.189
704.3	3.007	0.767	1.62	4.57	13.11	0.255	0.539	1.520	4.360
752.0	3.109	4.28	8.08	21.58	43.34	1.375	2.601	6.943	13.94
770.0	3.137	7.80	15.93	22.94	55.18	2.479	5.062	10.47	17.54
788.1	3.183	12.68	23.74	42.46	67.70	3.986	7.457	13.34	21.27
801.9	3.192	19.66	30.67	49.53	76.01	6.126	9.556	15.43	23.68
912.3	3.413	29.59	43.65	66.41	105.61	8.671	12.79	19.46	30.94
									$\lambda = 2767.87\text{Å}$
749.2	2.196			3.30	10.23			1.501	4.655
767.3	2.219	0.781	1.82	5.37	14.98	0.352	0.818	2.420	6.751
832.0	2.311	4.51	10.05	21.30	36.56	1.950	4.351	9.218	15.82

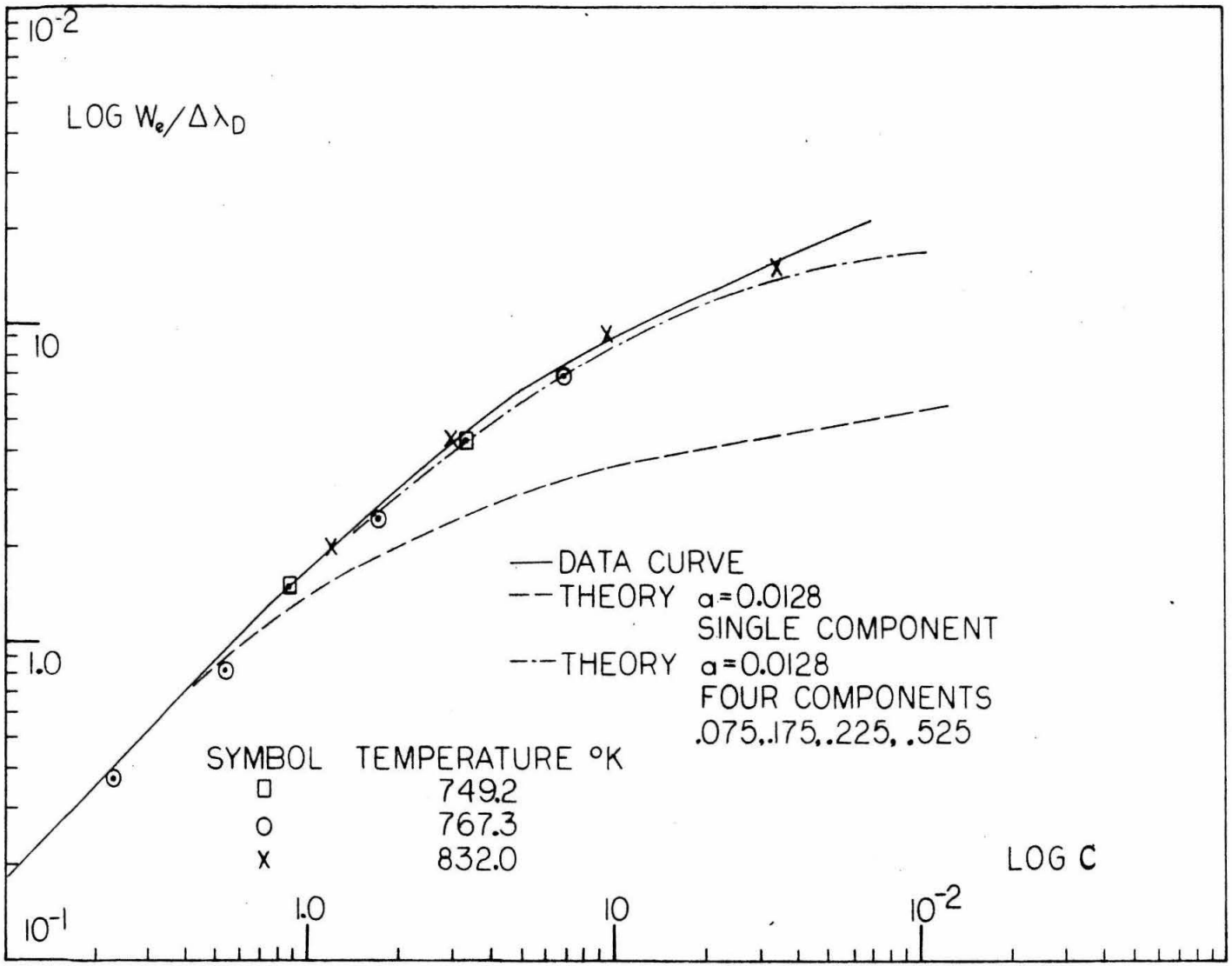

FIGURE 26 CURVE OF GROWTH OF T_L λ=2667.87 A°

TABLE 20

Calculations For The f-Value Of Tl. λ=2767.87 Å

E.P.=0.0000 eV

T (^{o}K)	C(T), (L)	Nfx10^{-10}	NfTx10^{-13}	Pfx10^{8}	Px10^{7}	f^{*}(abs)
749.2	0.822(3)	3.280	2.457	0.335	1.48	0.226
	3.24 (4)	3.274	2.453	0.334		0.226
767.3	0.199(1)	6.544	5.021	0.684	2.72	0.251
	0.480(2)	6.256	4.801	0.654		0.240
	1.55 (3)	6.248	4.794	0.653		0.240
	6.82 (4)	6.147	4.717	0.643		0.236
832.0	1.19 (1)	41.73	33.89	4.62	21.5	0.215
	2.51 (2)	33.96	28.25	3.85		0.179
	8.37 (3)	35.12	29.22	3.99		0.186
	34.2 (4)	36.35	30.24	4.12		0.192

$\bar{f}$(abs)=0.219 ± 0.020

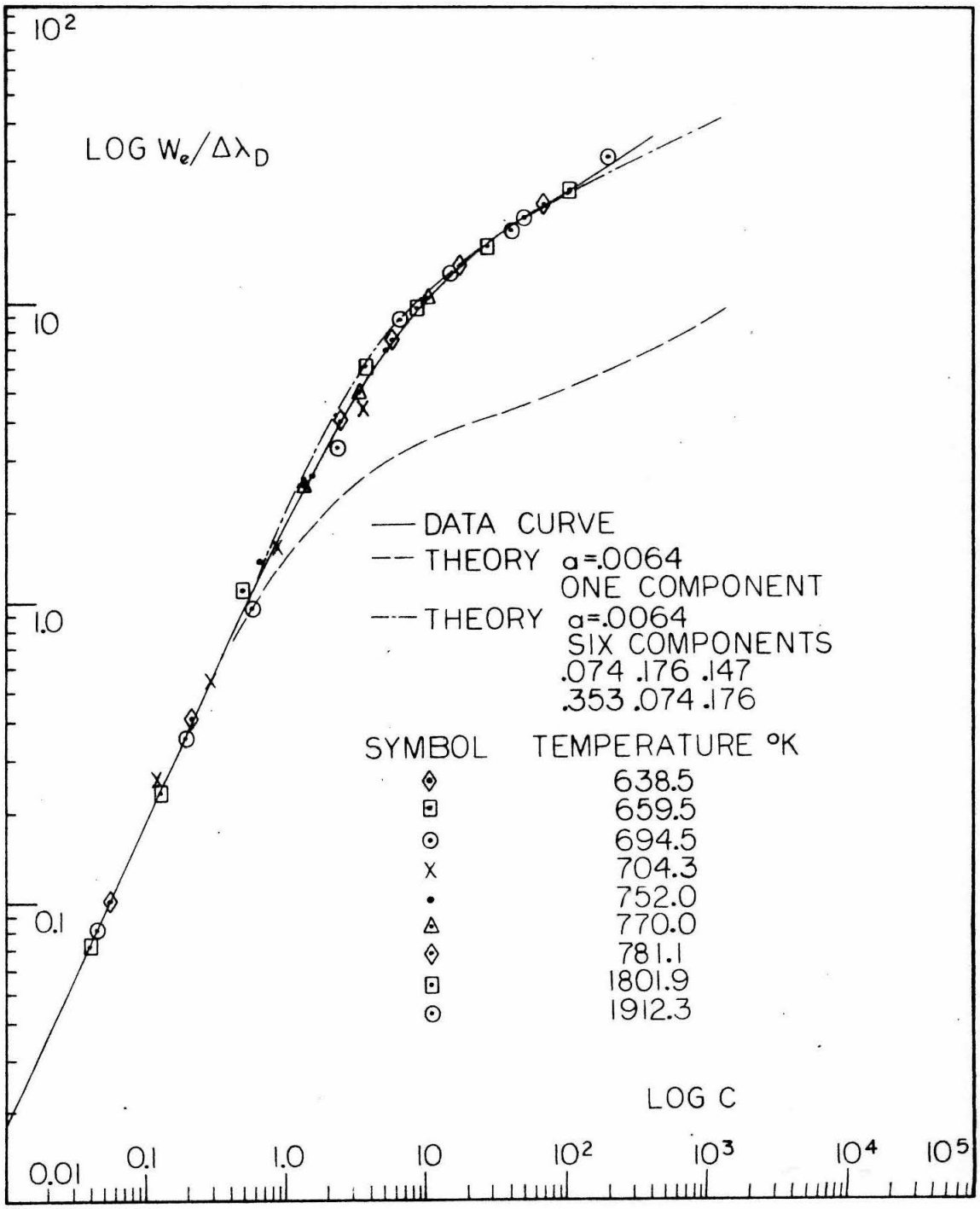

FIGURE 27 CURVE OF GROWTH OF Tl λ=3775.72 A°

TABLE 21

Calculations For The f-Value Of Tl. λ=3775.72 Å

L.P.=0.0000 eV

T (°K)	C(T), (L)	$Nf \times 10^{-10}$	$NfT \times 10^{-13}$	$Pf \times 10^{9}$	$P \times 10^{7}$	f*(abs)
638.5	0.060(3)	0.152	0.097	0.132	0.011	0.120
	0.235(4)	0.154	0.099	0.134		0.122
659.5	0.042(2)	0.358	0.236	0.321	0.030	0.107
	0.135(3)	0.356	0.235	0.320		0.107
	0.615(4)	0.411	0.271	0.370		0.123
694.0	0.200(2)	1.749	1.314	1.65	0.149	0.111
	0.545(3)	1.479	1.026	1.40		0.094
	2.15 (4)	1.478	1.025	1.40		0.094
704.3	0.142(1)	3.161	2.225	3.03	0.252	0.120
	0.302(2)	2.175	1.868	2.55		0.101
	0.905(3)	2.469	1.738	2.37		0.094
	3.41 (4)	2.357	1.659	2.26		0.090
752.0	0.790(1)	18.17	14.37	19.6	1.54	0.127
	1.66 (2)	15.08	11.93	16.2		0.105
	5.55 (3)	15.65	12.38	16.9		0.110
	22.0 (4)	15.73	12.43	17.0		0.111
770.0	1.57 (1)	36.55	28.15	38.3	2.95	0.130
	3.59 (2)	33.02	25.43	34.6		0.117
	11.2 (3)	31.96	24.61	33.5		0.114
	47.6 (4)	34.94	26.94	36.7		0.124

(cont'd)

TABLE 21a

Calculations For The f-Value Of Tl. λ=3775.72 Å

E.P.=0.0000 eV

T (^{o}K)	C(T), (L)	$Nf \times 10^{-10}$	$NfT \times 10^{-13}$	$Pf \times 10^{9}$	$P \times 10^{7}$	f(abs)*
788.1	2.68 (1)	63.11	49.73	67.8	5.95	0.114
	6.35 (2)	59.07	46.55	63.5		0.107
	19.4 (3)	55.95	44.08	60.1		0.101
	71.8 (4)	55.76	44.17	60.2		0.101
801.9	4.10 (1)	97.29	78.0	106.5	9.80	0.109
	9.50 (2)	89.12	71.4	97.2		0.099
	30.1 (3)	88.68	71.1	96.6		0.099
	120. (4)	88.94	71.3	97.3		0.099
912.3	7.05 (1)	198.3	162.5	222.	210.	0.106
	16.3 (2)	162.6	148.3	202.		0.096
	53.5 (3)	165.5	151.0	206.		0.098
	218.0 (4)	170.9	155.9	313.		0.101

$\bar{f}$(abs)=0.108 ± 0.010

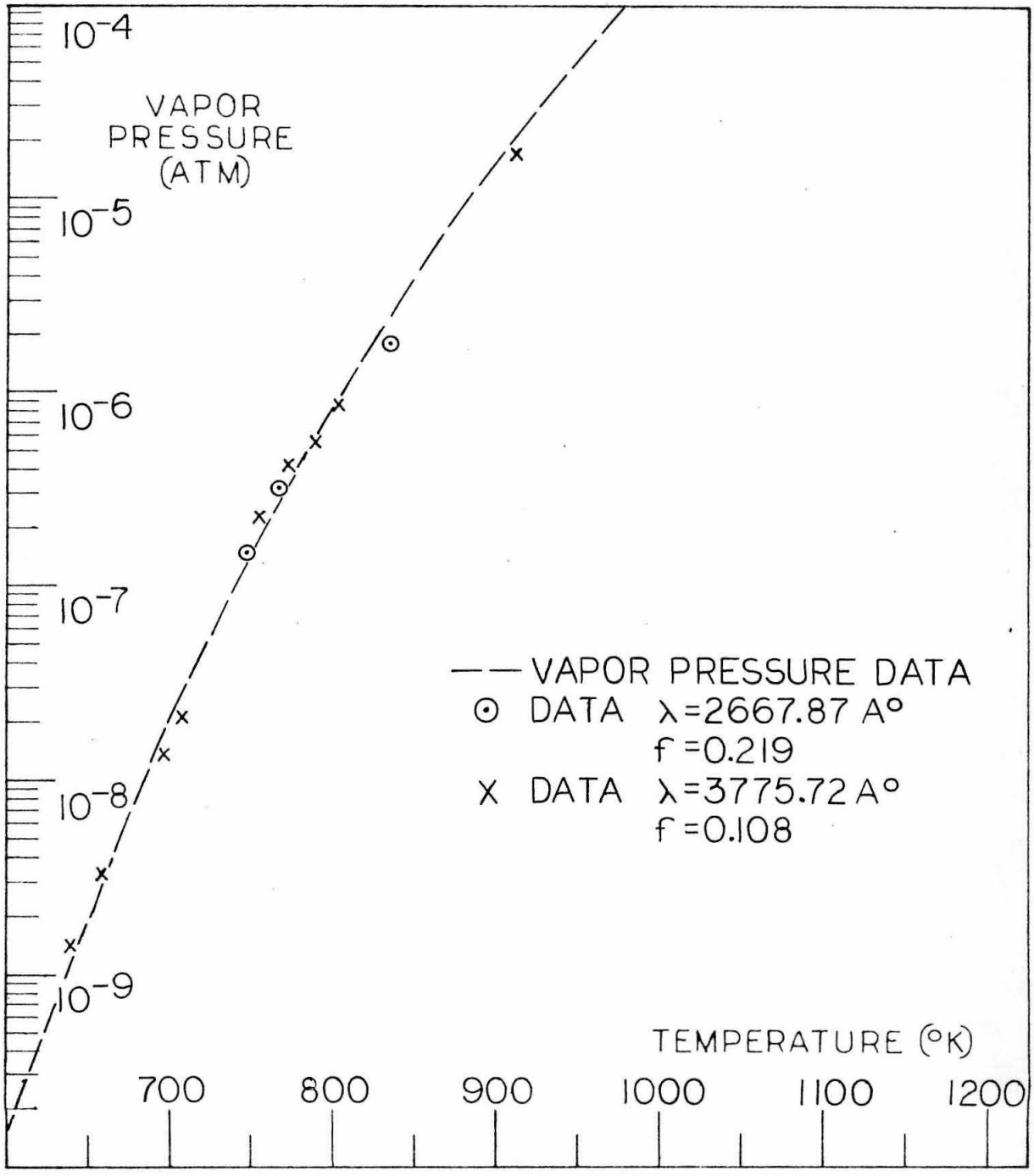

FIGURE 28 VAPOR PRESSURE OF Tl VS TEMPERATURE

VIII. THE RESULTS FOR TIN AND LEAD

A. The Sn and Pb lines measured were part of a multiplet $6p\ ^3P - 7s\ ^3P$ with only four of the lines present. The other two lines are forbidden by the $j = 0, \pm 1$ rule (ie., $j = 2 \rightarrow j = 0$) and the $j = 0$ to $j = 0$ forbidden rule. The f-value for Pb, λ2833 is well known, but those for Tin are not. In the case of Sn, the two excited levels are at 0.21eV and 0.425eV which gives them appreciable population at the temperatures used. For Pb, on the other hand, the levels are at 0.96eV and 1.3eV for the $j = 1$ and $j = 2$ states, respectively. In the temperature range studied, the upper state population is only a very small fraction of the total N.

B. Of the Tin lines, only the λ2863 line was measured at high enough $W/\Delta\lambda_D$'s to consider the hyperfine splitting. Tin consists of 83.7% of even isotopes 112, 114, 116, 118, and 122 which have no appreciable splitting. The 16.8% odd isotopes 115, 117, and 119 have $I = \frac{1}{2}$, yielding two components separated from the even isotopes by +6.5mÅ and -13mÅ with 0.33 and 0.67 intensities. These, however, only amount to about 6% and 10% of the total line. The curve of growth in figure 29 verifies that this line is nearly a single component line. Figures 30 and 31 show the curves of growth of the λ3009 ($j = 1$ to $j = 1$) and 3175 ($j = 2$ to $j = 1$) lines, respectively. The data are presented in tables 22 and 24, and the calculations in tables 23 and 25. The results are

$f(\lambda 2863) = 0.332 \pm 0.027$

$f(\lambda 3009) = 0.0419 \pm 0.0013$

$f(\lambda 3175) = 0.0651 \pm 0.0061$

The vapor pressure data used was that recommended by the University of California Metallurgy Department[17] derived by F. D. Gaidos and revised in 1962 by R. L. Orr.

Previously, Prokof'ev, Nagibina, and Petrova[43] found an arc emission value for 2863 of 0.24. Recently, J. Link[15] got a result of 0.20. The result here is higher than either. The Tin result came from a long run during which several traverses in temperature were made, and therefore, the only difficulty would seem to be the vapor pressure data. Link's results on the λ3009Å line were 0.030, and on the λ3175Å line they were 0.063. His relative f-values are not in agreement with this experiment. The relative f-values obtained in this experiment should be the most reliable, due to the equilibrium conditions involved. The difficulties lie in the ability to calculate the relative populations, which depend on the temperature.

C. The Pb, λ2833 line was used as a reference in section IV, paragraph D. There it was shown, that the curve of growth (figure 33) nicely fits the four-component theory. The data and calculations are presented in tables 26 and 27, and the result given there is

$f(\lambda 2833) = 0.229 \pm 0.018$

A result in excellent agreement with this was previously

obtained by Bell and King[13], and a calculation by T. Helliwell[6] gives 0.23. Therefore, it is safe to conclude the value 0.23 is well established, since all methods seem to be in excellent agreement.

The data on the other lines of the multiplet (tables 28, 29, and 30) are shown below with those of Bell and King, and Helliwell.

	Vapor Pressure	Atomic Beam	Calculations
f(3683)	= 0.243 ± 0.030	0.165	0.168
f(3639)	= 0.106 ± 0.010	0.092	0.088
f(4057)	= 0.419 ± 0.023	0.350	0.365

The results tabulated by Corliss and Bozman[21] are 0.213, 0.087 and 0.46, respectively. In each case the data obtained in this experiment were higher than those of King and Helliwell. The difference could be explained on the basis of an error in the high temperature vapor pressure data of about 10 to 20%. The results of Corliss and Bozman could be in error easily through the temperature calibration of the arc source.

The fit to the vapor pressure data is shown in figure 37 (the curves of growth are figures 34, 35, and 36) and matches reasonably well over a 400°K range so that the current data seem to be as reliable as the vapor pressure. The results of King and Helliwell being in agreement, the implication is that the vapor pressure data are low in the temperature region above 1000°K.

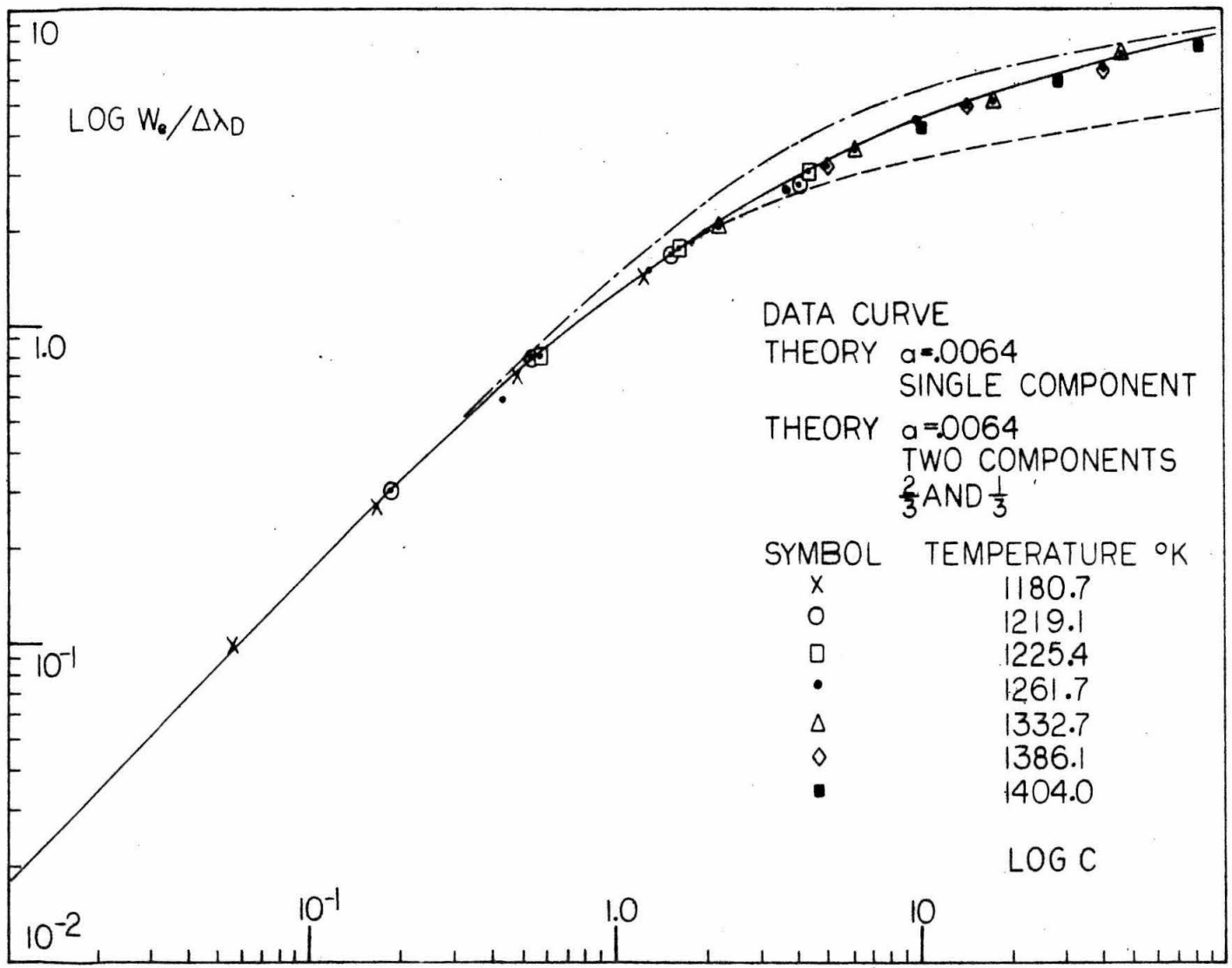

FIGURE 29 CURVE OF GROWTH OF Sn λ=2863.33 A°

TABLE 22

Experimental Data For **Sn.** $\lambda = 2863.33\,\text{Å}$

T (°K)	$\Delta\lambda_D$ (mÅ)	W_{L1} (mÅ) L1=0.27	W_{L2} (mÅ) L2=0.78	W_{L3} (mÅ) L3=2.22	W_{L4} (mÅ) L4=5.93	$W_{L1}/\Delta\lambda_D$	$W_{L2}/\Delta\lambda_D$	$W_{L3}/\Delta\lambda_D$	$W_{L4}/\Delta\lambda_D$
1180.7	3.890	0.385	1.06	2.68	5.47	0.099	0.272	0.688	1.405
1219.1	3.964	1.18	3.13	7.01	11.18	0.299	0.792	1.770	2.820
1225.4	3.966	1.24	3.11	7.01	12.16	0.315	0.785	1.768	3.065
1261.7	4.014	2.31	5.82	10.92	17.56	0.575	1.452	2.722	4.374
1332.7	4.116	4.15	9.40	14.83	22.10	1.006	2.285	3.603	5.368
1386.1	4.208	8.71	13.72	21.79	31.78	2.070	3.621	5.180	7.551
1404.0	4.234	13.64	21.30	27.17	36.60	3.221	5.030	6.402	8.502

TABLE 23

Calculations For The f-Value Of Sn. λ=2863.33 Å

E.P.=0.0000 eV

T (^{o}K)	C(T), (L)	Hfx10^{-11}	HfTx10^{-14}	Pfx10^{8}	Px10^{7}	f(abs)
1180.7	0.058(1)	0.204	0.339	0.461	0.152	0.302
	0.161(2)	0.916	0.325	0.442		0.291
	0.455(3)	0.195	0.323	0.441		0.291
	1.14 (4)	0.183	0.304	0.413		0.271
1219.1	0.180(1)	0.646	1.142	1.55	0.481	0.322
	0.518(2)	0.643	1.136	1.54		0.322
	1.49 (3)	0.650	1.149	1.56		0.324
	3.78 (4)	0.616	1.091	1.49		0.310
1225.4	0.178(1)	0.639	1.096	1.56	1.525	0.297
	0.504(2)	0.670	1.197	1.63		0.310
	1.61 (3)	0.702	1.253	1.72		0.328
	4.55 (4)	0.743	1.326	1.82		0.346
1261.7	0.371(1)	1.349	2.546	3.46	1.18	0.295
	1.23 (2)	1.547	2.922	3.98		0.337
	3.46 (3)	1.528	2.886	3.93		0.333
	9.31 (4)	1.540	2.909	3.96		0.335
1332.7	2.04 (1)	7.601	15.40	20.8	5.20	0.400
	5.80 (2)	7.480	15.17	20.7		0.398
	15.5 (3)	7.049	14.29	19.6		0.377
	43.3 (4)	7.361	14.93	20.4		0.393

(cont'd)

TABLE 23a

Calculations For The f-Value Of Sn. λ=2863.33 Å

L.P.=0.0000 eV

T (°K)	C(T), (L)	Nfx10^{-11}	NfTx10^{-14}	Pfx10^{8}	Px10^{7}	f(abs)
1386.1	4.42 (1)	16.84	38.22	52.1	14.7	0.354
	12.2 (2)	16.07	36.51	49.8		0.339
	32.7 (3)	15.14	34.40	46.8		0.320
	99.8 (4)	17.30	39.29	53.4		0.364
1404.0	8.30 (1)	31.81	74.67	101.8	20.4	*0.499
	22.9 (2)	30.38	71.31	97.1		*0.476
	61.4 (3)	28.62	67.18	91.6		*0.449
	172. (4)	30.01	70.46	96.0		*0.471

$\bar{f}$(abs)=0.332 ± 0.027

* Without using the data at 1404.0°K which is on the end of the curve of growth, and which doesn't overlap the data at 1386.1.

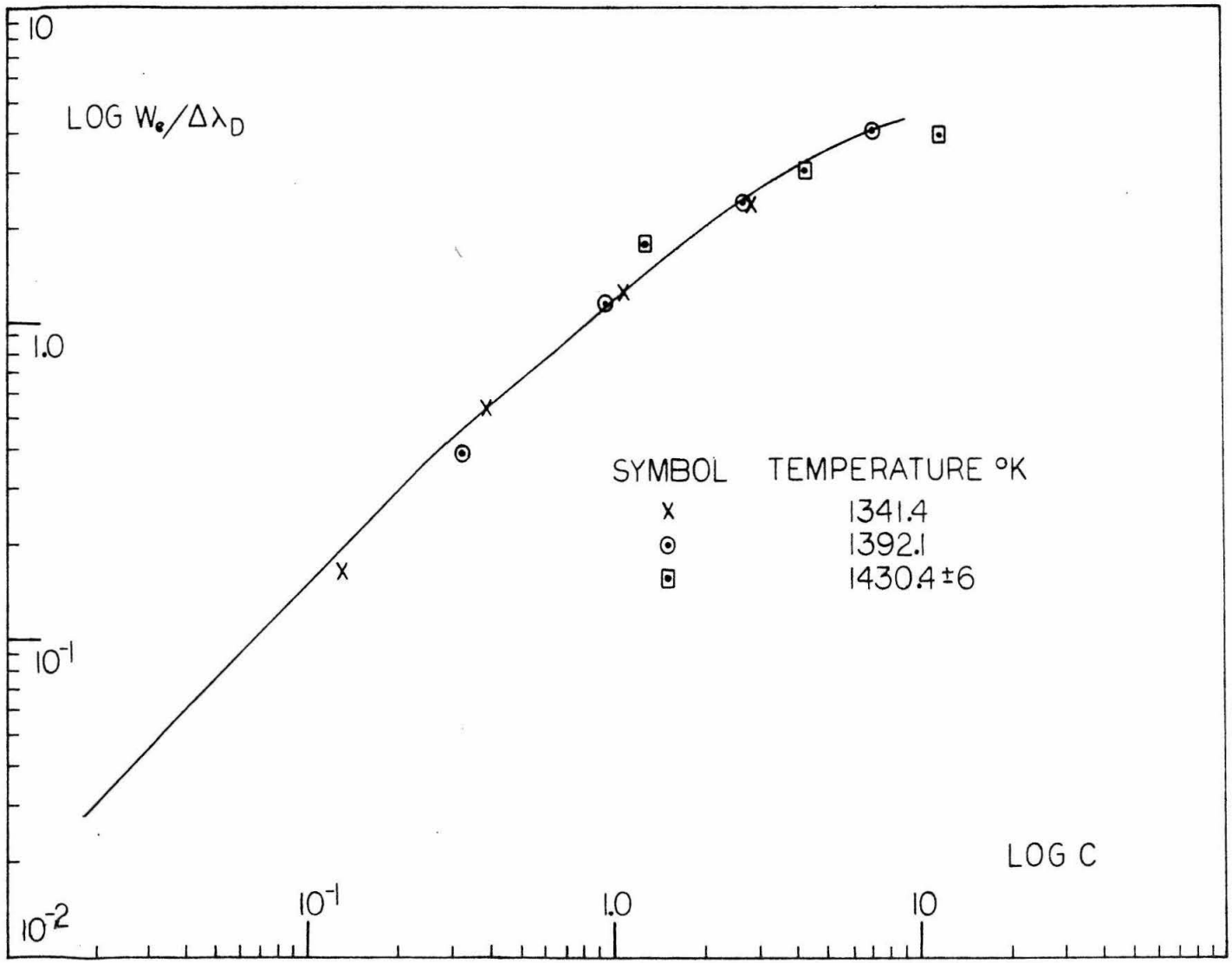

FIGURE 30 CURVE OF GROWTH OF SN λ=3009.4 A°

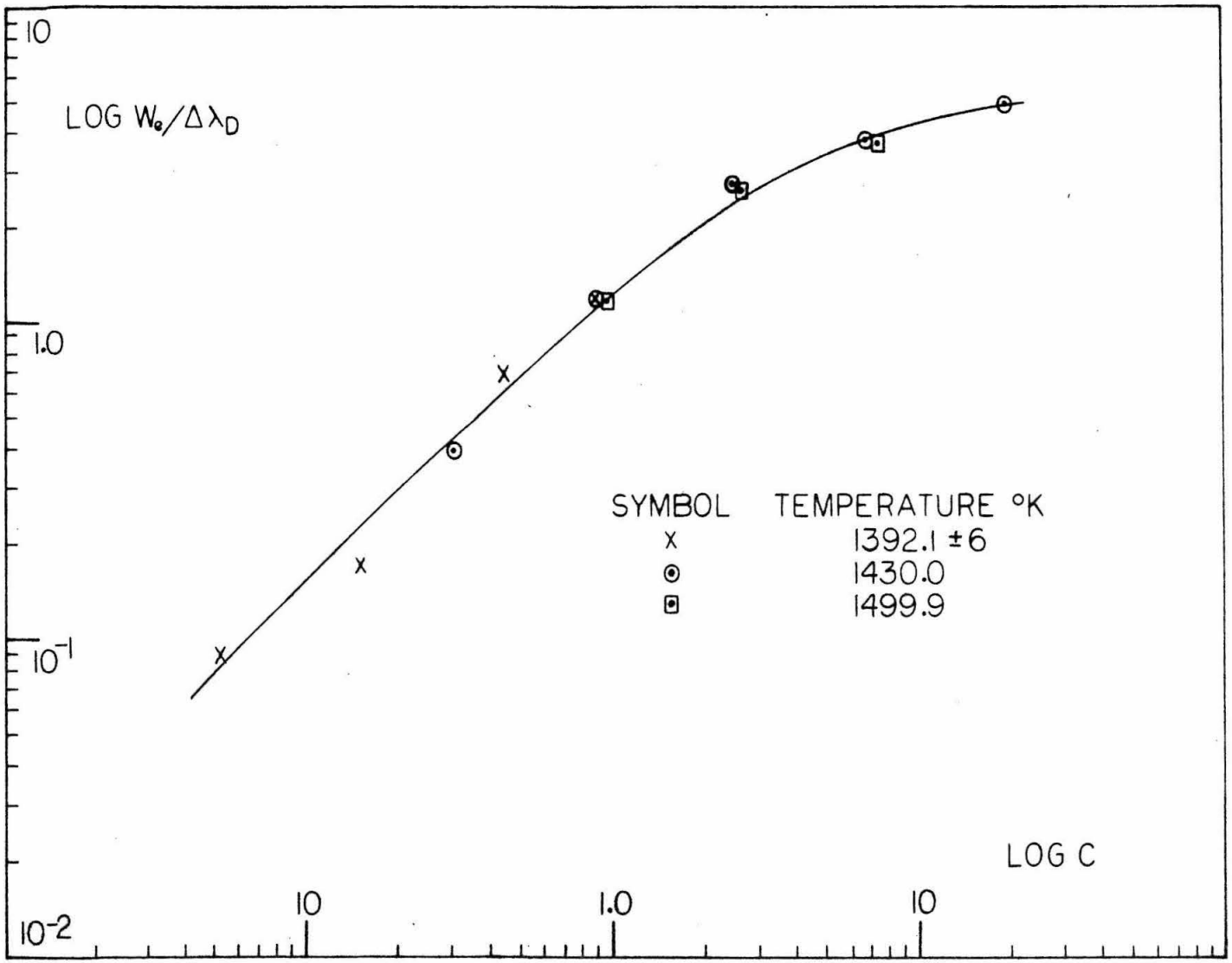

FIGURE 31 CURVE OF GROWTH OF Sn λ=3175.05 A°

TABLE 24

Experimental Data For Sn. $\lambda = 3009.14\text{Å}$

T (°K)	$\Delta\lambda_D$(mÅ)	W_{L1}(mÅ) L1=0.27	W_{L2}(mÅ) L2=0.78	W_{L3}(mÅ) L3=2.22	W_{L4}(mÅ) L4=5.93	$W_{L1}/\Delta\lambda_D$	$W_{L2}/\Delta\lambda_D$	$W_{L3}/\Delta\lambda_D$	$W_{L4}/\Delta\lambda_D$
1341.4	4.348	0.46	2.30	5.40	10.01	0.160	0.529	1.242	2.301
1392.1	4.428	1.64	5.22	10.58	17.75	0.370	1.179	2.389	4.008
									$\lambda = 3175.05\text{Å}$
1430.0	4.738	1.84	5.20	12.85	17.20	0.376	1.112	2.749	3.679
1499.9	4.853	5.38	12.74	16.72	23.21	1.108	2.625	3.449	4.283

Some data taken at 1392°K for $\lambda = 3175\text{Å}$ but temperature varied 6°K. This data appears on curve of growth only. The same is true for $\lambda = 3009\text{Å}$ at 1430°K.

TABLE 25

Calculations For The f-Value Of Sn.

λ=3009.14 Å

E.P.=0.2098 eV

T (°K)	C(T), (L)	Nfx10^{-11}	NfTx10^{-14}	Pfx10^{7}	Px10^{6}	f*(abs)
1341.4	0.124(1)	0.443	1.570	0.257	0.635	0.0405
	0.383(2)	0.472	1.683	0.275		0.0433
	1.08 (3)	0.468	1.659	0.271		0.0427
	2.82 (4)	0.458	1.622	0.265		0.0417
1392.1	0.297(1)	1.103	4.667	0.636	1.60	0.0398
	0.945(2)	1.187	5.023	0.685		0.0428
	2.66 (3)	1.174	4.968	0.677		0.0423
	7.12 (4)	1.177	4.988	0.678		0.0423

$\bar{f}$(abs)=0.0419 ± 0.0013

λ=3175.05 Å

E.P.=0.4250 eV

1430.0	0.287(1)	1.009	15.60	2.13	3.25	0.0655
	0.940(2)	1.135	17.55	2.39		0.0735
	2.88 (3)	1.138	17.59	2.40		0.0736
	6.69 (4)	1.063	16.43	2.24		0.0689
1499.9	0.930(1)	3.300	47.14	6.43	10.8	0.0595
	2.84 (2)	3.488	49.83	6.79		0.0627
	6.60 (3)	3.449	49.27	6.72		0.0622
	19.0 (4)	3.070	43.85	5.98		0.0554

$\bar{f}$(abs)=0.0651 ± 0.0061

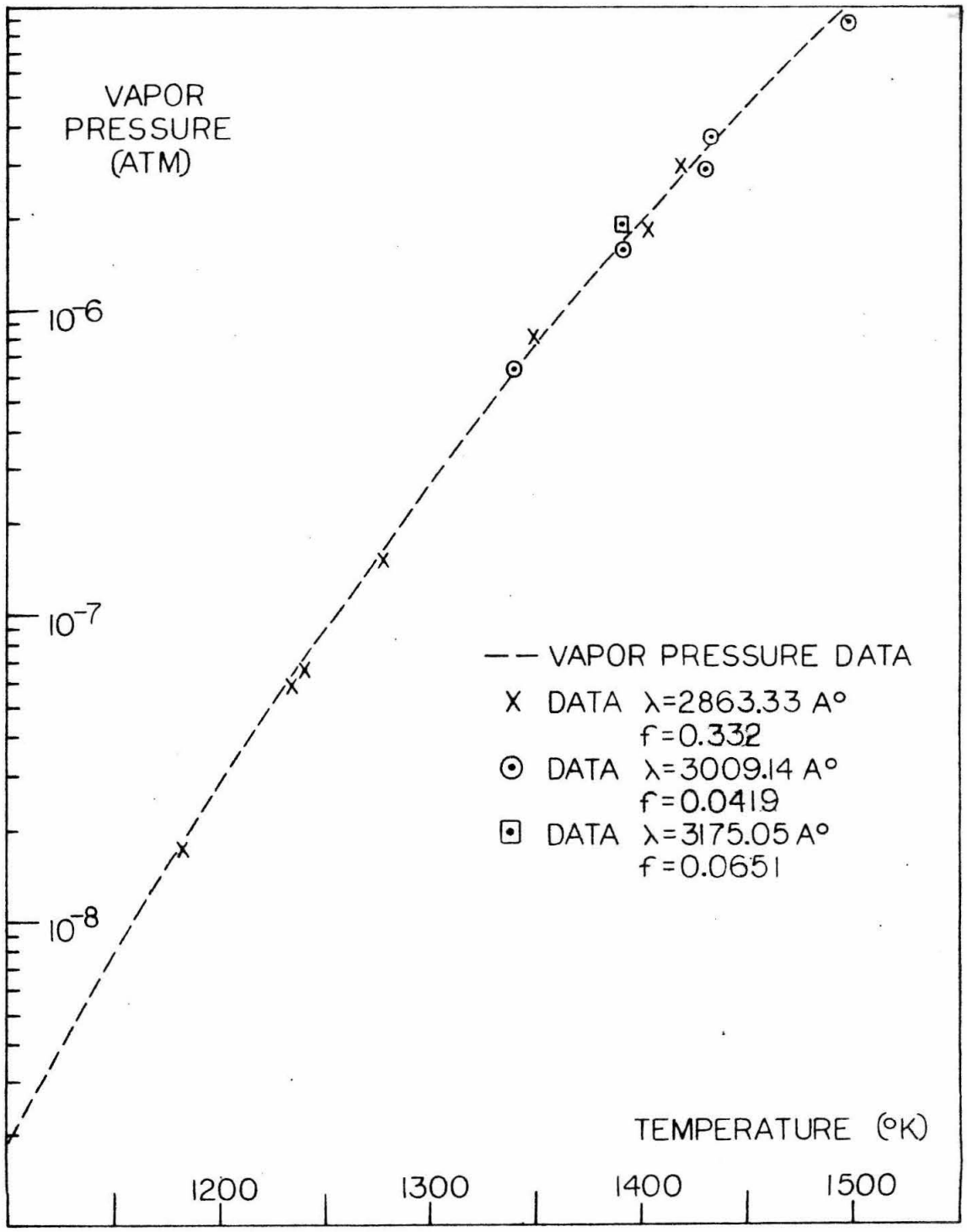

FIGURE 32 VAPOR PRESSURE OF Sn

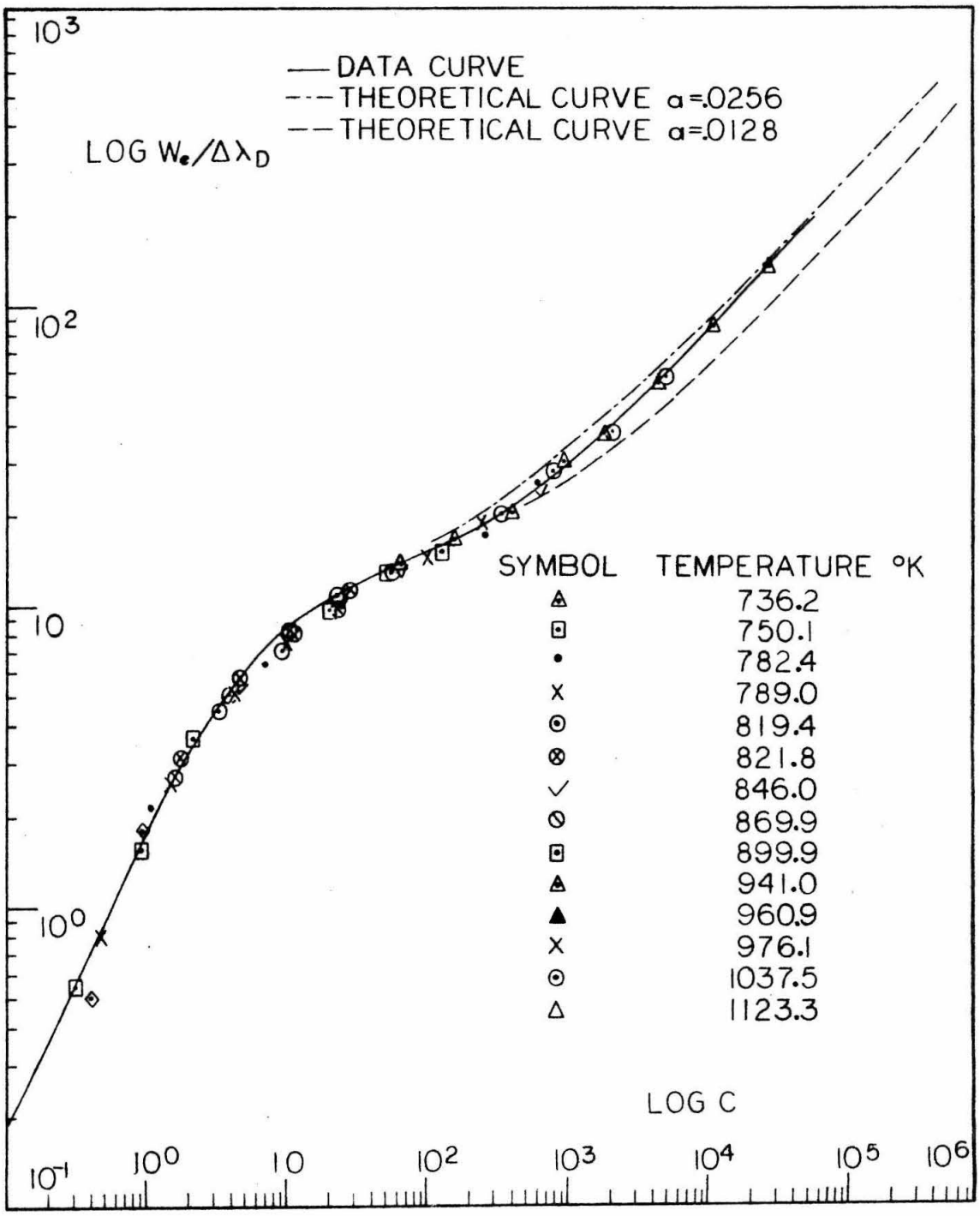

FIGURE 33 CURVE OF GROWTH OF Pb λ=2833.06 A°

TABLE 26

Experimental Data For Pb. $\lambda = 2833.06$ Å

T (°K).	$\Delta\lambda_D$ (mÅ)	W_{L1} (mÅ) L1=0.43	W_{L2} (mÅ) L2=0.96	W_{L3} (mÅ) L3=2.53	W_{L4} (mÅ) L4=6.21	$W_{L1}/\Delta\lambda_D$	$W_{L2}/\Delta\lambda_D$	$W_{L3}/\Delta\lambda_D$	$W_{L4}/\Delta\lambda_D$
736.2	2.325			1.19	4.25			0.515	1.830
750.1	2.346		1.29	3.61	8.40		0.550	1.540	3.581
782.4	2.394		5.05	9.65	15.57		2.111	4.031	6.505
789.0	2.407	1.96	6.19	12.43	18.63	0.815	2.571	5.161	7.740
819.4	2.453	6.50	11.12	17.64	24.78	2.690	4.532	7.190	10.10
821.8	2.458	7.30	14.60	20.35	28.09	3.130	5.930	8.280	11.43
846.0	2.493	12.67	20.77	25.28	31.54	5.081	8.332	10.14	12.65
869.9	2.529	19.58	24.78	33.38	39.34	7.741	9.802	13.20	15.56
941.0	2.630			46.08	70.61			17.52	26.85
960.9	2.656	38.01	46.50	59.17	83.58	14.31	17.51	22.28	31.47
976.1	2.675	42.04	52.75	62.17	95.17	15.72	19.72	23.24	35.58
1037.5	2.760	57.19	77.18	106.8	163.0	20.72	27.96	38.69	59.05
1123.3	2.872	109.3	160.5	243.0	392.6	38.05	55.88	84.59	136.7

TABLE 27

Calculations For The f-Value Of Pb. λ=2833.06 Å

I.P.=0.0000 eV

T (°K)	C(T), (L)	Pfx10^{-11}	nPfx10^{-14}	Pfx10^{8}	Px10^{7}	f*(abs)
736.2	0.440(3)	0.104	0.076	0.105	0.053	0.198
	1.51 (4)	0.142	0.105	0.142		0.268
750.1	0.311(2)	0.190	0.143	0.194	0.092	0.211
	0.920(3)	0.213	0.160	0.219		0.238
	2.40 (4)	0.227	0.170	0.232		0.252
782.4	1.22 (2)	0.761	0.595	0.811	0.332	0.244
	3.95 (3)	0.934	0.731	0.996		0.300
	6.32 (4)	0.608	0.475	0.648		0.195
789.0	1.52 (2)	0.951	0.750	1.02	0.428	0.238
	3.95 (3)	0.932	0.735	1.00		0.234
	8.91 (4)	0.862	0.681	0.929		0.217
819.4	1.62 (1)	2.307	1.890	2.58	1.22	0.211
	3.39 (2)	2.162	1.772	2.42		0.198
	23.1 (4)	2.278	1.867	2.54		0.208
824.8	1.90 (1)	2.712	2.228	3.04	1.34	0.227
	4.90 (2)	3.133	2.574	3.51		0.262
	10.1 (3)	2.450	2.014	2.74		0.204
	28.2 (4)	2.786	2.289	3.12		0.233

(cont'd)

TABLE 27a

Calculations For The f-Value Of Pb. λ=2833.06 Å

L.P.=0.0000 eV

T (°K)	C(T), (L)	Mfx10^{-11}	MfTx10^{-14}	Pfx10^{8}	Px10^{7}	f*(abs)
846.0	4.25(1)	6.153	5.205	7.09	2.85	0.249
	9.80(2)	6.364	5.384	7.34		0.258
	19.5 (3)	4.799	4.059	5.53		0.194
	50.5 (4)	5.062	4.282	5.84		0.205
869.9	8.30(1)	12.19	10.60	14.5	6.20	0.234
	17.5 (2)	11.51	10.01	13.6		0.219
	50.5 (3)	12.60	10.96	15.0		0.242
	104. (4)	10.57	9.20	12.6		0.203
941.0	245. (3)	64.01	60.23	82.1	39.7	0.207
	705. (4)	74.46	70.07	95.5		0.241
960.9	66. (1)	101.8	97.84	133.	65.4	0.203
	175. (2)	120.8	116.0	158.		0.242
	395. (3)	103.6	101.7	135.		0.206
	4120. (4)	119.5	114.8	156.		0.239
976.1	93.5 (1)	145.2	141.7	193.	99.5	0.194
	285. (2)	198.2	193.4	264.		0.265
	560. (3)	147.8	142.9	199.		0.200
	1680. (4)	180.7	176.4	240.		0.241

(cont'd)

TABLE 27b

Calculations For The f-Value Of Pb. λ=2833.06 Å

L.P.=0.0000 eV

T (^{o}K)	C(T), (L)	Nfx10^{-11}	NfTx10^{-14}	Pfx10^{8}	Px10^{7}	f(abs)
1037.5	365.(1)	585.0	606.9	827.	383.	0.216
	920.(2)	660.3	685.0	934.		0.244
	2110.(3)	574.7	596.2	812.		0.212
	5250.(4)	582.7	604.5	824.		0.215
1123.3	1950.(1)	3252.	3653.	4980.	2100.	0.237
	4450.(2)	3323.	3732.	5090.		0.242
	11100.(3)	3146.	3535.	4820.		0.230
	28500.(4)	3291.	3747.	5110.		0.243

$\bar{f}$(abs)=0.229 ± 0.018

TABLE 28

Experimental Data For Pb. $\lambda = 3683.48$ Å

T (°K)	$\Delta\lambda_D$ (mÅ)	W_{L1} (mÅ) L1=0.43	W_{L2} (mÅ) L2=0.96	W_{L3} (mÅ) L3=2.53	W_{L4} (mÅ) L4=6.21	$W_{L1}/\Delta\lambda_D$	$W_{L2}/\Delta\lambda_D$	$W_{L3}/\Delta\lambda_D$	$W_{L4}/\Delta\lambda_D$
976.1	3.441		0.19	0.52			0.055	0.152	
1039.8	3.551				7.85				2.21
1095.2	3.645		3.83	7.69	17.35		1.05	2.11	4.76
1139.9	3.716		8.62	17.09	26.68		2.32	4.60	7.18
1152.2	3.736	6.50	14.23	23.13	29.96	1.74	3.81	6.19	8.02
1162.4	3.754	9.35	16.56	25.68	31.57	2.49	4.41	6.84	8.41
1303.0	3.993	32.06	37.93	46.52	51.95	8.03	9.50	11.65	13.01
									$\lambda = 4057.83$ Å
1203.2	4.238	3.51	8.41	17.35	30.01	0.828	1.984	4.094	7.080
									$\lambda = 3639.58$ Å
1035.2	3.507			1.06	2.61			0.304	0.745
1162.4	3.709	2.08	4.38	9.35	18.73	0.560	1.182	2.520	5.050
1303.0	3.946	23.36	33.07	47.04	63.85	5.92	8.38	11.92	16.10

TABLE 29

Calculations for the f-Value of Pb. λ=3683.48 Å

E.P.= 0.9694 eV

T (°K)	C(T), (L)	Nfx10^{-10}	NfTx10^{-17}	Pfx10^{5}	Px10^{4}	f*(abs)
976.1	0.033(2)	0.175	0.166	0.226	0.095	0.238
	0.087(3)	0.176	0.167	0.228		0.240
1039.8	1.59 (4)	1.33	0.950	1.29	0.420	0.307
1095.2	0.776(2)	4.18	2.02	2.75	1.25	0.220
	1.56 (3)	3.46	1.67	2.30		0.184
	4.52 (4)	3.91	1.89	2.58		0.206
1139.9	1.76 (2)	10.07	3.68	5.02	2.61	0.192
	4.11 (3)	8.93	3.26	4.45		0.170
	11.0 (4)	9.72	3.55	4.84		0.185
1152.2	1.26 (1)	16.19	5.57	8.62	3.31	0.230
	3.36 (2)	18.75	6.45	8.77		0.265
	7.62 (3)	16.66	5.73	7.81		0.236
	17.6 (4)	15.70	5.40	7.30		0.220
1162.4	1.48 (1)	19.01	6.19	8.44	3.83	0.220
	3.68 (2)	21.21	6.91	9.42		0.246
	9.66 (3)	20.91	6.81	9.28		0.242
	21.9 (4)	19.52	6.36	8.67		0.226
1303.0	16.54 (1)	226.7	36.11	49.2	17.0	0.289
	36.58 (2)	224.8	35.79	48.8		0.287
	99.20 (3)	231.3	36.83	50.2		0.295
	242.5 (4)	230.4	36.69	50.0		0.294

$\bar{f}$(abs) = 0.243 ± 0.030

TABLE 30

Calculations for the f-Value of Pb. $\lambda = 4057.83$ Å

E.P. = 1.320 eV

T (°K)	C(T), (L)	$Nf \times 10^{-10}$	$NfT \times 10^{-17}$	$Pf \times 10^{5}$	$P \times 10^{4}$	f(abs)
1203.0	0.570(1)	2.539	0.235	32.0	8.1	0.395
	1.42 (2)	2.855	0.264	36.0		0.444
	3.60 (3)	2.651	0.245	33.4		0.412
	9.25 (4)	2.733	0.258	34.5		0.425

$\bar{f}$(abs) = 0.419 ± 0.023

$\lambda = 3639.58$ Å

E.P. = 0.9694 eV

1035.2	0.182(3)	0.380	0.281	0.383	0.41	0.093
	0.478(4)	0.408	0.302	0.411		0.100
1162.4	0.339(1)	4.405	1.435	1.955	1.73	0.113
	0.781(2)	4.715	1.536	2.093		0.121
	1.80 (3)	3.979	1.296	1.765		0.102
	4.62 (4)	4.172	1.359	1.851		0.107
1303.0	6.13 (1)	85.28	13.58	18.5	17.0	0.109
	12.92 (2)	80.70	12.85	17.5		0.103
	35.07 (3)	82.96	13.21	18.0		0.106
	86.37 (4)	83.90	13.36	18.2		0.107

$\bar{f}$ = 0.106 ± 0.010

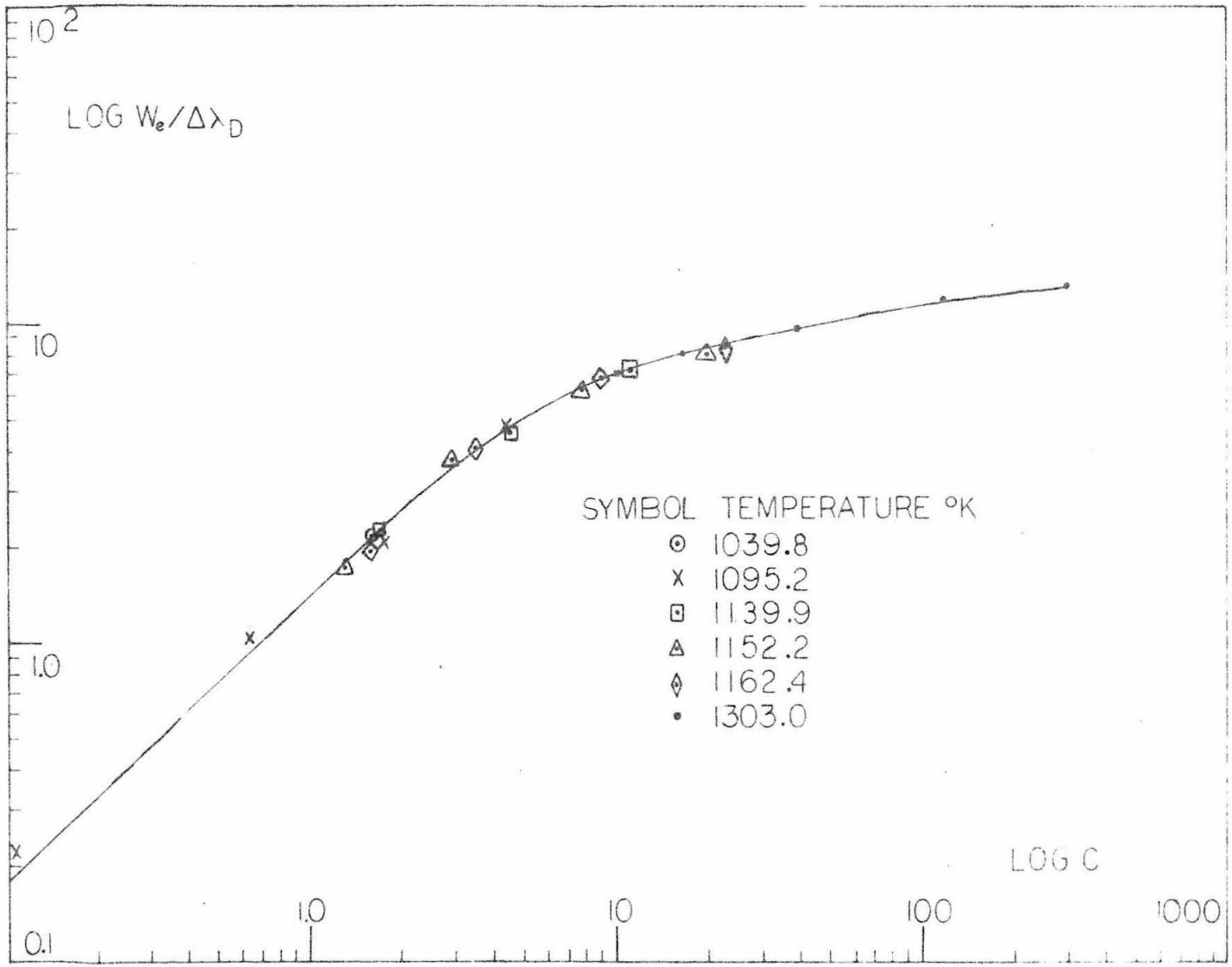

FIGURE 34 CURVE OF GROWTH OF PB λ=3683.48 A°

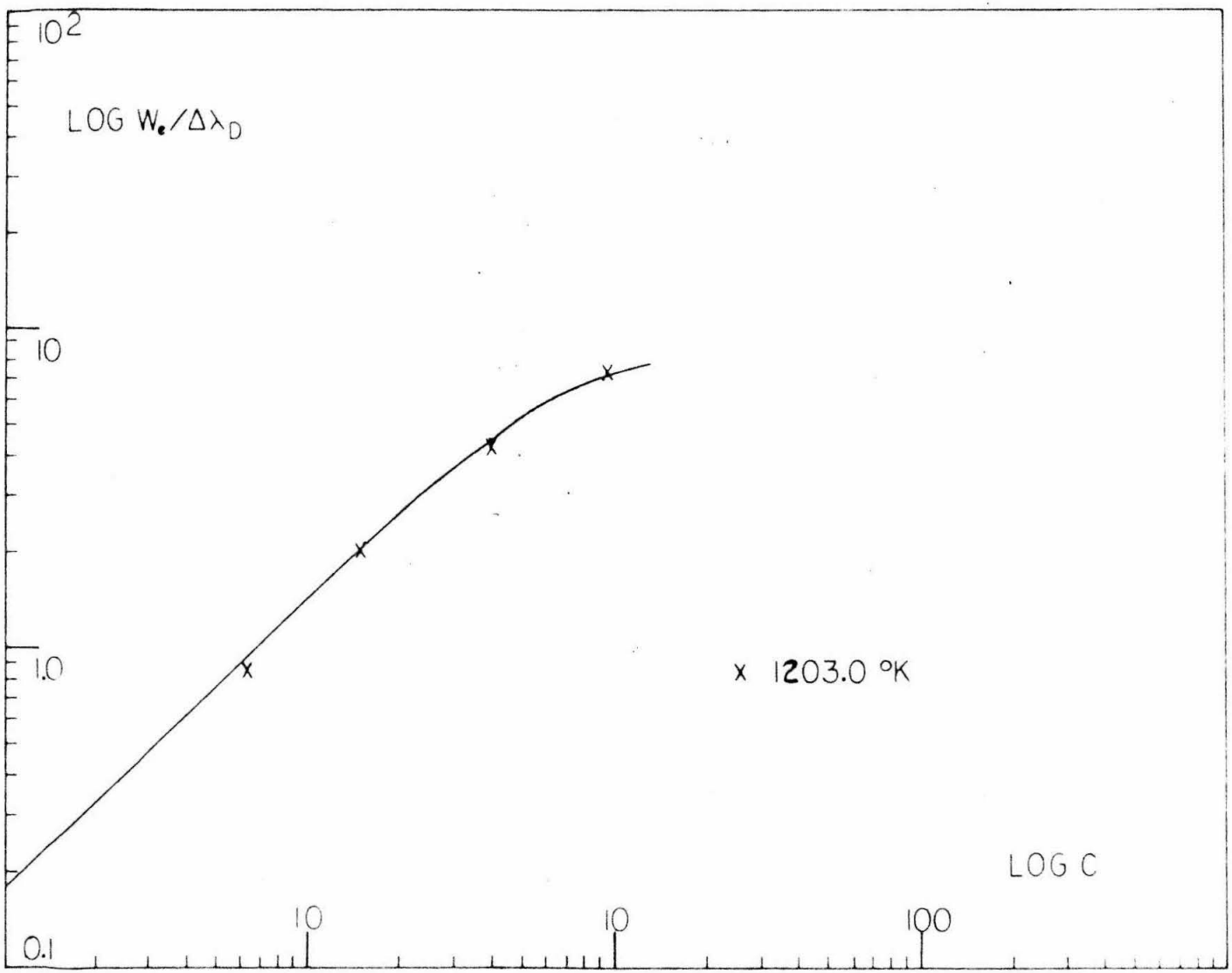

FIGURE 35 CURVE OF GROWTH OF Pb λ=4057.83A°

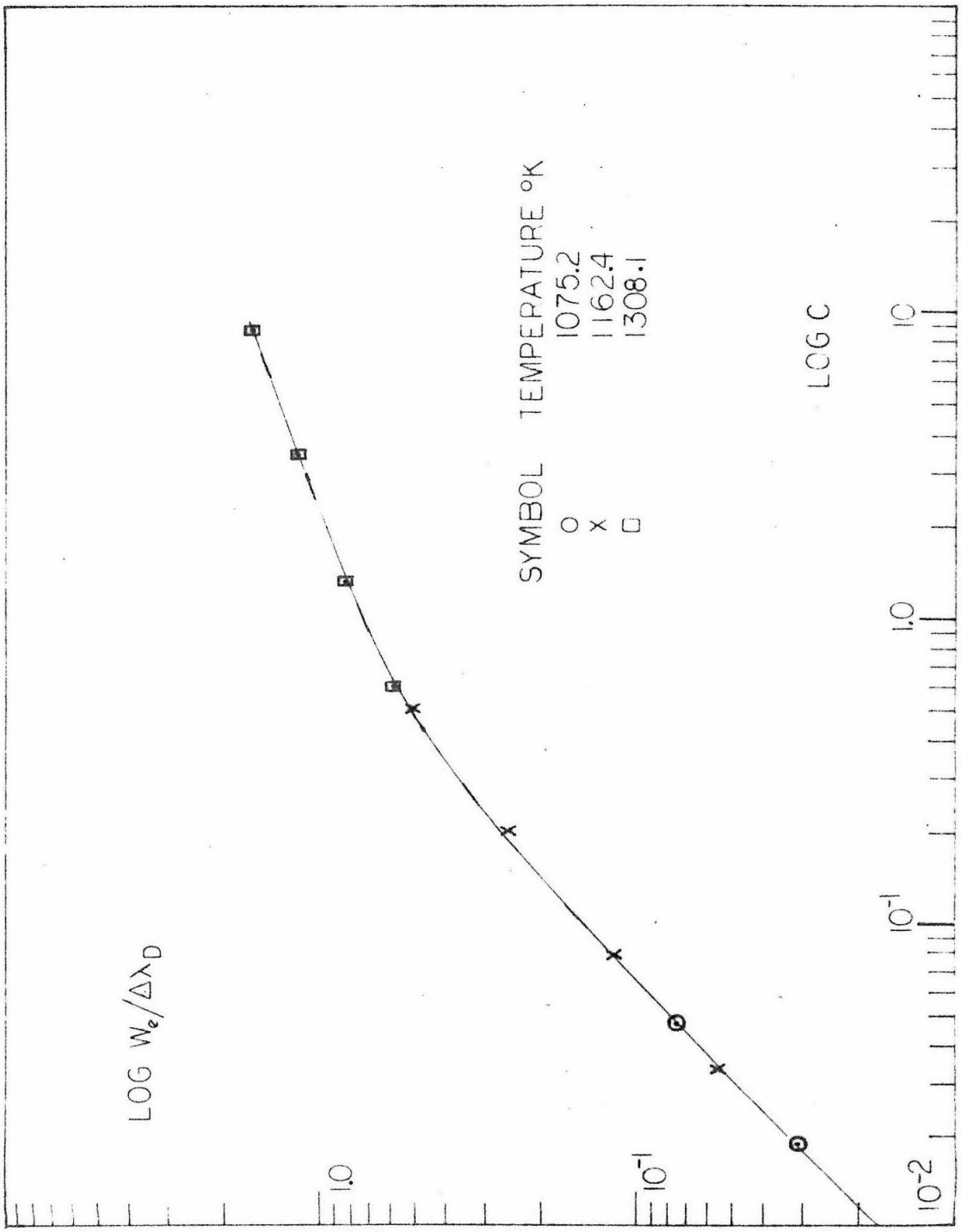

FIGURE 36 CURVE OF GROWTH OF PB 3639.58 A°

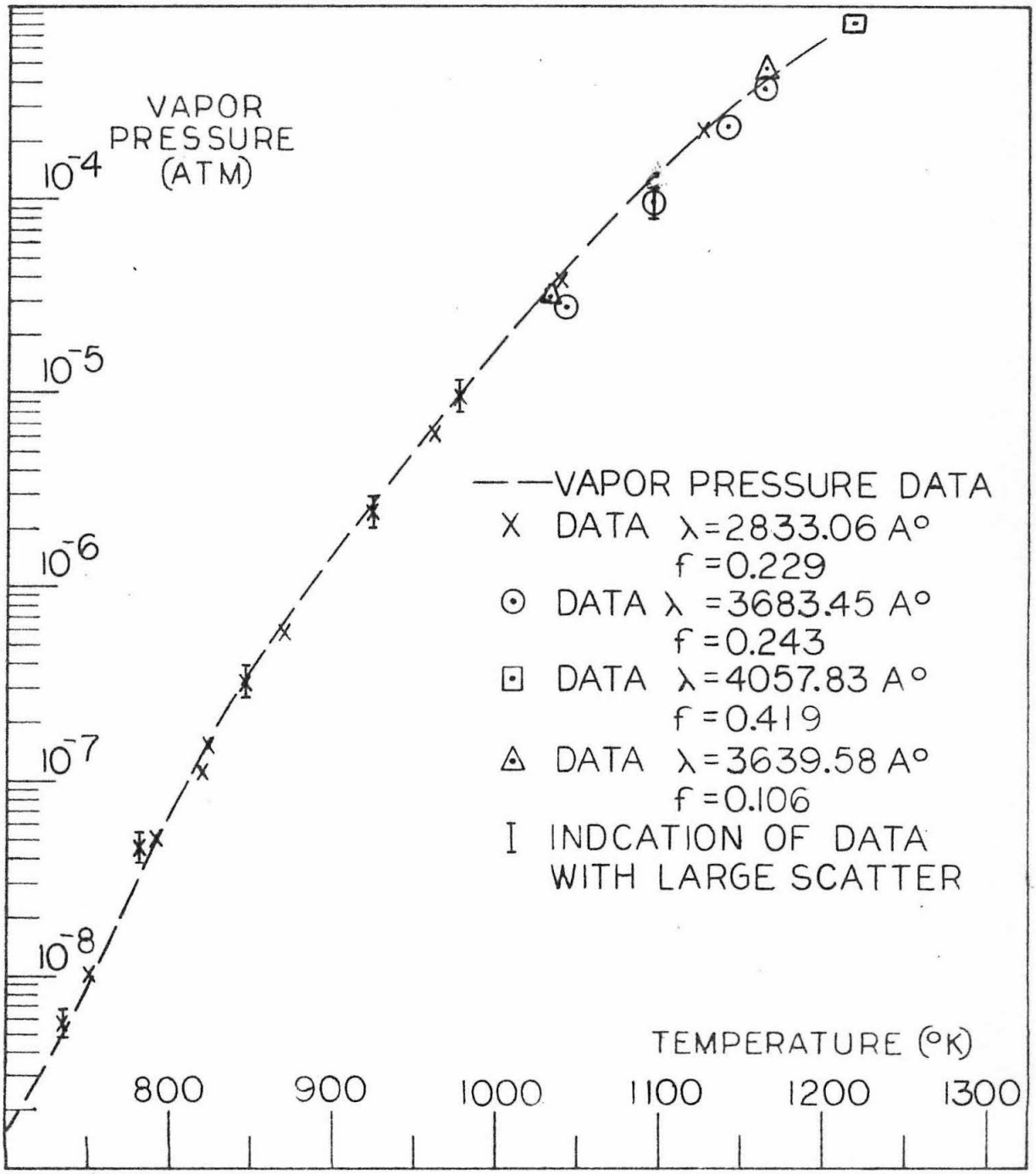

FIGURE 37 VAPOR PRESSURE OF Pb VS TEMPERATURE

IX. SUMMARY OF RESULTS AND COMMENTS OF ASTRO PHYSICAL INTEREST

A. The Experimental Results - A total of ten elements have been investigated and f-values of nineteen lines determined. It is of considerable interest to examine the data from the point of view that some other f-values could be predicted. For this purpose we summarize the data in Table 31.

B. Matrix Elements - The f-value is proportional to the dipole matrix element between initial and final states. In the simplest approximation the wave functions are separable so that

$$\langle \psi_u | z | \psi_\ell \rangle = \langle R_u \Theta_u \Phi_u | r \cos\theta | R_\ell \Theta_\ell \Phi_\ell \rangle$$

For a given term value the angular functions are the same so that for similar terms, one expects

$$gf \propto \frac{1}{\lambda} \sum_m \langle R_u | r | R_\ell \rangle^2 \qquad (23)$$

Going ahead further with this crude approximation, one realizes that in some fashion the average value of the radius, or most likely occuring radius, is proportional to the energy, so that,

$$\bar{r}_u - \bar{r}_\ell \propto E_u - E_\ell$$

Thus, one might hope to find that for a given transition

$$f \propto \lambda$$

One would hope to find that,

$$\text{Cu } \lambda 3247 < \text{Ag } \lambda 3281$$

implies,

$$f(3247) < f(3281)$$

TABLE 31

SUMMARY OF EXPERIMENTAL f-VALUE DETERMINATION

Elem	λ(Å)	Term	J_ℓ - ju	f-value
Cu	3247	4^2S-4^2P	1/2-3/2	0.322
	3274		1/2-1/2	0.153
Ag	3281	5^2S-5^2P	1/2-3/2	0.451
	3383		1/2-1/2	0.175
Au	2676	6^2S-6^2P	1/2-1/2	0.076
Ga	4033	4^2P-5^2S	1/2-1/2	0.095
In	3039	$5_p{}^2P-5d^2D$	1/2-3/2	0.339
	4101	5^2P-6^2S	1/2-1/2	0.172
Tl	2767	$6_p{}^2P-6d^2D$	1/2-3/2	0.219
	3775	6^2P-7^2S	1/2-1/2	0.108
Sn	2863	$5_p{}^3P-6S^3P$	0-1	0.332
	3009		1-1	0.0419
	3175		2-1	0.0651
Pb	2833	$6_p{}^3P-7s^3P$	0-1	0.229
	3603		1-0	0.243
	4057		2-1	0.419
	3639		1-1	0.106
Zn	3076	4^1S-4^3P	0-1	0.992×10^{-4}
Cd	3261		0-1	2.05×10^{-3}

In order to pursue the matter further, the values of log f were plotted against log λ, and a line was drawn connecting points for a given transition in different elements. The results are shown in figure 38. In every case the data occur in a monotonic fashion, that is, whenever

$$\lambda_1 > \lambda_2$$

$$f(\lambda_1) > f(\lambda_2)$$

Furthermore, the slopes are not dissimilar among transitions with the same Δj. In fact, the indication is that the $\Delta j = \pm 1$ transitions have a higher slope than the $\Delta j = 0$ transitions, which is not surprising since the overlap integrals are dependent on the angular momentum.

C. Predictions - On the basis of figure 38 one could predict the Al, $\lambda 3944\text{Å}$ line. This is the same transition as the Ga, $\lambda 4033\text{Å}$, the In, $\lambda 4101\text{Å}$, and the Tl, $\lambda 3775\text{Å}$ lines. The predicted f-value is found by drawing the curve between the above measured transitions and finding the ordinate at $\lambda = 3944\text{Å}$. A list of such crude empirical predictions is given in table 32 and a comparison to the values of Corliss and Bozman[21] is made. The predictions are certainly oversimplified but illustrate a possible method for extending the knowledge of transition probabilities for use in estimating atomic composition of radiating bodies.

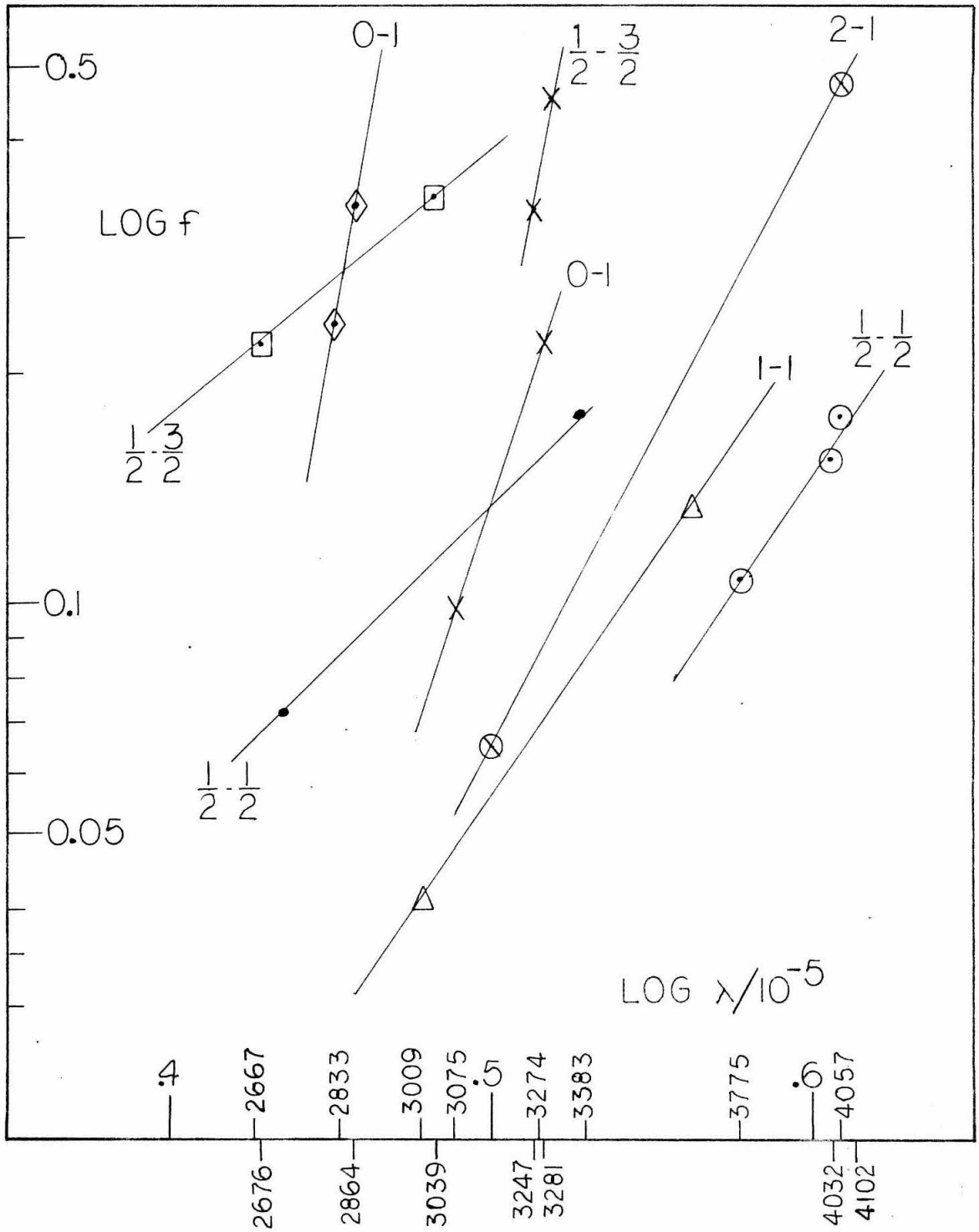

FIGURE 38 THE RELATIONSHIP BETWEEN f AND λ FOR THE ISOELECTRONIC SEQUENCES

TABLE 32

Element	λ(Å)	Prediction of f-Value	NBS Value
Al	3944	0.10	0.08
	2566	0.17	0.10
Ge	2497	0.07	0.22
Au	2428	0.07	0.08

It is apparent that these predictions do not agree well with the results of Corliss and Bozman. Not enough theoretical results are available for a good comparison.

In section XI there are suggestions for doing further experimental work to check this scheme of prediction against experimental evidence.

D. It is the purpose of this paragraph to review some of the astrophysical significance of the data obtained in the experiment described.

The reference on solar abundances used is the paper of Goldberg, Aller, and Muller[23]. In this paper the authors have predicted the abundances of the elements in the sun based on spectroscopic data. They have reviewed the literature and made a choice of f-value which they then use, with a curve of growth, to determine the abundances. Since they are always considering the linear portion of the curve of growth, their results are linearly dependent on the f-value.

Unfortunately, the lines used by them are not always the ones measured here. In these cases, the National Bureau of Standards Monograph[21] has been used to relate their choices to the f-values measured here. The method of relating f-values is chosen because the reference[21] is the most complete, if not the most accurate. The results of this comparison are shown in table 33. Aller's, et al, results were corrected to the values f_1, while f_2 are the results achieved here, and the ratio is shown in the right hand column.

The most severe discrepancies are in Copper, Zinc, and Tin. In the case of Copper, the authors get a result which is eight times lower than those derived by Unsold. The resulting correction here tends to make even Unsold's result seem too high.

The other of the three large discrepancies are listed below.

	Aller	Unsold	Corrected
$\log \frac{N_{Cu}}{N_H}$	5.04	5.95	6.24
$\log \frac{N_{Zn}}{N_H}$	4.40	4.78	4.81
$\log \frac{N_{Sn}}{N_H}$	1.54		0.71

TABLE 33

COMPARISON OF f-VALUES WITH ALLER, ET AL

Elem	λ(Å)	Aller gf	Corrected (NBS) λ(Å)	Corrected (NBS) f_1	Exp. Results f_2(abs)	Ratio f_2/f_1
Cu	8092	0.081	3247	0.020	0.322	15.7
	7933	0.039	3274	0.010	0.153	
Ag	3281	1.77	3281	0.885	0.451	0.45
	3383	0.89	3383	0.445	0.175	
Zn	4811	0.152	3076	3.8×10^{-5}	9.92×10^{-5}	2.61
Cd	3261	2.2×10^{-3}	3261	2.2×10^{-3}	2.2×10^{-3}	1.00
Ga	4172	0.742	4033	0.168	0.095	0.56
In	4511	0.871	4101	0.311	0.172	0.55
Sn	3801	1.42	2863	2.25	0.332	0.15
Pb	3639	0.760	3639	0.280	0.106	0.55
	3683	1.23	3683	0.410	0.243	
	4057	1.74	4057	0.348	0.419	1.2

The remaining discrepancies are probably no greater than the accuracy of the equivalent width measurements and can be found from table 33.

X. AN AUXILIARY EXPERIMENT

There are two main classes of experiments on f-value determination. The first class provides a density measurement and a line width. The second gives a relative f-value for various lines of a given element, by estimating relative occupation numbers of various states.

As an auxiliary experiment a third type was done which is basically different from previous experiments. This experiment does the following:

1. Gives a new method of measuring density and therefore an absolute f-value in a manner similar to the usual determinations.
2. Offers a possibility of measuring the ratio of the f-values of different elements without measuring density.
3. Gives an excellent means of finding the curve of growth without isotope splitting for comparison purposes.

The experiment consists of chemically isolating a particular radioactive isotope (such as Zn^{65}) in such a manner that all of the other (Zn) isotopes are absent, and that at a known time all of the daughter isotopes are absent (i.e., Cu). Then the parent (Zn^{65}) isotope is electroplated on an inert metallic wire such as Pt (which has very low vapor pressures compared to both Zn and Cu). The wire is placed in a step cell, evacuated, and sealed off.

Consequently, the radioactive decay process is counted directly. That is, the γ -radiation in the process

$$Zn^{65} \rightarrow Cu^{65} + \beta^{+} + \gamma$$

is counted and a direct measurement of the total number of Zn^{65} atoms is made. This number must be small enough so that complete vaporization is possible.

Subsequently, the cell is placed in the electric furnace and brought up to a sufficiently high temperature that all of the atoms are in vapor form. The $W/\Delta\lambda_D$ values are measured for all four optical path lengths. Also the $W/\Delta\lambda_D$ are measured for the Cu line. The experiment is repeated at intervals of 100 days or so. (Zn^{65} half-life is about 200 days.)

The results include, then, measurements of part of the curve of growth at various times. The following are known quantities:

1. N(Zn) at each time $\pm$ 10%
2. N(Cu)/N(Zn) $\pm$1%
3. N(Zn, t_1)/N(Zn, t_2) $\pm$1%

If the $W/\Delta\lambda_D$ is plotted versus C the results are:

1. f(Zn) $\pm$20% from the usual method.
2. f(Cu)/f(Zn) $\pm$10% from the knowledge of the half life.
3. $\frac{\Delta}{\Delta t}\left(\frac{W}{\Delta\lambda_D}\right)$ and $\frac{\Delta}{\Delta t} N(Zn^{65})$ from comparison of the various data and from the half life.

The third of these results is the one which allows a new type of absolute f-value determination. If the total N is kept

small enough to be near the linear portion of the curve of growth then

$$\frac{W}{\Delta\lambda_D} = \frac{\sqrt{\pi}\, n_o \lambda^2 N f L}{\Delta\lambda_D} + \text{Corr } O(a) \qquad (24)$$

Therefore,

$$\frac{\Delta}{\Delta t}\left(\frac{W}{\Delta\lambda_D}\right) = \frac{\sqrt{\pi}\, n_o \lambda^2 N L}{\Delta\lambda_D}\,\frac{\Delta}{\Delta t} N \qquad (25)$$

or for the parent,

$$\frac{\Delta}{\Delta t}\left(\log \frac{W}{\Delta\lambda_D}\right) = -\gamma^{-1}$$

The γ term is the decay constant of the process. For the daughter atom, the experiment can be checked, i.e.,

$$\frac{\Delta}{\Delta t}\left(\log \frac{W}{\Delta\lambda_D}\right)_{Cu} = -\frac{\Delta}{\Delta t}\left(\log \frac{W}{\Delta\lambda_D}\right)_{Zn}. \qquad (26)$$

<u>The main point is that equation 26 is independent of N.</u> The experiment has been started with Zn^{65} and studied for Cd^{109}, Au^{199}, and other isotopes. The results are obviously slowly obtained since the best isotopes have the longest half-lives.

XI. SUGGESTIONS FOR FURTHER RESEARCH

A. The experiment discussed in Section X is already underway on the $Zn^{65} \rightarrow Cu^{65}$ radioactive decay schemes. There are considerable chemical handling problems to be met, including the isolation of the element, and the filling of a step cell with about 10^{11} atoms. These will, it appears, be only temporary obstacles. Other isotopes and their reactions, which are suitable to this experiment, include the following,

$$Cd^{109} \rightarrow Ag^{109} + \beta^+ + \gamma$$

$$Au^{199} \rightarrow Hg^{199} + \beta^- + \gamma$$

$$Tl^{204} \rightarrow Hg^{204} + K$$
$$\quad\quad \rightarrow Pb^{204} + \beta^-$$

$$In^{114*} \rightarrow Sn^{114} + \beta^-$$
$$\quad\quad\quad \rightarrow Cd^{114} + \beta^+$$

For the most part, one must use cyclotron prepared isotopes, made from an isotopically pure target, or one which produces only one long-lived product.

B. The limitations on the main experiment have been chiefly due to two causes. The first is that many interesting elements, such as the Sodium family and the Calcium family, react with quartz, and the second is that quartz deteriorates rapidly above 1400°K. These limitations could be removed by building a step cell of fused sapphire, which is available but difficult to work with.

The production of a sapphire cell would allow the extension of this work to include the following elements:

1. Na, K, Rb, Os
2. Ca, Mg, Sr
3. Au ($\lambda = 2497\text{Å}$)
4. Sc, Y
5. Mn, Fe, Cr, Ni

Even without sapphire, one very interesting extension would be to do the lines of the lower vapor pressure members of the rare earths. Pure isotopes are now available and the spectra are rich and of considerable astrophysical interest.

APPENDIX A - THE EQUATION FOR THE CURVE OF GROWTH

In this appendix the equations for the curve of growth will be examined from the standpoint of the possibility of numerical computation.

Consider the equation for the curve of growth, in the form:

$$x = \int dw \left[1-\exp -yG(w;a)\right] \tag{A1}$$

where,

$$x = \frac{W}{\Delta\lambda_D} \tag{A2}$$

$$y = \frac{\sqrt{\pi}\, r_0\, {}^{2}_{0} N L f}{\Delta\lambda_D} \tag{A3}$$

$$a = \frac{\Delta\lambda_N + \Delta\lambda_P}{\Delta\lambda_D} = \frac{\Delta\lambda_P}{\Delta\lambda_D} + \frac{4\pi r_0 f}{\Delta\lambda_D} \frac{\epsilon_1}{\epsilon_2} \tag{A4}$$

$$G = \frac{1}{\sqrt{\pi}} \int_{-\infty}^{\infty} \frac{a e^{-t^2} dt}{a^2 + (w-t)^2} \tag{A5}$$

The range of the parameter a is,

$$0.00004 < a < 0.4 \tag{A6}$$

It is customary for investigators to use the approximation a equals zero, since the solution for this approximation is well known. However, it will be shown that the solution is not accurate for values of $W/\Delta\lambda_D$ greater than one-half.

One might hope to expand x(y;a) in a Taylor Series about a = 0. Before proceeding it should be remarked that another form for G(w;a) due to Reiche[44] is possible,

if one notices that,

$$\frac{a}{a^2+(w-t)^2} = \int_0^\infty e^{-ax} \cos(w-t)x \, dx$$

So that equation A5 may be written (reversing the order of integration) as,

$$G = \frac{1}{\sqrt{\pi}} \int_0^\infty e^{-at} \left[\int_{-\infty}^{\infty} e^{-z^2} \cos(w-z)t \, dz \right] dt$$

Since,

$$\cos(w-t)z = (\cos wt)(\cos tz)+(\sin wt)(\sin tz)$$

and since,

$$(\sin wt)(\sin tz) = -(\sin wt)(\sin -tz)$$

only the even term contributes. That is,

$$G = \frac{1}{\sqrt{\pi}} \int_0^\infty e^{-at} \int_{-\infty}^{\infty} e^{-z^2} (\cos wt)(\cos zt) dz \, dt \qquad (A7)$$

Integration over z gives,

$$G = \frac{1}{\sqrt{\pi}} \int_0^\infty e^{-at-t^2/4} (\cos wt) dt$$

Changing variables leads to the form,

$$G = \frac{2}{\pi^{1/4}} \int_0^\infty e^{-2at-t^2} (\cos 2wt) dt$$

which may also be written

$$G = \frac{2e^{a^2}}{\pi^{1/2}} \left[\cos 2wa \int_0^\infty e^{-t^2} (\cos 2wt) dt + \sin 2wa \int_0^\infty e^{-t^2} (\sin 2wt) dt \right]$$

$$= \frac{2}{\pi^{1/2}} \left[F_1(w;a)+F_2(w;a) \right] \qquad (A8)$$

with

$$F_1(w;a) = e^{a^2}\cos 2wa \int e^{-t^2}(\cos 2wt)dt \qquad (A9)$$

$$F_2(w;a) = e^{a^2}\sin 2wa \int e^{-t^2}(\sin 2wt)dt \qquad (A10)$$

It is pertinent to notice that

$$\int e^{-t^2}(\cos 2wt)dt = \tfrac{1}{2}\sqrt{\pi}\, e^{-w^2} \qquad (A11)$$

and

$$\int e^{-t^2}(\sin 2wt)dt = e^{-w^2}\int_0^w e^{u^2}du = H(w) \qquad (A12)$$

with

$$H(w\to\infty) = 0(e^{-w^2})$$

From the proceeding we can construct the solution as a Taylor Series in the variable a about the point a = 0. The first two terms can be calculated but higher terms are very difficult. The first term has been calculated by many authors as

$$x_0 = \frac{y}{\sqrt{\pi}}\left(1 - \frac{y}{2!\ 2} + \frac{y^2}{3!\ 3} - \cdots\cdots\right) \qquad (A13)$$

The second term is derived from,

$$\left.\frac{dx}{da}\right|_{a=0} = -\frac{2y}{\sqrt{\pi}}\int \frac{dH(w)}{dw}\cdot \exp{-ye^{-w^2}}dw \qquad (A14)$$

where H(w) is given by A12. Mitchel & Zemansky have investigated H(w) and since H(w) goes to zero very rapidly as w increases, A14 converges nicely. In fact, H'(w) is an even function of w, therefore,

$$\left.\frac{dx}{da}\right|_{a=0} = -\frac{4y}{\sqrt{\pi}}\int \frac{d}{dw}\left(e^{-w^2}\int_0^w e^{u^2}du\right)\cdot \exp{-ye^{-w^2}}dw \qquad (A15)$$

This term has been numerically worked out by Unsold[25]. The succeeding terms contribute appreciably to the solution but are very difficult to compute.

One could facilitate the computation of the function H(w) by solving the analogue problem. The method would be to solve the differential equation obeyed by the function H(w).

$$\frac{dH}{dw} = 1-2wH(w) \qquad (A16)$$

This equation is simple to solve since the end point values are known.

It seems more realistic to calculate equation A1 directly on a computing machine. The program for doing this is given in Appendix B and the numerical results are given in Appendix C.

Figure 39 is a summary of the results of the digital computer study of the variation of x versus y for various constant values of the parameter a.

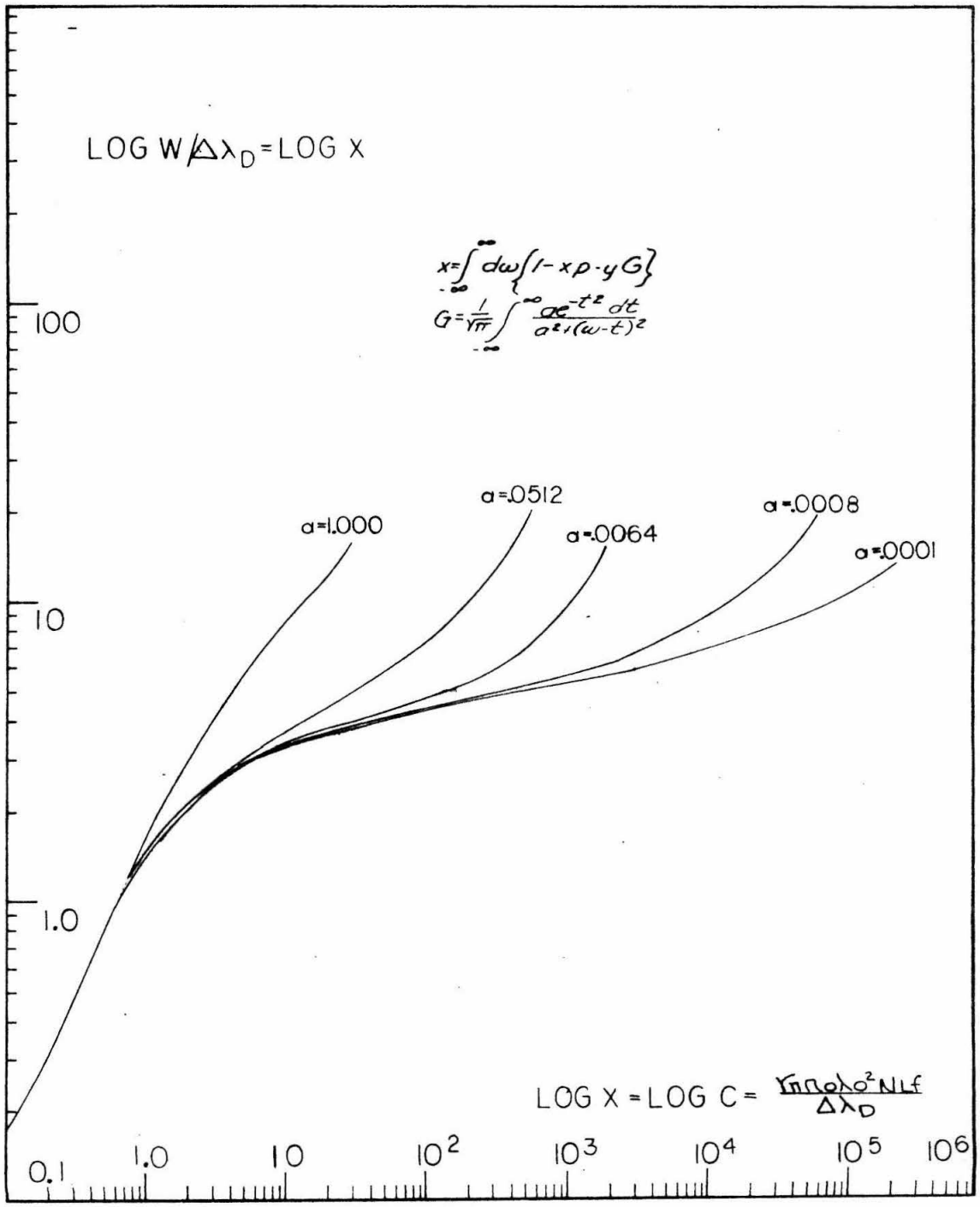

FIGURE 39 CURVE OF GROWTH FUNCTION

APPENDIX B - COMPUTER PROGRAM FOR CURVE OF GROWTH

1. ALGEBRAIC MANIPULATION

The problem is to compute x where

$$x = \int_{-\infty}^{\infty} \left\{ 1-\exp -yG \right\} \, dw \tag{B1}$$

with

$$G(w) = \frac{1}{\sqrt{\pi}} \int_{-\infty}^{\infty} \frac{ae^{-t^2}}{a^2+(w-t)^2} \, dt \tag{B2}$$

It was decided to evaluate both of the integrals as differential equations.

Making use of the equation

$$\int_{-\infty}^{\infty} f(x)dx = \int_{0}^{\infty} \left[f(-x)+f(x) \right] dx \tag{B3}$$

equation B2 becomes

$$G(w) = \frac{1}{\sqrt{\pi}} \int_{0}^{\infty} \left[\frac{ae^{-t^2}}{a^2+(w+t)^2} + \frac{ae^{-t^2}}{a^2+(w-t)^2} \right] dt \tag{B4}$$

From equation B4 it is obvious that G(w) = G(-w). Using this result and equation B3 again, x can be written in the form

$$x = 2 \int_{0}^{\infty} \left[1-\exp(yG) \right] \, dw \tag{B5}$$

2. NUMERICAL PROCEDURE

At the installation used, the Adams Method has been the standard procedure for solving simultaneous non-linear differential equations on the IBM 7090. This particular

Adams routine* controls the computing interval in such a way as to maintain any desired pre-set accuracy. Several versions of this routine have been coded and two separate versions more used in this one problem since an integration (for G(w)0 is to be completed at each step of the other integration (for x).

Thus, equation B5 was written in the form

$$\frac{dx}{dw} = 2\left[1-\exp(yG)\right]$$

and integrated from w = 0 to a w such that the succeeding stepwise contributions to the value of the integral would not change the final value of the integral in the fourth place. At each step of this integration, equation B4 was integrated similarly. In the actual program, since x is to be found for several values of y, it was not necessary to integrate B4 at each step for each y. On the first pass (taking the first value for y) a table of values, w versus G(w), was constructed and additional table values were computed and added to the table only when neighboring table values indicated that a linear interpolation would not maintain the desired four place accuracy.

*Differential Equations Subroutine D2 CL DEQ, SHARE Distribution No. 248.

3. THE PROGRAM

The following program was written in the FORTRAN language. (A description of this language may be found in any of the several FORTRAN Manuals published by IBM.) The subroutine which integrates equation B4 was coded as a FORTRAN subroutine and the subroutine which integrates equation B5 was coded as a function and is called directly from the FORTRAN library tape. The program is given in the remainder of this appendix.

APPENDIX B - PROGRAM FOR 7090 COMPUTER

```
*     XEQ
      COMMON  A,W,GEE
      DIMENSION WT(1500)  ,GT(1500)
      DIMENSION D(25)
      N=1
      LOCD=XLOCF(D)
      EQUIVALENCE (D(1),N),(D(2),X),(D(3),Y1),(D(4),DY1,E1),
     1(D(5),Y2),(D(6),DY2,E2),(D(7),Y3),(D(8),DY3,E3),
     2(D(9),Y4),(D(10),DY4,E4),(D(11),Y5),(D(12),DY5,E5),
     3(D(13),Y6),(D(14),DY6,E6),(D(15),Y7),(D(16),DY7,E7),
     4(D(17),Y8),(D(18),DY8,E8),(D(19),Y9),(D(20),DY9,E9),
     5(D(21),Y10),(D(22),DY10,E10),(D(23),Y11),(D(24),DY11,E11),
     6(D(25),Y12),(D(26),DY12,E12),(D(27),Y13),(D(28),DY13,E13),
     7(D(29),Y14),(D(30),DY14,E14),(D(31),Y15),(D(32),DY15,E15),
     8(D(33),Y16),(D(34),DY16,E16),(D(35),Y17),(D(36),DY17,E17),
     9(D(37),Y18),(D(38),DY18,E18),(D(39),Y19),(D(40),DY19,E19)
      EQUIVALENCE (D(41),Y20),(D(42),DY20,E20),(D(43),Y21),
     1(D(44),DY21,E21),(D(45),Y22),(D(46),DY22,E22),(D(47),Y23),
     2(D(48),DY23,E23),(D(49),Y24),(D(50),DY24,E24),(D(51),Y25),
     3(D(52),DY25,E25),(D(53),Y26),(D(54),DY26,E26),(D(55),Y27),
     4(D(56),DY27,E27),(D(57),Y28),(D(58),DY28,E28),(D(59),Y29),
     5(D(60),DY29,E29),(D(61),Y30),(D(62),DY30,E30),(D(63),Y31),
     6(D(64),DY31,E31),(D(65),Y32),(D(66),DY32,E32),(D(67),Y33),
     7(D(68),DY33,E33),(D(69),Y34),(D(70),DY34,E34),(D(71),Y35),
     8(D(72),DY35,E35),(D(73),Y36),(D(74),DY36,E36),(D(75),Y37),
     9(D(76),DY37,E37),(D(77),Y38),(D(78),DY38,E38),(D(79),Y39)
      EQUIVALENCE (D(80),DY39,E39),(D(81),Y40),(D(82),DY40,E40),
     1(D(83),Y41),(D(84),DY41,E41),(D(85),Y42),(D(86),DY42,E42),
     2(D(87),Y43),(D(88),DY43,E43),(D(89),Y44),(D(90),DY44,E44),
     3(D(91),Y45),(D(92),DY45,E45),(D(93),Y46),(D(94),DY46,E46),
     4(D(95),Y47),(D(96),DY47,E47),(D(97),Y48),(D(98),DY48,E48),
     5(D(99),Y49),(D(100),DY49,E49),(D(101),Y50),(D(102),DY50,E50)
      EQUIVALENCE (D(5),DX)
      E=2.7182818
      JPAGE=2
20    READ INPUT TAPE 7,900,A,DYI
      IF (A) 21,910,21
21    JPAGE=JPAGE+1
      WRITE OUTPUT TAPE 6,906,JPAGE
      WRITE OUTPUT TAPE 6,902,A
      JPRNT=56
      J=1
32    WT(J)=0.
      GT(J)=0.
      J=J+1
      IF (J-1500) 32,32,35
35    Y=DYI
      YLG=LOGF(Y)*.43429448
623   X=0.0
      JAKEP=1
      FLAG=0.
      Y1=0.
629   E1=1.E-5
      DX=1.E-7
      I=XDESBF(LOCD)
624   JAKE=JAKEP
625   IF (GT(JAKE)) 595,600,595
595   IF (X-WT(JAKE))609,615,620
609   IF (GT(JAKE)*ABSF(GT(JAKE)-GT(JAKE-1))-.0006)611,608,608
```

```
 608  JAKEN=JAKE-1
      FLAG=1.
      XSAVE=X
      X=.5*(WT(JAKE)+WT(JAKE-1))
      GO TO 610
 611  S1=(GT(JAKE)-GT(JAKE-1))/(WT(JAKE)-WT(JAKE-1))
      G=S1*(X-WT(JAKE-1))+GT(JAKE-1)
      GO TO 617
 620  JAKE=JAKE+1
      IF (JAKE-1500) 625,625,630
 630  WRITE OUTPUT TAPE 6,635
 635  FORMAT (16H1 G TABLE FILLED)
      GO TO 20
 615  G=GT(JAKE)
 617  OPT=Y*G-.01
      IF (OPT) 618,618,616
 616  DY1=2.*(1.-EXPF(-Y*G))
      GO TO 103
 618  DY1=2.*(Y*G-(Y*G)**2/2.+(Y*G)**3/6.)
      GO TO 103
C     FIND G(W) BY ADAMS
 600  CONTINUE
 610  XSA1=WT(JAKE)
      XSA2=GT(JAKE)
      NA=1
      W=X
      CALL ADAMS(NA)
      GT(JAKE)=GEE
      G=GEE
C     PLACE NEW VALUES OF W AND G(W) INTO TABLE
 638  WT(JAKE)=X
 640  XSA3=WT(JAKE+1)
      XSA4=GT(JAKE+1)
      WT(JAKE+1)=XSA1
      GT(JAKE+1)=XSA2
      XSA1=XSA3
      XSA2=XSA4
      IF (GT(JAKE+1)) 645,6171,645
 6171 IF (FLAG) 6172,617,6172
 6172 JAKE=JAKEN
      FLAG=0.
      X=XSAVE
      GO TO 595
 645  JAKE=JAKE+1
      GO TO 640
 103  I=XDESDF(1)
 114  GO TO (106,624),I
 106  IF (X-WT(JAKEP)) 710,721,720
 720  JAKEP=JAKEP+1
      GO TO 106
 710  JAKEP=JAKEP-1
 721  IF (X-10.) 308,302,302
 302  TEST=ABSF((Y1-YY1)/YY1)
      IF (TEST-.0000005) 401,401,308
 308  YY1=Y1
 301  I=XDESFF(1)
      GO TO 624
 401  XX=Y1
      IF (XX-15.)421,421,20
```

```
421   IF(XX)441,431,431
431   XXLG=LOGF(XX)*.43429448
      WRITE OUTPUT TAPE 6,904,XX,Y,XXLG,YLG
      JPRNT=JPRNT-1
      IF (JPRNT) 436,436,441
436   JPAGE=JPAGE+1
      WRITE OUTPUT TAPE 6,906,JPAGE
      WRITE OUTPUT TAPE 6,902,A
      JPRNT=56
441   YLG=LOGF(Y)*.43429448+.1
      Y=EXPF(YLG*2.30258509)
      GO TO 623
900   FORMAT (7F10.0)
902   FORMAT (1H 5X,E11.4/1H )
904   FORMAT (1H 5X,E11.4,5X,E11.4,12X,F7.4,5X,F7.4)
906   FORMAT (1H166X,1HA,I3/1H0/1H )
910   CALL EXIT
      STOP 7777
      END



      SUBROUTINE SETUP (TA,YA,NSIGA,NPRINT,TPRINT,NA)
      COMMON  A,W,GEE
      DIMENSION TA(2),YA(50),NSIGA(50)
      YA(1)=0.
      TA(2)=1.E-7
      NSIGA(1)=5
      RETURN
      END



      SUBROUTINE DIFEQ (TA,YA,DYA,NA)
      COMMON  A,W,GEE
      DIMENSION TA(2),YA(50),DYA(50)
      DYA(1)=A*EXPF(-TA(1)**2)*(1./(A**2+(W+TA(1))**2)+1./(A**2
     1+(W-TA(1))**2))/3.1415927
      RETURN
      END



      SUBROUTINE PRINT (TA,YA,DYA,NA)
      COMMON  A,W,GEE
      DIMENSION TA(2),YA(50),DYA(50)
2     IF (TA(1)-10.) 5,5,3
3     IF (ABSF((YA(1)-YPRE)/YPRE)-.000001) 4,4,5
5     YPRE=YA(1)
      RETURN
4     GEE=YA(1)
      NA=0
      RETURN
      END
```

APPENDIX C

TABLES OF CURVE OF GROWTH

A = 0.0001

X	Y	LOG X	LOG Y
0.1767E-01	1.0000E-02	-1.7527	-2.0000
0.2223E-01	0.1259E-01	-1.6530	-1.9000
0.2795E-01	0.1585E-01	-1.5535	-1.8000
0.3514E-01	0.1995E-01	-1.4542	-1.7000
0.4415E-01	0.2512E-01	-1.3551	-1.6000
0.5547E-01	0.3162E-01	-1.2559	-1.5000
0.6963E-01	0.3981E-01	-1.1572	-1.4000
0.8735E-01	0.5012E-01	-1.0587	-1.3000
0.1095E-00	0.6310E-01	-0.9607	-1.2000
0.1370E-00	0.7943E-01	-0.8632	-1.1000
0.1713E-00	0.1000E-00	-0.7663	-1.0000
0.2137E-00	0.1259E-00	-0.6702	-0.9000
0.2660E-00	0.1585E-00	-0.5751	-0.8000
0.3303E-00	0.1995E-00	-0.4812	-0.7000
0.4086E-00	0.2512E-00	-0.3888	-0.6000
0.5033E 00	0.3162E-00	-0.2982	-0.5000
0.6167E 00	0.3981E-00	-0.2099	-0.4000
0.7508E 00	0.5012E 00	-0.1245	-0.3000
0.9072E 00	0.6310E 00	-0.0423	-0.2000
0.1086E 01	0.7943E 00	0.0358	-0.1000
0.1286E 01	0.1000E 01	0.1093	0.0000
0.1504E 01	0.1259E 01	0.1774	0.1000
0.1735E 01	0.1585E 01	0.2394	0.2000
0.1972E 01	0.1995E 01	0.2949	0.3000
0.2206E 01	0.2512E 01	0.3436	0.4000
0.2430E 01	0.3162E 01	0.3856	0.5000
0.2638E 01	0.3981E 01	0.4213	0.6000
0.2830E 01	0.5012E 01	0.4517	0.7000
0.3005E 01	0.6310E 01	0.4779	0.8000
0.3167E 01	0.7943E 01	0.5006	0.9000
0.3318E 01	0.1000E 02	0.5209	1.0000
0.3462E 01	0.1259E 02	0.5393	1.1000
0.3599E 01	0.1585E 02	0.5561	1.2000
0.3730E 01	0.1995E 02	0.5717	1.3000
0.3856E 01	0.2512E 02	0.5861	1.4000
0.3978E 01	0.3162E 02	0.5997	1.5000
0.4096E 01	0.3981E 02	0.6124	1.6000
0.4211E 01	0.5012E 02	0.6244	1.7000
0.4323E 01	0.6310E 02	0.6357	1.8000
0.4432E 01	0.7943E 02	0.6466	1.9000
0.4538E 01	0.1000E 03	0.6569	2.0000
0.4642E 01	0.1259E 03	0.6667	2.1000
0.4745E 01	0.1585E 03	0.6762	2.2000
0.4845E 01	0.1995E 03	0.6853	2.3000
0.4945E 01	0.2512E 03	0.6941	2.4000
0.5041E 01	0.3162E 03	0.7025	2.5000
0.5139E 01	0.3981E 03	0.7109	2.6000
0.5235E 01	0.5012E 03	0.7189	2.7000
0.5330E 01	0.6310E 03	0.7267	2.8000
0.5424E 01	0.7943E 03	0.7343	2.9000
0.5517E 01	1.0000E 03	0.7417	3.0000
0.5611E 01	0.1259E 04	0.7491	3.1000
0.5706E 01	0.1585E 04	0.7564	3.2000
0.5803E 01	0.1995E 04	0.7637	3.3000

TABLES OF CURVE OF GROWTH

A = 0.0001

X	Y	LOG X	LOG Y
0.5902E 01	0.2512E 04	0.7710	3.4000
0.6007E 01	0.3162E 04	0.7786	3.5000
0.6116E 01	0.3981E 04	0.7864	3.6000
0.6232E 01	0.5012E 04	0.7946	3.7000
0.6357E 01	0.6310E 04	0.8033	3.8000
0.6493E 01	0.7943E 04	0.8124	3.9000
0.6641E 01	1.0000E 04	0.8222	4.0000
0.6807E 01	0.1259E 05	0.8330	4.1000
0.6994E 01	0.1585E 05	0.8447	4.2000
0.7206E 01	0.1995E 05	0.8577	4.3000
0.7452E 01	0.2512E 05	0.8723	4.4000
0.7736E 01	0.3162E 05	0.8885	4.5000
0.8069E 01	0.3981E 05	0.9068	4.6000
0.8462E 01	0.5012E 05	0.9275	4.7000
0.8926E 01	0.6310E 05	0.9507	4.8000
0.9476E 01	0.7943E 05	0.9766	4.9000
0.1013E 02	1.0000E 05	1.0055	5.0000
0.1090E 02	0.1259E 06	1.0374	5.1000
0.1181E 02	0.1585E 06	1.0724	5.2000
0.1289E 02	0.1995E 06	1.1103	5.3000
0.1415E 02	0.2512E 06	1.1509	5.4000

TABLES OF CURVE OF GROWTH

A = 0.0002

X	Y	LOG X	LOG Y
0.1767E-01	1.0000E-02	-1.7528	-2.0000
0.2222E-01	0.1259E-01	-1.6532	-1.9000
0.2794E-01	0.1585E-01	-1.5537	-1.8000
0.3513E-01	0.1995E-01	-1.4543	-1.7000
0.4415E-01	0.2512E-01	-1.3551	-1.6000
0.5545E-01	0.3162E-01	-1.2561	-1.5000
0.6960E-01	0.3981E-01	-1.1574	-1.4000
0.8731E-01	0.5012E-01	-1.0590	-1.3000
0.1094E-00	0.6310E-01	-0.9609	-1.2000
0.1370E-00	0.7943E-01	-0.8634	-1.1000
0.1712E-00	0.1000E-00	-0.7665	-1.0000
0.2136E-00	0.1259E-00	-0.6704	-0.9000
0.2659E-00	0.1585E-00	-0.5752	-0.8000
0.3301E-00	0.1995E-00	-0.4813	-0.7000
0.4084E-00	0.2512E-00	-0.3889	-0.6000
0.5031E 00	0.3162E-00	-0.2984	-0.5000
0.6165E 00	0.3981E-00	-0.2101	-0.4000
0.7505E 00	0.5012E 00	-0.1246	-0.3000
0.9069E 00	0.6310E 00	-0.0425	-0.2000
0.1086E 01	0.7943E 00	0.0357	-0.1000
0.1286E 01	0.1000E 01	0.1092	0.0000
0.1504E 01	0.1259E 01	0.1772	0.1000
0.1735E 01	0.1585E 01	0.2393	0.2000
0.1971E 01	0.1995E 01	0.2948	0.3000
0.2205E 01	0.2512E 01	0.3435	0.4000
0.2429E 01	0.3162E 01	0.3854	0.5000
0.2637E 01	0.3981E 01	0.4211	0.6000
0.2829E 01	0.5012E 01	0.4516	0.7000
0.3004E 01	0.6310E 01	0.4777	0.8000
0.3166E 01	0.7943E 01	0.5005	0.9000
0.3317E 01	0.1000E 02	0.5207	1.0000
0.3460E 01	0.1259E 02	0.5390	1.1000
0.3597E 01	0.1585E 02	0.5559	1.2000
0.3728E 01	0.1995E 02	0.5714	1.3000
0.3853E 01	0.2512E 02	0.5859	1.4000
0.3975E 01	0.3162E 02	0.5994	1.5000
0.4093E 01	0.3981E 02	0.6121	1.6000
0.4208E 01	0.5012E 02	0.6241	1.7000
0.4321E 01	0.6310E 02	0.6356	1.8000
0.4430E 01	0.7943E 02	0.6464	1.9000
0.4537E 01	0.1000E 03	0.6568	2.0000
0.4642E 01	0.1259E 03	0.6667	2.1000
0.4746E 01	0.1585E 03	0.6763	2.2000
0.4848E 01	0.1995E 03	0.6855	2.3000
0.4949E 01	0.2512E 03	0.6945	2.4000
0.5049E 01	0.3162E 03	0.7032	2.5000
0.5149E 01	0.3981E 03	0.7118	2.6000
0.5248E 01	0.5012E 03	0.7200	2.7000
0.5350E 01	0.6310E 03	0.7284	2.8000
0.5452E 01	0.7943E 03	0.7365	2.9000
0.5555E 01	1.0000E 03	0.7447	3.0000
0.5662E 01	0.1259E 04	0.7532	3.1000
0.5773E 01	0.1585E 04	0.7614	3.2000
0.5888E 01	0.1995E 04	0.7700	3.3000

TABLES OF CURVE OF GROWTH

A = 0,0002

X	Y	LOG X	LOG Y
0.6008E 01	0.2512E 04	0.7787	3.4000
0.6141E 01	0.3162E 04	0.7883	3.5000
0.6283E 01	0.3981E 04	0.7982	3.6000
0.6439E 01	0.5012E 04	0.8088	3.7000
0.6611E 01	0.6310E 04	0.8203	3.8000
0.6806E 01	0.7943E 04	0.8329	3.9000
0.7026E 01	1.0000E 04	0.8467	4.0000
0.7280E 01	0.1259E 05	0.8621	4.1000
0.7574E 01	0.1585E 05	0.8793	4.2000
0.7916E 01	0.1995E 05	0.8985	4.3000
0.8318E 01	0.2512E 05	0.9200	4.4000
0.8791E 01	0.3162E 05	0.9440	4.5000
0.9351E 01	0.3981E 05	0.9708	4.6000
0.1001E 02	0.5012E 05	1.0006	4.7000
0.1080E 02	0.6310E 05	1.0334	4.8000
0.1173E 02	0.7943E 05	1.0692	4.9000
0.1282E 02	1.0000E 05	1.1079	5.0000
0.1410E 02	0.1259E 06	1.1491	5.1000

TABLES OF CURVE OF GROWTH

A = 0.0004

X	Y	LOG X	LOG Y
0.1766E-01	1.0000E-02	-1.7529	-2.0000
0.2222E-01	0.1259E-01	-1.6533	-1.9000
0.2794E-01	0.1585E-01	-1.5538	-1.8000
0.3513E-01	0.1995E-01	-1.4543	-1.7000
0.4414E-01	0.2512E-01	-1.3552	-1.6000
0.5545E-01	0.3162E-01	-1.2561	-1.5000
0.6960E-01	0.3981E-01	-1.1574	-1.4000
0.8731E-01	0.5012E-01	-1.0589	-1.3000
0.1094E-00	0.6310E-01	-0.9609	-1.2000
0.1370E-00	0.7943E-01	-0.8634	-1.1000
0.1712E-00	0.1000E-00	-0.7665	-1.0000
0.2136E-00	0.1259E-00	-0.6704	-0.9000
0.2659E-00	0.1585E-00	-0.5752	-0.8000
0.3301E-00	0.1995E-00	-0.4814	-0.7000
0.4084E-00	0.2512E-00	-0.3869	-0.6000
0.5031E 00	0.3162E-00	-0.2984	-0.5000
0.6164E 00	0.3981E-00	-0.2101	-0.4000
0.7506E 00	0.5012E 00	-0.1246	-0.3000
0.9069E 00	0.6310E 00	-0.0424	-0.2000
0.1086E 01	0.7943E 00	0.0357	-0.1000
0.1286E 01	0.1000E 01	0.1092	0.0000
0.1504E 01	0.1259E 01	0.1773	0.1000
0.1735E 01	0.1585E 01	0.2393	0.2000
0.1972E 01	0.1995E 01	0.2949	0.3000
0.2206E 01	0.2512E 01	0.3435	0.4000
0.2430E 01	0.3162E 01	0.3855	0.5000
0.2638E 01	0.3981E 01	0.4213	0.6000
0.2830E 01	0.5012E 01	0.4518	0.7000
0.3006E 01	0.6310E 01	0.4779	0.8000
0.3168E 01	0.7943E 01	0.5007	0.9000
0.3320E 01	0.1000E 02	0.5211	1.0000
0.3463E 01	0.1259E 02	0.5394	1.1000
0.3600E 01	0.1585E 02	0.5563	1.2000
0.3732E 01	0.1995E 02	0.5720	1.3000
0.3859E 01	0.2512E 02	0.5865	1.4000
0.3982E 01	0.3162E 02	0.6001	1.5000
0.4101E 01	0.3981E 02	0.6129	1.6000
0.4217E 01	0.5012E 02	0.6250	1.7000
0.4331E 01	0.6310E 02	0.6366	1.8000
0.4442E 01	0.7943E 02	0.6475	1.9000
0.4552E 01	0.1000E 03	0.6582	2.0000
0.4659E 01	0.1259E 03	0.6683	2.1000
0.4766E 01	0.1585E 03	0.6781	2.2000
0.4872E 01	0.1995E 03	0.6877	2.3000
0.4977E 01	0.2512E 03	0.6970	2.4000
0.5081E 01	0.3162E 03	0.7060	2.5000
0.5190E 01	0.3981E 03	0.7152	2.6000
0.5297E 01	0.5012E 03	0.7240	2.7000
0.5411E 01	0.6310E 03	0.7332	2.8000
0.5525E 01	0.7943E 03	0.7424	2.9000
0.5646E 01	1.0000E 03	0.7518	3.0000
0.5773E 01	0.1259E 04	0.7614	3.1000
0.5910E 01	0.1585E 04	0.7716	3.2000
0.6058E 01	0.1995E 04	0.7823	3.3000

TABLES OF CURVE OF GROWTH

A = 0.0004

X	Y	LOG X	LOG Y
0.6219E 01	0.2512E 04	0.7937	3.4000
0.6399E 01	0.3162E 04	0.8061	3.5000
0.6600E 01	0.3981E 04	0.8195	3.6000
0.6829E 01	0.5012E 04	0.8344	3.7000
0.7092E 01	0.6310E 04	0.8507	3.8000
0.7396E 01	0.7943E 04	0.8690	3.9000
0.7752E 01	1.0000E 04	0.8894	4.0000
0.8167E 01	0.1259E 05	0.9121	4.1000
0.8658E 01	0.1585E 05	0.9374	4.2000
0.9235E 01	0.1995E 05	0.9654	4.3000
0.9917E 01	0.2512E 05	0.9964	4.4000
0.1072E 02	0.3162E 05	1.0302	4.5000
0.1167E 02	0.3981E 05	1.0670	4.6000
0.1278E 02	0.5012E 05	1.1064	4.7000
0.1408E 02	0.6310E 05	1.1484	4.8000

TABLES OF CURVE OF GROWTH

A = 0.0008

X	Y	LOG X	LOG Y
0.1766E-01	1.0000E-02	-1.7529	-2.0000
0.2222E-01	0.1259E-01	-1.6533	-1.9000
0.2794E-01	0.1585E-01	-1.5538	-1.8000
0.3513E-01	0.1995E-01	-1.4544	-1.7000
0.4413E-01	0.2512E-01	-1.3553	-1.6000
0.5543E-01	0.3162E-01	-1.2562	-1.5000
0.6958E-01	0.3981E-01	-1.1575	-1.4000
0.8730E-01	0.5012E-01	-1.0590	-1.3000
0.1094E-00	0.6310E-01	-0.9610	-1.2000
0.1369E-00	0.7943E-01	-0.8635	-1.1000
0.1712E-00	0.1000E-00	-0.7666	-1.0000
0.2136E-00	0.1259E-00	-0.6705	-0.9000
0.2659E-00	0.1585E-00	-0.5753	-0.8000
0.3301E-00	0.1995E-00	-0.4813	-0.7000
0.4083E-00	0.2512E-00	-0.3890	-0.6000
0.5030E 00	0.3162E-00	-0.2985	-0.5000
0.6163E 00	0.3981E-00	-0.2102	-0.4000
0.7504E 00	0.5012E 00	-0.1247	-0.3000
0.9070E 00	0.6310E 00	-0.0424	-0.2000
0.1086E 01	0.7943E 00	0.0358	-0.1000
0.1286E 01	0.1000E 01	0.1093	0.0000
0.1504E 01	0.1259E 01	0.1772	0.1000
0.1736E 01	0.1585E 01	0.2395	0.2000
0.1972E 01	0.1995E 01	0.2950	0.3000
0.2207E 01	0.2512E 01	0.3437	0.4000
0.2431E 01	0.3162E 01	0.3858	0.5000
0.2640E 01	0.3981E 01	0.4216	0.6000
0.2832E 01	0.5012E 01	0.4521	0.7000
0.3008E 01	0.6310E 01	0.4783	0.8000
0.3171E 01	0.7943E 01	0.5012	0.9000
0.3324E 01	0.1000E 02	0.5216	1.0000
0.3468E 01	0.1259E 02	0.5401	1.1000
0.3607E 01	0.1585E 02	0.5571	1.2000
0.3739E 01	0.1995E 02	0.5728	1.3000
0.3867E 01	0.2512E 02	0.5874	1.4000
0.3992E 01	0.3162E 02	0.6012	1.5000
0.4113E 01	0.3981E 02	0.6142	1.6000
0.4232E 01	0.5012E 02	0.6265	1.7000
0.4348E 01	0.6310E 02	0.6382	1.8000
0.4462E 01	0.7943E 02	0.6495	1.9000
0.4575E 01	0.1000E 03	0.6604	2.0000
0.4688E 01	0.1259E 03	0.6710	2.1000
0.4801E 01	0.1585E 03	0.6813	2.2000
0.4914E 01	0.1995E 03	0.6914	2.3000
0.5029E 01	0.2512E 03	0.7015	2.4000
0.5147E 01	0.3162E 03	0.7115	2.5000
0.5269E 01	0.3981E 03	0.7217	2.6000
0.5395E 01	0.5012E 03	0.7320	2.7000
0.5527E 01	0.6310E 03	0.7425	2.8000
0.5671E 01	0.7943E 03	0.7536	2.9000
0.5823E 01	1.0000E 03	0.7651	3.0000
0.5993E 01	0.1259E 04	0.7776	3.1000
0.6180E 01	0.1585E 04	0.7910	3.2000
0.6389E 01	0.1995E 04	0.8054	3.3000

TABLES OF CURVE OF GROWTH

A = 0.0008

X	Y	LOG X	LOG Y
0.6626E 01	0.2512E 04	0.8213	3.4000
0.6897E 01	0.3162E 04	0.8386	3.5000
0.7212E 01	0.3981E 04	0.8581	3.6000
0.7576E 01	0.5012E 04	0.8795	3.7000
0.8007E 01	0.6310E 04	0.9035	3.8000
0.8510E 01	0.7943E 04	0.9300	3.9000
0.9104E 01	1.0000E 04	0.9592	4.0000
0.9802E 01	0.1259E 05	0.9913	4.1000
0.1062E 02	0.1585E 05	1.0263	4.2000
0.1159E 02	0.1995E 05	1.0641	4.3000
0.1272E 02	0.2512E 05	1.1045	4.4000
0.1403E 02	0.3162E 05	1.1471	4.5000

TABLES OF CURVE OF GROWTH

A = 0.0016

X	Y	LOG X	LOG Y
0.1766E-01	1.0000E-02	-1.7530	-2.0000
0.2222E-01	0.1259E-01	-1.6533	-1.9000
0.2794E-01	0.1585E-01	-1.5538	-1.8000
0.3512E-01	0.1995E-01	-1.4545	-1.7000
0.4413E-01	0.2512E-01	-1.3553	-1.6000
0.5543E-01	0.3162E-01	-1.2563	-1.5000
0.6958E-01	0.3981E-01	-1.1575	-1.4000
0.8728E-01	0.5012E-01	-1.0591	-1.3000
0.1094E-00	0.6310E-01	-0.9609	-1.2000
0.1369E-00	0.7943E-01	-0.8635	-1.1000
0.1712E-00	0.1000E-00	-0.7665	-1.0000
0.2136E-00	0.1259E-00	-0.6704	-0.9000
0.2659E-00	0.1585E-00	-0.5752	-0.8000
0.3301E-00	0.1995E-00	-0.4813	-0.7000
0.4084E-00	0.2512E-00	-0.3889	-0.6000
0.5031E 00	0.3162E-00	-0.2983	-0.5000
0.6164E 00	0.3981E-00	-0.2101	-0.4000
0.7506E 00	0.5012E 00	-0.1246	-0.3000
0.9072E 00	0.6310E 00	-0.0423	-0.2000
0.1086E 01	0.7943E 00	0.0359	-0.1000
0.1286E 01	0.1000E 01	0.1094	0.0000
0.1505E 01	0.1259E 01	0.1776	0.1000
0.1737E 01	0.1585E 01	0.2397	0.2000
0.1974E 01	0.1995E 01	0.2953	0.3000
0.2209E 01	0.2512E 01	0.3441	0.4000
0.2433E 01	0.3162E 01	0.3862	0.5000
0.2643E 01	0.3981E 01	0.4221	0.6000
0.2836E 01	0.5012E 01	0.4527	0.7000
0.3013E 01	0.6310E 01	0.4790	0.8000
0.3177E 01	0.7943E 01	0.5020	0.9000
0.3331E 01	0.1000E 02	0.5225	1.0000
0.3477E 01	0.1259E 02	0.5412	1.1000
0.3616E 01	0.1585E 02	0.5583	1.2000
0.3751E 01	0.1995E 02	0.5742	1.3000
0.3882E 01	0.2512E 02	0.5891	1.4000
0.4009E 01	0.3162E 02	0.6031	1.5000
0.4134E 01	0.3981E 02	0.6164	1.6000
0.4258E 01	0.5012E 02	0.6292	1.7000
0.4379E 01	0.6310E 02	0.6414	1.8000
0.4500E 01	0.7943E 02	0.6532	1.9000
0.4622E 01	0.1000E 03	0.6649	2.0000
0.4745E 01	0.1259E 03	0.6762	2.1000
0.4871E 01	0.1585E 03	0.6876	2.2000
0.5000E 01	0.1995E 03	0.6990	2.3000
0.5134E 01	0.2512E 03	0.7105	2.4000
0.5275E 01	0.3162E 03	0.7222	2.5000
0.5426E 01	0.3981E 03	0.7345	2.6000
0.5587E 01	0.5012E 03	0.7472	2.7000
0.5765E 01	0.6310E 03	0.7608	2.8000
0.5961E 01	0.7943E 03	0.7753	2.9000
0.6179E 01	1.0000E 03	0.7909	3.0000
0.6427E 01	0.1259E 04	0.8080	3.1000
0.6710E 01	0.1585E 04	0.8267	3.2000
0.7037E 01	0.1995E 04	0.8474	3.3000

TABLES OF CURVE OF GROWTH

A = 0.0016

X	Y	LOG X	LOG Y
0.7415E 01	0.2512E 04	0.8701	3.4000
0.7858E 01	0.3162E 04	0.8953	3.5000
0.8376E 01	0.3981E 04	0.9230	3.6000
0.8984E 01	0.5012E 04	0.9535	3.7000
0.9699E 01	0.6310E 04	0.9867	3.8000
0.1054E 02	0.7943E 04	1.0227	3.9000
0.1152E 02	1.0000E 04	1.0614	4.0000
0.1266E 02	0.1259E 05	1.1025	4.1000
0.1399E 02	0.1585E 05	1.1459	4.2000

TABLES OF CURVE OF GROWTH

A = 0.0032

X	Y	LOG X	LOG Y
0.1766E-01	1.0000E-02	-1.753[illegible]	-2.000[illegible]
0.2222E-01	0.1259E-01	-1.653[illegible]	-1.9000
0.2794E-01	0.1585E-01	-1.5537	-1.8000
0.3512E-01	0.1995E-01	-1.4545	-1.7000
0.4413E-01	0.2512E-01	-1.3553	-1.6000
0.5545E-01	0.3162E-01	-1.2561	-1.5000
0.6960E-01	0.3981E-01	-1.1574	-1.4000
0.8731E-01	0.5012E-01	-1.0590	-1.3000
0.1094E-00	0.6310E-01	-0.9609	-1.2000
0.1370E-00	0.7943E-01	-0.8634	-1.1000
0.1712E-00	0.1000E-00	-0.7664	-1.0000
0.2136E-00	0.1259E-00	-0.6703	-0.9000
0.2660E-00	0.1585E-00	-0.5752	-0.8000
0.3302E-00	0.1995E-00	-0.4812	-0.7000
0.4085E-00	0.2512E-00	-0.3888	-0.6000
0.5033E 00	0.3162E-00	-0.2982	-0.5000
0.6168E 00	0.3981E-00	-0.2099	-0.4000
0.7511E 00	0.5012E 00	-0.1243	-0.3000
0.9077E 00	0.6310E 00	-0.0421	-0.2000
0.1087E 01	0.7943E 00	0.0362	-0.1000
0.1288E 01	0.1000E 01	0.1098	0.0000
0.1507E 01	0.1259E 01	0.1760	0.1000
0.1739E 01	0.1585E 01	0.2402	0.2000
0.1977E 01	0.1995E 01	0.2959	0.3000
0.2212E 01	0.2512E 01	0.3449	0.4000
0.2438E 01	0.3162E 01	0.3871	0.5000
0.2650E 01	0.3981E 01	0.4232	0.6000
0.2844E 01	0.5012E 01	0.4539	0.7000
0.3023E 01	0.6310E 01	0.4804	0.8000
0.3188E 01	0.7943E 01	0.5038	0.9000
0.3345E 01	0.1000E 02	0.5244	1.0000
0.3494E 01	0.1259E 02	0.5433	1.1000
0.3637E 01	0.1585E 02	0.5607	1.2000
0.3776E 01	0.1995E 02	0.5770	1.3000
0.3912E 01	0.2512E 02	0.5924	1.4000
0.4045E 01	0.3162E 02	0.6070	1.5000
0.4178E 01	0.3981E 02	0.6209	1.6000
0.4309E 01	0.5012E 02	0.6344	1.7000
0.4442E 01	0.6310E 02	0.6476	1.8000
0.4577E 01	0.7943E 02	0.6605	1.9000
0.4715E 01	0.1000E 03	0.6735	2.0000
0.4858E 01	0.1259E 03	0.6865	2.1000
0.5008E 01	0.1585E 03	0.6997	2.2000
0.5167E 01	0.1995E 03	0.7133	2.3000
0.5338E 01	0.2512E 03	0.7274	2.4000
0.5525E 01	0.3162E 03	0.7423	2.5000
0.5730E 01	0.3981E 03	0.7582	2.6000
0.5959E 01	0.5012E 03	0.7752	2.7000
0.6219E 01	0.6310E 03	0.7937	2.8000
0.6513E 01	0.7943E 03	0.8138	2.9000
0.6853E 01	1.0000E 03	0.8359	3.0000
0.7246E 01	0.1259E 04	0.8601	3.1000
0.7704E 01	0.1585E 04	0.8867	3.2000
0.8240E 01	0.1995E 04	0.9159	3.3000

TABLES OF CURVE OF GROWTH

A = 0.0032

X	Y	LOG X	LOG Y
0.8866E 01	0.2512E 04	0.9477	3.4000
0.9601E 01	0.3162E 04	0.9823	3.5000
0.1046E 02	0.3981E 04	1.0195	3.6000
0.1146E 02	0.5012E 04	1.0592	3.7000
0.1262E 02	0.6310E 04	1.1011	3.8000
0.1397E 02	0.7943E 04	1.1451	3.9000

TABLES OF CURVE OF GROWTH

A = 0.0064

X	Y	LOG X	LOG Y
0.1766E-01	1.0000E-02	-1.7530	-2.0000
0.2222E-01	0.1259E-01	-1.6533	-1.9000
0.2794E-01	0.1585E-01	-1.5538	-1.8000
0.3512E-01	0.1995E-01	-1.4544	-1.7000
0.4414E-01	0.2512E-01	-1.3552	-1.6000
0.5544E-01	0.3162E-01	-1.2562	-1.5000
0.6960E-01	0.3981E-01	-1.1574	-1.4000
0.8731E-01	0.5012E-01	-1.0589	-1.3000
0.1094E-00	0.6310E-01	-0.9609	-1.2000
0.1370E-00	0.7943E-01	-0.8633	-1.1000
0.1712E-00	0.1000E-00	-0.7664	-1.0000
0.2137E-00	0.1259E-00	-0.6703	-0.9000
0.2660E-00	0.1585E-00	-0.5751	-0.8000
0.3302E-00	0.1995E-00	-0.4812	-0.7000
0.4086E-00	0.2512E-00	-0.3887	-0.6000
0.5035E 00	0.3162E-00	-0.2980	-0.5000
0.6171E 00	0.3981E-00	-0.2096	-0.4000
0.7516E 00	0.5012E 00	-0.1240	-0.3000
0.9084E 00	0.6310E 00	-0.0417	-0.2000
0.1088E 01	0.7943E 00	0.0367	-0.1000
0.1289E 01	0.1000E 01	0.1104	0.0000
0.1509E 01	0.1259E 01	0.1788	0.1000
0.1743E 01	0.1585E 01	0.2412	0.2000
0.1982E 01	0.1995E 01	0.2970	0.3000
0.2219E 01	0.2512E 01	0.3462	0.4000
0.2448E 01	0.3162E 01	0.3887	0.5000
0.2661E 01	0.3981E 01	0.4251	0.6000
0.2858E 01	0.5012E 01	0.4561	0.7000
0.3041E 01	0.6310E 01	0.4830	0.8000
0.3210E 01	0.7943E 01	0.5065	0.9000
0.3371E 01	0.1000E 02	0.5278	1.0000
0.3525E 01	0.1259E 02	0.5472	1.1000
0.3675E 01	0.1585E 02	0.5653	1.2000
0.3823E 01	0.1995E 02	0.5824	1.3000
0.3968E 01	0.2512E 02	0.5986	1.4000
0.4114E 01	0.3162E 02	0.6142	1.5000
0.4261E 01	0.3981E 02	0.6295	1.6000
0.4411E 01	0.5012E 02	0.6445	1.7000
0.4565E 01	0.6310E 02	0.6595	1.8000
0.4727E 01	0.7943E 02	0.6746	1.9000
0.4898E 01	0.1000E 03	0.6900	2.0000
0.5080E 01	0.1259E 03	0.7059	2.1000
0.5279E 01	0.1585E 03	0.7225	2.2000
0.5496E 01	0.1995E 03	0.7401	2.3000
0.5738E 01	0.2512E 03	0.7588	2.4000
0.6010E 01	0.3162E 03	0.7789	2.5000
0.6320E 01	0.3981E 03	0.8007	2.6000
0.6675E 01	0.5012E 03	0.8245	2.7000
0.7084E 01	0.6310E 03	0.8503	2.8000
0.7559E 01	0.7943E 03	0.8785	2.9000
0.8113E 01	1.0000E 03	0.9092	3.0000
0.8758E 01	0.1259E 04	0.9424	3.1000
0.9510E 01	0.1585E 04	0.9782	3.2000
0.1039E 02	0.1995E 04	1.0165	3.3000

TABLES OF CURVE OF GROWTH

A = 0.0064

X	Y	LOG X	LOG Y
0.1141E 02	0.2512E 04	1.0572	3.4000
0.1259E 02	0.3162E 04	1.0999	3.5000
0.1395E 02	0.3981E 04	1.1445	3.6000

TABLES OF CURVE OF GROWTH

A = 0.0128

X	Y	LOG X	LOG Y
0.1766E-01	1.0000E-02	-1.7529	-2.0000
0.2222E-01	0.1259E-01	-1.6532	-1.9000
0.2794E-01	0.1585E-01	-1.5537	-1.8000
0.3513E-01	0.1995E-01	-1.4543	-1.7000
0.4415E-01	0.2512E-01	-1.3551	-1.6000
0.5545E-01	0.3162E-01	-1.2561	-1.5000
0.6961E-01	0.3981E-01	-1.1573	-1.4000
0.8733E-01	0.5012E-01	-1.0589	-1.3000
0.1094E-00	0.6310E-01	-0.9609	-1.2000
0.1370E-00	0.7943E-01	-0.8632	-1.1000
0.1713E-00	0.1000E-00	-0.7663	-1.0000
0.2137E-00	0.1259E-00	-0.6701	-0.9000
0.2661E-00	0.1585E-00	-0.5749	-0.8000
0.3305E-00	0.1995E-00	-0.4808	-0.7000
0.4090E-00	0.2512E-00	-0.3883	-0.6000
0.5041E 00	0.3162E-00	-0.2975	-0.5000
0.6180E 00	0.3981E-00	-0.2090	-0.4000
0.7529E 00	0.5012E 00	-0.1233	-0.3000
0.9104E 00	0.6310E 00	-0.0408	-0.2000
0.1091E 01	0.7943E 00	0.0377	-0.1000
0.1294E 01	0.1000E 01	0.1118	0.0000
0.1515E 01	0.1259E 01	0.1805	0.1000
0.1751E 01	0.1585E 01	0.2433	0.2000
0.1993E 01	0.1995E 01	0.2995	0.3000
0.2235E 01	0.2512E 01	0.3492	0.4000
0.2467E 01	0.3162E 01	0.3922	0.5000
0.2686E 01	0.3981E 01	0.4292	0.6000
0.2890E 01	0.5012E 01	0.4609	0.7000
0.3079E 01	0.6310E 01	0.4884	0.8000
0.3257E 01	0.7943E 01	0.5128	0.9000
0.3427E 01	0.1000E 02	0.5350	1.0000
0.3593E 01	0.1259E 02	0.5555	1.1000
0.3757E 01	0.1585E 02	0.5748	1.2000
0.3921E 01	0.1995E 02	0.5933	1.3000
0.4086E 01	0.2512E 02	0.6113	1.4000
0.4255E 01	0.3162E 02	0.6289	1.5000
0.4431E 01	0.3981E 02	0.6465	1.6000
0.4615E 01	0.5012E 02	0.6642	1.7000
0.4811E 01	0.6310E 02	0.6823	1.8000
0.5023E 01	0.7943E 02	0.7009	1.9000
0.5255E 01	0.1000E 03	0.7206	2.0000
0.5512E 01	0.1259E 03	0.7413	2.1000
0.5799E 01	0.1585E 03	0.7633	2.2000
0.6124E 01	0.1995E 03	0.7870	2.3000
0.6496E 01	0.2512E 03	0.8127	2.4000
0.6922E 01	0.3162E 03	0.8402	2.5000
0.7416E 01	0.3981E 03	0.8702	2.6000
0.7989E 01	0.5012E 03	0.9025	2.7000
0.8653E 01	0.6310E 03	0.9372	2.8000
0.9427E 01	0.7943E 03	0.9744	2.9000
0.1032E 02	1.0000E 03	1.0138	3.0000
0.1136E 02	0.1259E 04	1.0554	3.1000
0.1256E 02	0.1585E 04	1.0988	3.2000
0.1393E 02	0.1995E 04	1.1440	3.3000

TABLES OF CURVE OF GROWTH

A = 0.0256

X	Y	LOG X	LOG Y
0.1766E-01	1.0000E-02	-1.7529	-2.0000
0.2222E-01	0.1259E-01	-1.6532	-1.9000
0.2795E-01	0.1585E-01	-1.5537	-1.8000
0.3513E-01	0.1995E-01	-1.4543	-1.7000
0.4415E-01	0.2512E-01	-1.3550	-1.6000
0.5547E-01	0.3162E-01	-1.2560	-1.5000
0.6963E-01	0.3981E-01	-1.1572	-1.4000
0.8735E-01	0.5012E-01	-1.0587	-1.3000
0.1095E-00	0.6310E-01	-0.9606	-1.2000
0.1371E-00	0.7943E-01	-0.8629	-1.1000
0.1714E-00	0.1000E-00	-0.7659	-1.0000
0.2140E-00	0.1259E-00	-0.6697	-0.9000
0.2665E-00	0.1585E-00	-0.5743	-0.8000
0.3310E-00	0.1995E-00	-0.4802	-0.7000
0.4097E-00	0.2512E-00	-0.3875	-0.6000
0.5049E 00	0.3162E-00	-0.2968	-0.5000
0.6196E 00	0.3981E-00	-0.2079	-0.4000
0.7552E 00	0.5012E 00	-0.1219	-0.3000
0.9141E 00	0.6310E 00	-0.0390	-0.2000
0.1096E 01	0.7943E 00	0.0400	-0.1000
0.1302E 01	0.1000E 01	0.1145	0.0000
0.1527E 01	0.1259E 01	0.1837	0.1000
0.1767E 01	0.1585E 01	0.2472	0.2000
0.2015E 01	0.1995E 01	0.3043	0.3000
0.2264E 01	0.2512E 01	0.3548	0.4000
0.2505E 01	0.3162E 01	0.3989	0.5000
0.2735E 01	0.3981E 01	0.4369	0.6000
0.2950E 01	0.5012E 01	0.4699	0.7000
0.3153E 01	0.6310E 01	0.4987	0.8000
0.3347E 01	0.7943E 01	0.5247	0.9000
0.3536E 01	0.1000E 02	0.5486	1.0000
0.3724E 01	0.1259E 02	0.5710	1.1000
0.3914E 01	0.1585E 02	0.5926	1.2000
0.4109E 01	0.1995E 02	0.6137	1.3000
0.4311E 01	0.2512E 02	0.6346	1.4000
0.4526E 01	0.3162E 02	0.6557	1.5000
0.4755E 01	0.3981E 02	0.6772	1.6000
0.5004E 01	0.5012E 02	0.6993	1.7000
0.5279E 01	0.6310E 02	0.7225	1.8000
0.5584E 01	0.7943E 02	0.7470	1.9000
0.5929E 01	0.1000E 03	0.7729	2.0000
0.6319E 01	0.1259E 03	0.8007	2.1000
0.6766E 01	0.1585E 03	0.8303	2.2000
0.7279E 01	0.1995E 03	0.8621	2.3000
0.7872E 01	0.2512E 03	0.8961	2.4000
0.8558E 01	0.3162E 03	0.9324	2.5000
0.9350E 01	0.3981E 03	0.9708	2.6000
0.1027E 02	0.5012E 03	1.0114	2.7000
0.1132E 02	0.6310E 03	1.0539	2.8000
0.1253E 02	0.7943E 03	1.0981	2.9000
0.1392E 02	1.0000E 03	1.1437	3.0000

TABLES OF CURVE OF GROWTH

A = 0.0512

X	Y	LOG X	LOG Y
0.1767E-01	1.0000E-02	-1.7528	-2.0000
0.2223E-01	0.1259E-01	-1.6531	-1.9000
0.2795E-01	0.1585E-01	-1.5536	-1.8000
0.3514E-01	0.1995E-01	-1.4541	-1.7000
0.4417E-01	0.2512E-01	-1.3549	-1.6000
0.5549E-01	0.3162E-01	-1.2558	-1.5000
0.6966E-01	0.3981E-01	-1.1570	-1.4000
0.8742E-01	0.5012E-01	-1.0584	-1.3000
0.1096E-00	0.6310E-01	-0.9602	-1.2000
0.1372E-00	0.7943E-01	-0.8625	-1.1000
0.1716E-00	0.1000E-00	-0.7654	-1.0000
0.2143E-00	0.1259E-00	-0.6690	-0.9000
0.2670E-00	0.1585E-00	-0.5735	-0.8000
0.3318E-00	0.1995E-00	-0.4791	-0.7000
0.4111E-00	0.2512E-00	-0.3861	-0.6000
0.5072E 00	0.3162E-00	-0.2948	-0.5000
0.6228E 00	0.3981E-00	-0.2057	-0.4000
0.7602E 00	0.5012E 00	-0.1191	-0.3000
0.9212E 00	0.6310E 00	-0.0357	-0.2000
0.1107E 01	0.7943E 00	0.0441	-0.1000
0.1317E 01	0.1000E 01	0.1195	0.0000
0.1549E 01	0.1259E 01	0.1899	0.1000
0.1798E 01	0.1585E 01	0.2547	0.2000
0.2057E 01	0.1995E 01	0.3133	0.3000
0.2320E 01	0.2512E 01	0.3655	0.4000
0.2579E 01	0.3162E 01	0.4115	0.5000
0.2829E 01	0.3981E 01	0.4516	0.6000
0.3068E 01	0.5012E 01	0.4868	0.7000
0.3297E 01	0.6310E 01	0.5182	0.8000
0.3522E 01	0.7943E 01	0.5468	0.9000
0.3746E 01	0.1000E 02	0.5736	1.0000
0.3976E 01	0.1259E 02	0.5994	1.1000
0.4215E 01	0.1585E 02	0.6248	1.2000
0.4468E 01	0.1995E 02	0.6502	1.3000
0.4741E 01	0.2512E 02	0.6759	1.4000
0.5038E 01	0.3162E 02	0.7023	1.5000
0.5366E 01	0.3981E 02	0.7297	1.6000
0.5733E 01	0.5012E 02	0.7584	1.7000
0.6146E 01	0.6310E 02	0.7886	1.8000
0.6615E 01	0.7943E 02	0.8205	1.9000
0.7151E 01	0.1000E 03	0.8544	2.0000
0.7765E 01	0.1259E 03	0.8902	2.1000
0.8472E 01	0.1585E 03	0.9280	2.2000
0.9284E 01	0.1995E 03	0.9678	2.3000
0.1022E 02	0.2512E 03	1.0094	2.4000
0.1129E 02	0.3162E 03	1.0527	2.5000
0.1252E 02	0.3981E 03	1.0975	2.6000
0.1392E 02	0.5012E 03	1.1435	2.7000

TABLES OF CURVE OF GROWTH

A = 0.1024

X	Y	LOG X	LOG Y
0.1767E-01	1.0000E-02	-1.7527	-2.0000
0.2223E-01	0.1259E-01	-1.6531	-1.9000
0.2796E-01	0.1585E-01	-1.5535	-1.8000
0.3516E-01	0.1995E-01	-1.4540	-1.7000
0.4419E-01	0.2512E-01	-1.3547	-1.6000
0.5552E-01	0.3162E-01	-1.2555	-1.5000
0.6973E-01	0.3981E-01	-1.1566	-1.4000
0.8751E-01	0.5012E-01	-1.0579	-1.3000
0.1097E-00	0.6310E-01	-0.9596	-1.2000
0.1375E-00	0.7943E-01	-0.8617	-1.1000
0.1720E-00	0.1000E-00	-0.7644	-1.0000
0.2149E-00	0.1259E-00	-0.6677	-0.9000
0.2680E-00	0.1585E-00	-0.5719	-0.8000
0.3333E-00	0.1995E-00	-0.4771	-0.7000
0.4134E-00	0.2512E-00	-0.3836	-0.6000
0.5108E 00	0.3162E-00	-0.2917	-0.5000
0.6283E 00	0.3981E-00	-0.2018	-0.4000
0.7686E 00	0.5012E 00	-0.1143	-0.3000
0.9340E 00	0.6310E 00	-0.0297	-0.2000
0.1126E 01	0.7943E 00	0.0515	-0.1000
0.1345E 01	0.1000E 01	0.1286	0.0000
0.1589E 01	0.1259E 01	0.2010	0.1000
0.1855E 01	0.1585E 01	0.2682	0.2000
0.2136E 01	0.1995E 01	0.3296	0.3000
0.2426E 01	0.2512E 01	0.3849	0.4000
0.2717E 01	0.3162E 01	0.4341	0.5000
0.3005E 01	0.3981E 01	0.4779	0.6000
0.3288E 01	0.5012E 01	0.5169	0.7000
0.3568E 01	0.6310E 01	0.5524	0.8000
0.3850E 01	0.7943E 01	0.5854	0.9000
0.4140E 01	0.1000E 02	0.6170	1.0000
0.4445E 01	0.1259E 02	0.6479	1.1000
0.4774E 01	0.1585E 02	0.6789	1.2000
0.5131E 01	0.1995E 02	0.7102	1.3000
0.5526E 01	0.2512E 02	0.7424	1.4000
0.5967E 01	0.3162E 02	0.7757	1.5000
0.6463E 01	0.3981E 02	0.8104	1.6000
0.7024E 01	0.5012E 02	0.8466	1.7000
0.7663E 01	0.6310E 02	0.8844	1.8000
0.8393E 01	0.7943E 02	0.9239	1.9000
0.9226E 01	0.1000E 03	0.9650	2.0000
0.1018E 02	0.1259E 03	1.0077	2.1000
0.1127E 02	0.1585E 03	1.0518	2.2000
0.1251E 02	0.1995E 03	1.0971	2.3000
0.1391E 02	0.2512E 03	1.1435	2.4000

TABLES OF CURVE OF GROWTH

A = 1.0000

X	Y	LOG X	LOG Y
0.1770E-01	1.0000E-02	-1.7520	-2.0000
0.2229E-01	0.1259E-01	-1.6519	-1.9000
0.2805E-01	0.1585E-01	-1.5521	-1.8000
0.3530E-01	0.1995E-01	-1.4523	-1.7000
0.4441E-01	0.2512E-01	-1.3526	-1.6000
0.5586E-01	0.3162E-01	-1.2529	-1.5000
0.7023E-01	0.3981E-01	-1.1535	-1.4000
0.8834E-01	0.5012E-01	-1.0539	-1.3000
0.1110E-00	0.6310E-01	-0.9546	-1.2000
0.1395E-00	0.7943E-01	-0.8554	-1.1000
0.1752E-00	0.1000E-00	-0.7564	-1.0000
0.2199E-00	0.1259E-00	-0.6577	-0.9000
0.2758E-00	0.1585E-00	-0.5594	-0.8000
0.3455E-00	0.1995E-00	-0.4616	-0.7000
0.4325E-00	0.2512E-00	-0.3640	-0.6000
0.5402E 00	0.3162E-00	-0.2674	-0.5000
0.6739E 00	0.3981E-00	-0.1714	-0.4000
0.8384E 00	0.5012E 00	-0.0766	-0.3000
0.1040E 01	0.6310E 00	0.0171	-0.2000
0.1286E 01	0.7943E 00	0.1094	-0.1000
0.1584E 01	0.1000E 01	0.1997	0.0000
0.1940E 01	0.1259E 01	0.2879	0.1000
0.2362E 01	0.1585E 01	0.3734	0.2000
0.2856E 01	0.1995E 01	0.4558	0.3000
0.3425E 01	0.2512E 01	0.5347	0.4000
0.4071E 01	0.3162E 01	0.6097	0.5000
0.4792E 01	0.3981E 01	0.6805	0.6000
0.5585E 01	0.5012E 01	0.7470	0.7000
0.6446E 01	0.6310E 01	0.8093	0.8000
0.7376E 01	0.7943E 01	0.8678	0.9000
0.8378E 01	0.1000E 02	0.9232	1.0000
0.9467E 01	0.1259E 02	0.9762	1.1000
0.1066E 02	0.1585E 02	1.0276	1.2000
0.1197E 02	0.1995E 02	1.0782	1.3000
0.1343E 02	0.2512E 02	1.1282	1.4000

XIII - BIBLIOGRAPHY

(1) Bates and Damgard; Phil. Trans. Roy. Soc. of London A 242, 108 (1949)

(2) J. Hargreaves; Proc. Camb. Phil. Soc 25, 75 (1928)

(3) Bates and Damgard; Astrophys. J 107, 383 (1948)

(4) D. R. Hartree and W. Hartree; Proc. Roy. Soc. A 164, 167 (1938)

(5) B. Misra; Ph.D. Thesis Univ. of London (1948)

(6) T. Helliwell; Astrophys. J 133, 566 (1961)

(7) P. Atlick; U.C.R.L. 10510 (Oct. 1962)

(8) A. S. King and R. B. King; Astrophys. J 87, 24 (1938)

(9) R. B. King and D. C. Stockbarger; Astrophys. J 91, 488 (1940)

(10) F. A. Estabrook; Ph.D. Thesis California Inst. of Technology (1950)

(11) H. Kopferman and G. Wessel; Zeits. f. Phys. 130, 100 (1951)

(12) G. D. Bell, M. H. Davis, R. B. King, P. M. Routly; Astrophys. J 127, 775 (1958)

(13) G. D. Bell and R. B. King; Astrophys. J 133, 718 (1960)

(14) G. Lawrence; Ph.D. Thesis California Inst. of Technology (1963)

(15) J. Link; Ph.D. Thesis California Inst. of Technology (1963)

(16) O. S. Rozhdestvenskii and N. P. Penkin; Optical Trans. Prob. (N.S.F.) 127 (1960)

(17) Y. D. Ostrovskii and N. P. Penkin; Optical Trans. Prob. (N.S.F.) 415 (1960)

(18) K. Ziock; Zeits. f. Phys. 147, 99 (1957)

Bibliography - cont'd

(19) C. Ottinger and K. Ziock; Zeits. Naturforsch 16a, 720 (1961)

(20) W. Demtroder; Zeits. f. Phys. 166, 42 (1962)

(21) C. H. Corliss and W. R. Bozman; (N.B.S. Monograph 53) (July 1962)

(22) L. H. Aller; The Abundance of the Elements (Interscience) (1961)

(23) L. H. Aller, L. Goldberg, and E. A. Muller; Astrophys. J Suppl. V, 1 (1960)

(24) J. L. Greenstein and L. H. Aller; Astrophys. J Suppl. V 139 (1960)

(25) A. Unsold; Physik der Sterneatmospharen (J. Springer, Berlin) (1938)

(26) E. Lindholm; Loc. Cit., 1

(27) Selected Values for the Thermodynamic Properties of Metals and Alloys (U.C.B.) (1960)

(28) D. R. Stulle and G. C. Sinke; Thermodynamic Properties of the Elements (Amer. Chem. Soc.) (1956)

(29) K. K. Kelley; Contributions to the Data on Theoretical Metallurgy III Bulletin 383 U. S. Bureau of Mines

(30) Landholt - Bornstein; Zohlenwerte u. Funktionen 1 (J. Springer, Berlin) (1950)

(31) A. C. G. Mitchel and M. W. Zemansky; Resonance Radiation and Excited Atoms (Macmillan Co.) (1934)

(32) G. D. Bell; Ph.D. Thesis California Inst. of Technology (1957)

(33) H. G. Kuhn; Atomic Spectra (Acad. Press) (1962)

(34) E. Hinnov and H. Kohn; J. Opt. Soc. Am. 47, 156 (1957)

(35) B. M. Glennon and W. L. Wiese; (N.B.S. Monograph 50) (Aug. 1962)

(36) P. Soleillet; Compt. rend 204, 253 (1937)

Bibliography - cont'd

(37) J. Auslander; Helv. Phys. Acta 11, 562 (1938)

(38) A. Gatlow and F. Schneider; Angew Chem. 71, 181 (1959)

(39) W. Kuhn; Kgl. Danske Videnskab Selskab Mat-fys. 7, 1 (1926)

(40) H. D. Koenig and A. Ellett; Phys. Rev. 39, 576 (1932)

(41) J. S. Anderson; J. Chem. Soc. (London) 1943, 141 (1943)

(42) A. P. Lyubimov and Y. N. Lyubimov; Obrabotka Stali i Splavov. Moskov Inst. 36, 191 (1957)

(43) Prokof'ev, Nagibina, and Petrova; Zeits. f. Physik 48, 276 (1928)

(44) F. Reiche; Verh. d. D. Phys. Ges. 15, 3 (1913)